REASSESSMENT OF A HISTORICAL COLLECTION OF SAUROPOD DINOSAURS FROM THE NORTHERN MORRISON FORMATION OF WYOMING, WITH IMPLICATIONS FOR SAUROPOD BIOGEOGRAPHY

EMANUEL TSCHOPP
American Museum of Natural History, Division of Paleontology, New York; Museu da Lourinhã, Lourinhã, Portugal

SUSANNAH C.R. MAIDMENT
Natural History Museum, London

MATTHEW C. LAMANNA
Section of Vertebrate Paleontology, Carnegie Museum of Natural History, Pittsburgh

MARK A. NORELL
American Museum of Natural History, Division of Paleontology, New York

BULLETIN OF THE AMERICAN MUSEUM OF NATURAL HISTORY
Number 437, 79 pp., 31 figures, 22 tables
Issued November 4, 2019

 ISSN 0003-0090

CONTENTS

ABSTRACT

The Upper Jurassic Morrison Formation of the western United States preserves one of the best-known Mesozoic paleoecosystems worldwide. The formation crops out over an area from New Mexico and Oklahoma to Montana and Utah and encompasses a time span of approximately eight million years. Recent studies indicate a high diversity of gigantic, herbivorous sauropod dinosaurs, but the geographic and temporal distributions of species or even genera of these animals remain poorly understood. In particular, sauropod specimens from northern outcrops of the formation have rarely been studied in detail, and temporal relationships among sites are imprecise. Here, we reassess the taxonomic diversity of the sauropods from a historic Carnegie Museum locality in northern Wyoming. Previous referrals of material to the well-known diplodocid genera *Apatosaurus* and *Diplodocus* cannot be confidently confirmed; instead, all these specimens more likely represent elements from the recently recognized *Galeamopus*. Specimens previously assigned to *Camarasaurus* and *Haplocanthosaurus* could not be referred to these genera based on apomorphies, due to a lack of detailed knowledge concerning the genus- and species-level taxonomy of these sauropods. Our findings imply that many referrals of incomplete diplodocid skeletons to *Apatosaurus* and *Diplodocus* must be reassessed. These reassessments are particularly important with regard to specimens from northern localities of the Morrison Formation, as it is becoming increasingly evident that diplodocids from this area were distinct from better-known, more southerly taxa. This geographic segregation does not seem to apply to nondiplodocid sauropods; however, these taxa are also in need of systematic revision, which may reveal species-level patterns similar to those observed in Diplodocidae.

INTRODUCTION

The Upper Jurassic Morrison Formation of the western United States preserves one of the best-studied Mesozoic terrestrial ecosystems. The formation has been explored for nearly 150 years and produced the first bones of sauropod dinosaurs in North America (Cope, 1877a). The richness and diversity of the Morrison Formation paleoecosystem is surprising, but was recognized early in the history of its study: many of the most familiar dinosaurs—animals such as *Stegosaurus* Marsh, 1877a, *Allosaurus* Marsh, 1877b, *Diplodocus* Marsh, 1878, and *Brontosaurus* Marsh, 1879—were found in these strata during the 1870s. However, although the dinosaur fauna of the formation seems to be well known, the majority of the remains are from outcrops in Colorado, Utah, and southern Wyoming. Only recently have more specimens, and sites, from more northerly exposures been excavated and described (Harris and Dodson, 2004; Schwarz et al., 2007; Tschopp and Mateus, 2013a, 2013b, 2017; Foth et al., 2015; Maidment et al., 2015, 2018; Woodruff and Foster, 2017; Maltese et al., 2018; Tschopp et al., 2018a; Woodruff et al., 2018). Many of these new finds from northern Wyoming and Montana cannot be confidently referred to any known species, and some have been designated as type specimens of new taxa. Due to the scarcity of data, however, it remains unclear whether these apparent faunal differences are temporal or geographic in nature.

In the past, Upper Jurassic outcrops in northern Wyoming and Montana have been explored by several institutions (e.g., the Howe Quarry excavated by the AMNH; see Brown, 1935, and a compilation of quarries is provided in Foster, 2003; fig. 1). However, specimens from these historical sites have rarely been formally described. The Red Fork of the Powder River (RFPR) locality of the Carnegie Museum is one such site.

Located on the east side of the Bighorn Mountains, about 20 km west of the town of Kaycee, Wyoming, RFPR was excavated in 1902 and 1903 by William H. Utterback and became important because it is the type locality of the diplodocine sauropod *Galeamopus hayi* (Holland, 1924). This

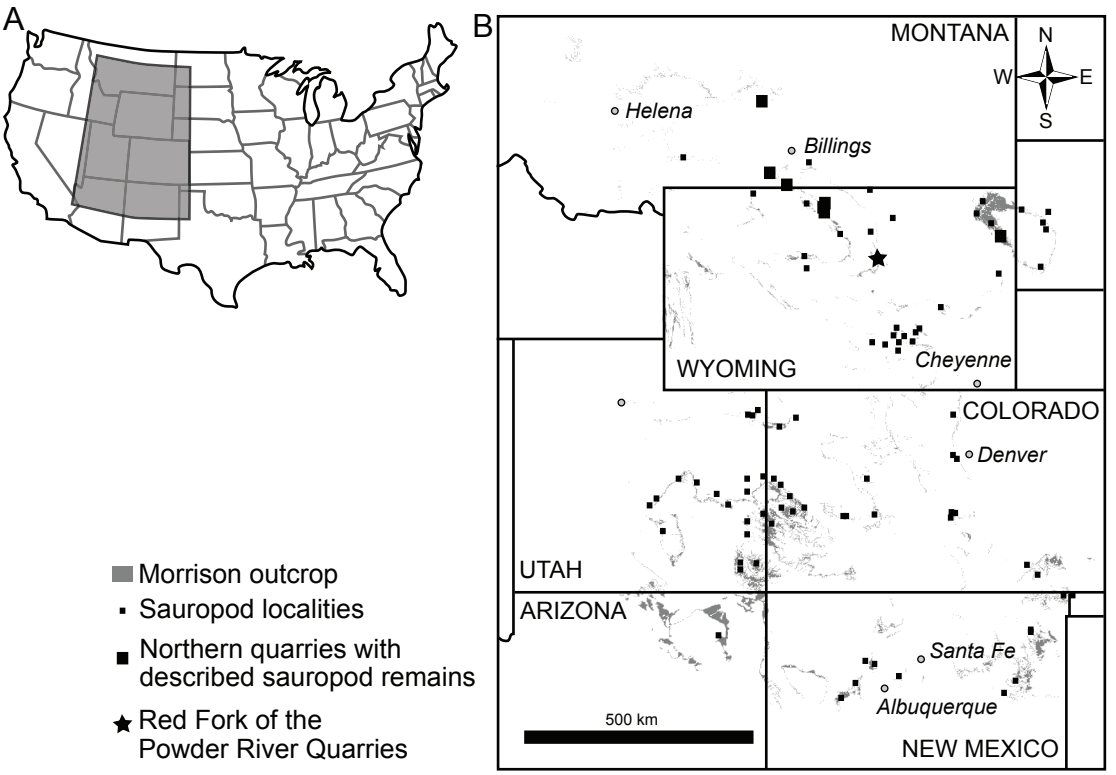

FIG. 1. Morrison Formation quarries that have produced sauropods. **A,** General area of the Morrison Formation depositional basin. **B,** Outcrops and single sauropod localities within the extent of the Morrison Formation. Note the fewer number of quarries in northern Wyoming and Montana compared with southern Wyoming, Colorado, and Utah.

species was initially assigned to *Diplodocus*, based on a fairly complete, associated specimen (HMNS 175, previously CM 662; Holland, 1924), and was recently referred to a new genus (Tschopp et al., 2015a). However, only the braincase, interclavicle, radius, and ulna of this specimen have been described (Hatcher, 1903; Holland, 1906, 1924; Tschopp and Mateus, 2013a). Other specimens from a second site at this locality were tentatively referred to the well-known genera *Apatosaurus*, *Camarasaurus*, *Diplodocus*, and *Haplocanthosaurus* (McIntosh, 1981; Wedel, 2001; Foster, 2003; Foster and Wedel, 2014). Here, we reassess the material from this second site (RFPR Quarry B) in order to more accurately map sauropod taxonomic distributions throughout the Morrison Formation.

History

After the successful excavation of the Carnegie Museum at Sheep Creek in Wyoming in 1899 and 1900, which resulted in the recovery and description of the new species *Diplodocus carnegii* Hatcher, 1901, "*Elosaurus*" *parvus* Peterson and Gilmore, 1902, and several other specimens (e.g., Hatcher, 1901, 1902, 1903; Peterson and Gilmore, 1902), the Carnegie Museum sent one of its employees, William H. Utterback, to Wyoming in April 1902. In late May, Utterback reached Wyoming but was delayed in Douglas due to heavy snow and poor road conditions. On June 5, he established his first camp on Crazy Woman Creek, approximately 32 km south of Buffalo, where he found outcrops similar to those in Cañon City, Colorado, where he had

worked for the Carnegie Museum at the Marsh-Felch Quarry the two years before. After 25 days of prospecting in the area, he finally made an apparently significant discovery and moved camp to the newly discovered site. In an unpublished letter to Carnegie Museum curator John B. Hatcher on June 28, 1902 (accessible at the Vertebrate Paleontology collections at CM), Utterback mentioned that there were at least a number of caudal vertebrae and limb bones, and that another skeleton was cropping out 300 feet from the specimen he planned to work on first. Most likely, that first skeleton is that which is now the holotype specimen of *Galeamopus hayi* HMNS 175 (previously CM 662; Holland, 1924; McIntosh, 1981; Tschopp et al., 2015a; Tschopp and Mateus, 2017). A few days later, he reported 16 caudal vertebrae, a sacrum, "a large number of limb bones as well other vert &c" (unpublished letter to Hatcher on July 3, 1902, Vertebrate Paleontology collections at CM). Utterback became increasingly demoralized by working alone and could find only inexperienced laborers in the area. In a letter dated September 20, 1902, he reported difficulties with removing overburden, which delayed his work. He also mentioned the first nights of temperatures below 0° C. Nonetheless, he managed to excavate "both ischia, another fibula a fine tibia, an astragalus, a great many vert of all kinds" and both scapulae. Utterback's reports on his finds were so promising that Hatcher mentioned the find to other museum curators, including Henry F. Osborn at the AMNH, who was apparently very jealous, and pushed his own field crew to find a similarly articulated sauropod (Brinkman, 2010). Before ending the excavation around October 10, 1902, Utterback unearthed more cervical and other vertebrae, plus a humerus, radius, ulna, and some foot bones. He did not manage to excavate the entire skeleton, estimating the time needed to do so was another six weeks to two months. Nevertheless, he sent a shipment of 22 boxes back to the Carnegie Museum, which arrived on November 15, 1902, and was accessioned under the number 2145 (CM Annual Reports, 1903). These boxes included 80 bones (suppl. table 1, available at https://doi.org/10.5531/sd.sp.36).

Utterback returned to the quarry on May 11, 1903, to continue excavation of the specimen that would become the holotype of *G. hayi*. Shortly after arrival, he reported that a Mr. Ross "of the University of Chicago is very anxious to learn the exact locality of our quarry," and he asked Hatcher to let him know if he heard anything about an expedition from Chicago to the area, because "there is a field just south of here that I want very much. Have been told of numerous finds down there" (unpublished letter to Hatcher on May 19, 1903, accessible at the Vertebrate Paleontology collections at CM). In his answer from May 26, 1903, Hatcher wrote that he did not know any Mr. Ross from Chicago, and suggested that Utterback "visit the localities some 15 to 20 miles to the south of your present location and spend a few days looking the ground over and locating any specimens you may think of value, leaving your name and the name of the Museum which you represent thereon." We currently do not know exactly where these localities may be, but it now seems clear that the mysterious "Mr. Ross" was actually Elmer S. Riggs from the Field Museum of Chicago, who was searching for new localities after his successful excavations near Fruita and Grand Junction, Colorado (Brinkman, 2010).

In a letter on June 1, 1903, Utterback first mentioned quarries A (which is now the type locality of *Galeamopus hayi*; Tschopp et al., 2015a) and B. With Quarry A showing signs of exhaustion, Utterback started to work on Quarry B (Brinkman, 2010). He described this site as "B or the lay out on the hill just above. It is I believe going to turn out some very fine bones." Just three days later, he already exposed "three ischia, two pubes, and about 15 vertebrae of different kinds as well as ribs &c."

Toward the end of June 1903, Utterback sent a sketch of the quarries (fig. 2) and mentioned the presence of possible *Stegosaurus* bones. The lists of the contents of the boxes contain a few mentions of "dorsal" or other

TABLE 1

Skeletal regions preserved in the sauropod genera from Red Fork of the Powder River Quarry B, as identified by McIntosh (1981)

Numbers indicate the minimum number of individuals based on overlapping specimens. Numbers with a question mark indicate questionable taxonomic identifications of the specimens representing a specific skeletal region (see text). Note that *Apatosaurus* and *Diplodocus* are represented by nonoverlapping skeletal regions. Also, four *Camarasaurus* individuals were previously identified based on pectoral girdle elements, but only three are confirmed in this study. Abbreviations: **acd,** anterior caudal vertebrae; **acv,** anterior cervical vertebrae; **adv,** anterior dorsal vertebrae; **bc,** braincase; **ch,** chevrons; **cr,** cervical ribs; **dr,** dorsal ribs; **fl,** forelimb; **fs,** facial skull; **hl,** hind limb; **lj,** lower jaw; **ma,** manus; **mcd,** midcaudal vertebrae; **mcv,** midcervical vertebrae; **mdv,** middorsal vertebrae; **pcd,** posterior caudal vertebrae; **pcg,** pectoral girdle; **pcv,** posterior cervical vertebrae; **pdv,** posterior dorsal vertebrae; **pe,** pes; **pvg,** pelvic girdle; **sv,** sacral vertebrae; **t,** teeth.

Taxon	fs	bc	lj	t	acv	mcv	pcv	cr	adv	mdv	pdv	dr	sv	acd	mcd	pcd	ch	pcg	fl	ma	pvg	hl	pe
Camarasaurus	–	–	1	–	1?	1?	–	–	1	1	–	1–2	–	2	1-2	1	2	3	2	1	3	2	–
Apatosaurus	–	–	–	–	–	–	–	–	–	–	–	–	–	1?	1?	–	–	–	2?	–	1?	–	1?
Diplodocus	–	–	–	–	–	–	–	–	1?	1?	–	–	–	–	–	1?	–	–	–	–	–	–	–
Haplocanthosaurus	–	–	–	–	–	–	–	–	–	–	–	–	–	–	1	–	–	–	–	–	–	–	–
not mentioned	–	–	–	–	–	–	–	–	–	–	1?	–	–	–	–	–	–	–	–	–	–	–	–

"plates" (suppl. table 1, available at https://doi.org/10.5531/sd.sp.36), but no *Stegosaurus* elements could be identified among the material later, and some of these plates turned out to be sternal plates (e.g., field number 198, which is part of the specimen CM 21775; McIntosh, 1981; E.T., personal obs., 2017). About a month later, Utterback reported some disappointment regarding the quality of the skeletons and was planning to give up the quarry soon thereafter. He also mentioned that Barnum Brown from the AMNH visited the quarry while searching for a new site in the Upper Jurassic. Utterback showed Brown the second site, as reported in field correspondence from Brown to Osborn (AMNH VPA 14, Box 2, Folder 13). In his letter, Brown also mentioned *Stegosaurus* as well as *Haplocanthus* (now *Haplocanthosaurus*; Hatcher, 1903), but also noted the relatively poor, crushed state of the bones, which was not as good as in the Beauvais Creek locality in Montana, where Brown was working at the time. Utterback quit work on Quarry B on August 11, 1903, but from his accounts in the letters to Hatcher, it seems plausible that he did not entirely exploit the bone layer. A total of 226 bones were sent back to Pittsburgh in 29 boxes that year, including 29 additional elements from Quarry A, and the rest from Quarry B (suppl. table 1, available at https://doi.org/10.5531/sd.sp.36). The boxes arrived at CM on November 18, 1903, and were accessioned under the number 2395 (CM Annual Reports 1904).

During a prospecting trip to the same sites in 2005 by one of us (E.T.) under the lead of Hans-Jakob Siber of the Sauriermuseum Aathal, Switzerland, some bones were located but not excavated. The land is owned privately, and we do not know of any other institution or private entity that has ever returned to further excavate Quarry B, although several people seem to have rediscovered it at least approximately (J. Foster, personal commun., 2019), and other sites close by have been worked by private collectors in recent years.

Geology

The Morrison Formation comprises a series of terrestrial sediments deposited in a broad, shallow basin that extended from New Mexico in the south to Montana in the north over a period of approximately eight million years during the Late Jurassic (Trujillo and Kowallis, 2015). The sediments comprise the deposits of distributive fluvial systems, including channel sandstones, which were especially well developed in the south of the area, but are less extensive in northern Wyoming (Owen et al., 2015, 2017), and accompanying overbank deposits. These latter sediments comprise varicolored siltstones with variably developed paleosol horizons (e.g., Demko et al., 2004) and gray lacustrine silts and limestones (Turner and Fishman, 1991; Dunagan, 1999; Dunagan and Turner, 2004).

The Red Fork of the Powder River quarries are located on the eastern side of the Bighorn Mountains, within the Powder River Basin. If Utterback's quarry sketch is accurate, quarries A and B are from the same stratigraphic level around a small hill (fig. 2). Quarry B appears to have been about 100 m northwest of Quarry A (according to Utterback's letter from June 28, 1902, and his quarry sketch). Sedimentological sections were not logged during the original excavations, nor during the prospecting trip in 2005, so the detailed sedimentology of the quarries themselves remains unknown. Turner and Peterson (1999) logged a section 50 km to the north at the Poison Creek quarries, also within the Powder River Basin. Here, remains of theropods, sauropods, and ornithischians were discovered (Turner and Peterson, 1999; Tucker, 2011; Erickson, 2014). At Poison Creek, the Morrison Formation appears to conformably overlie marine deposits of the Sundance Formation, as it does across the Bighorn Basin and in the Black Hills area. It is therefore likely that this applies to the area around the Red Fork of the Powder River as well. Marginal marine deposits of the Windy Hill Member (also named Windy Hill Sandstone Member in some publications; was

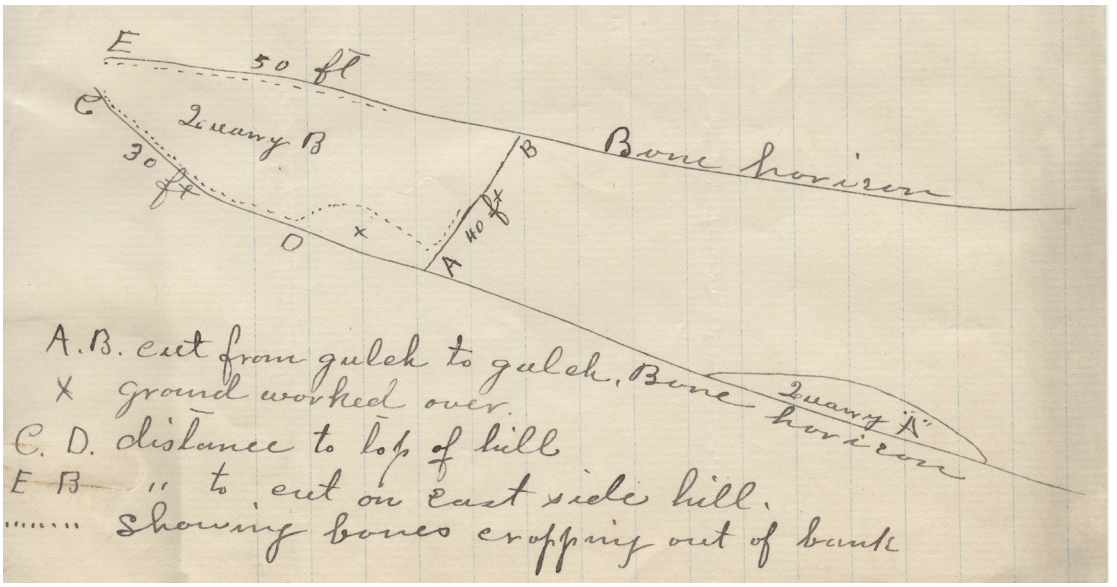

FIG. 2. Sketch of the location of the two quarries at the Red Fork of the Powder River (RFPR) showing that both lie in the same bone-bearing layer. Drawn by W. Utterback in 1903 and sent to J.B. Hatcher on June 30, 1903. No other historic drawings or charts relating to these RFPR quarries could be found at CM.

reassigned from the Sundance to the Morrison Formation by Peterson, 1994) were identified at the base of the Poison Creek section. The Windy Hill Member is overlain by silts with calcareous nodules in the lower parts, and occasional channel sandstones. The Poison Creek section, including the Windy Hill Member, is about 60 m thick.

Ostrom (1970) logged many sections of the Morrison and Cloverly formations in the Bighorn Basin and correlated them across the area. He recognized three units of the Morrison Formation, informally described as units I, II, and III. Units I and III are characterized by drab yellowish-gray-green silty mudstones, whereas unit II comprises 6 to 23 m of white to buff, massive to cross-laminated sandstone. Based on the stratigraphy of Ostrom (1970), at Poison Creek, unit I is represented by silts with calcareous nodules, unit II by a 5–6 m thick sandstone, which was the stratigraphic location of the Poison Creek quarries (Turner and Peterson, 1999), and unit III by the overlying siltstones, which Turner and Peterson (1999) identified as smectite rich based on their field character.

Unfortunately, correlation of the terrestrial deposits of the Morrison Formation across the Morrison basin has proven extremely difficult. Turner and Peterson (1999) attempted to correlate across the formation based on the "clay change," a purported change from ilitic clays in the lower part of the formation to smectitic clays in the upper parts; however, this alleged clay change has subsequently been disproven (Jennings and Hasiotis, 2006; Trujillo, 2006) and its resultant correlations must therefore be disregarded. A single radiometric date has been reported from the Morrison Formation of the Bighorn Basin (Kvale et al., 2001); Kvale et al. (2001) recovered a date of 151.5 ±4 Ma from the base of the formation at the Red Gulch dinosaur tracksite, near the community of Shell, 150 km northwest of the Red Fork of the Powder River quarries. The very large error bars on this date prevent it from being useful for correlative purposes. Mudstones from the Red Canyon Ranch Quarry, also near Shell, were investigated for radiometric dating twice, but primary zircons could not be recovered in any of the samples (Maidment et al., 2015; M.C.L., personal obs., 2017).

In Utah, where the sedimentology of the Morrison Formation has been best documented, deposits comprise thick channel sandstones of the Salt Wash and Vernal distributive fluvial systems (Owen et al., 2015, 2017). These are overlain by a thick sequence of gray, smectitic mudstones, with varicolored mudstones and isolated channel sand bodies in their upper parts (e.g., Turner and Peterson, 1999; Maidment et al., 2017). Because the Sundance Sea regressed to the north, it is likely that the base of the Morrison Formation is time transgressive, and the deposits at the base of the formation in the south are contemporaneous with shallow marine deposits of the Sundance Formation farther north in the basin. Furthermore, the sedimentological characteristics of the sediments in the upper part of the sections to the south are similar to those in the Bighorn Basin (Maidment, unpubl. data). Thus, it is likely that the Morrison Formation of the Bighorn Basin is broadly correlative with the upper parts of this formation in Utah and western Colorado (Maidment, unpubl. data). Radiometric dates for the upper part of the Morrison in Utah and western Colorado (Trujillo and Kowallis, 2015) all indicate a Tithonian age, and thus it is likely that the RFPR sauropods are also Tithonian in age. It is not possible to determine in which of Ostrom's (1970) units the quarries are located, because no stratigraphic section of the RFPR site exists.

Fauna

The CM Vertebrate Paleontology specimen database and McIntosh's (1981) catalog of the museum's nonavian dinosaur collection list the macronarian *Camarasaurus* and the diplodocoids *Apatosaurus*, *Diplodocus*, and *Haplocanthosaurus* as sauropods from RFPR. Additionally, a single caudal vertebra of *Allosaurus fragilis* (CM 36037) was recovered from the site. No nonsauropod herbivorous dinosaur taxon or additional theropod material was reported by McIntosh (1981), or could be found in the CM collections, even though both Utterback and Brown mentioned *Stegosaurus* in letters to their respective institutions (see above). Foster (2003) counted the minimum number of individuals in RFPR Quarry B as one *Allosaurus*, three adult and one juvenile *Camarasaurus*, one *Apatosaurus*, one *Diplodocus*, and one *Haplocanthosaurus*. However, *Diplodocus* and *Apatosaurus* are represented by nonoverlapping skeletal regions, and *Haplocanthosaurus* by a single specimen that consists of two anterior caudal vertebrae (table 1). The supposed *Diplodocus* is known from anterior dorsal, middorsal, and posterior to distal caudal vertebrae (following the terminology proposed by Tschopp et al., 2015a), whereas *Apatosaurus* is represented by anterior and midcaudal vertebrae and appendicular elements. Given that the recently erected diplodocid genus *Galeamopus*, which includes the species "*Diplodocus*" *hayi* known from RFPR Quarry A, has rather *Diplodocus*-like presacral vertebrae, but more *Apatosaurus*-like anterior and midcaudal vertebrae and limb elements (McIntosh, 1990a; Tschopp and Mateus, 2017), the specimens from RFPR Quarry B referred to *Diplodocus* and *Apatosaurus* may have been incorrectly identified. We reassess these referrals in the light of these more recent discoveries.

Institutional Abbreviations

AMNH FARB American Museum of Natural History, New York
BYU Museum of Paleontology, Brigham Young University, Provo, Utah
CM Carnegie Museum of Natural History, Pittsburgh, Pennsylvania
CMC Cincinnati Museum Center, Cincinnati, Ohio
FHPR Utah Field House of Natural History Museum, Vernal, Utah
GMNH Gunma Museum of Natural History, Tomioka, Japan
HMNS Houston Museum of Natural Science, Houston, Texas
LACM Natural History Museum of Los Angeles County, Los Angeles, California
MB.R. Museum für Naturkunde, Berlin, Germany
MIGM Museu Geológico do Instituto Geológico e Mineiro, Lisbon, Portugal

NSMT-PV National Science Museum, Tokyo, Japan
OMNH Sam Noble Museum, Norman, Oklahoma
SMA Sauriermuseum Aathal, Switzerland
TMP Royal Tyrrell Museum of Palaeontology, Drumheller, Canada
USNM National Museum of Natural History, Smithsonian Institution, Washington, D.C.
WDC Wyoming Dinosaur Center, Thermopolis, Wyoming
YPM Yale Peabody Museum of Natural History, New Haven, Connecticut

MATERIAL

The recovered material from RFPR Quarry A includes a semiarticulated, relatively complete skeleton that became the type specimen of *Galeamopus hayi* (originally CM 662, now HMNS 175; Holland, 1924; Tschopp et al., 2015a). This specimen has a complex history of ownership and curation (McIntosh, 1981). The skeleton, except the interclavicle (Tschopp and Mateus, 2013a) and possibly two dorsal vertebral neural arches and the left femur, was sent to the Cleveland Museum of Natural History in 1956. Once in Cleveland, the specimen was cataloged as CMNH 10670. According to McIntosh (1981: 20), a complete left femur and another fragmentary left femur, both cataloged as CM 94 (the paratype of *Diplodocus carnegii*, from Sheep Creek in Albany County, Wyoming), along with six caudal vertebrae of CM 94, were transferred to Cleveland to supplement CM 662/CMNH 10670. In his comments on CM 662, McIntosh (1981: 21) did not mention a femur where he listed the elements of the skeleton, but he also stated that "the left femur was not transferred to Cleveland . . . and its current whereabouts are unknown." Other than in this comment, neither McIntosh (1981) nor the CM Vertebrate Paleontology collection database explicitly mention a femur found with the skeleton of CM 662, although Utterback did mention a "very fine femur" in a letter to Hatcher dated October 1, 1902, and a femur is mentioned under the field number 73 in the contents of the accessioned boxes from RFPR Quarry A (suppl. table 1, available at https://doi.org/10.5531/sd.sp.36). Assuming it actually existed, the current whereabouts of this femur remain unclear, but according to a note from McIntosh ("*Diplodocus*, *Barosaurus*, *Amphicoelias*, Houston 662" notebook, p. 55; and "Book 17," p. 111; stored at the BYU Museum of Paleontology), it may be possible that the original left femur of CM 662 was erroneously labeled 1255 at some point during preparation. CM 1255 was initially applied to as yet unidentified material from Quarry N, Freezeout Hills (Carbon County, Wyoming), which was excavated during the same time as the RFPR quarries by Charles W. Gilmore (Brinkman, 2010). Preparation and curation of the specimens from Freezeout Hills likely also happened at about the same time as the material from RFPR, the unidentified elements of which received the general number CM 1256 (see below). The similar catalog number and likely contemporaneous excavation and curation of material from the two sites make it seem possible that elements could have been mixed up, and that the left femur excavated with the remainder of CM 662 was indeed mislabeled as CM 1255.

The move of CM 662 to Cleveland was apparently done upon the instruction of the Director of Carnegie Museum at the time, Graham Netting, who told J. LeRoy Kay, then Head of Vertebrate Paleontology at CM, to sell, trade, or give away dinosaur specimens, because there was no adequate storage room to house them, and also to "share the wealth." We do not know whether the specimen was ever mounted at CMNH, but given the timeframe it was there, this seems unlikely. Cleveland later sold the skeleton to the Houston Museum of Natural Science for $15,000 (A. McGee, personal commun., 2019), where it was cataloged as HMNS 175 (the reasons for and exact date of this transaction are not known to us). The specimen was first mounted at HMNS in 1975 and restored and remounted between 2013 and 2015. It is supplemented with a left femur originally cata-

loged as CM 94 and casts and models for other lacking elements. Of the material that remained at CM, the two dorsal neural arches are labeled both as CM 662 and CM 1256 on opposite sides of the bones, with the first of these specimens being from RFPR Quarry A, and the second from RFPR Quarry B (McIntosh, 1981). These partial vertebrae were later recataloged as CM 36041, and according to McIntosh (1981), it is more likely they came from Quarry B. In early 2019, a chevron marked "662" (in writing very similar or identical to that used in the CM Vertebrate Paleontology collection decades ago to mark specimen numbers on the specimens themselves) was found among the items of the late John S. McIntosh left to Daniel Chure, and donated by Chure to CM. Who gave this chevron to McIntosh and when and why it was given remains a mystery to us, as does the reason why not all bones of CM 662 were transferred to CMNH and later HMNS.

RFPR Quarry B, in contrast, produced numerous, mostly disarticulated sauropod dinosaur bones, plus a single theropod caudal vertebra (McIntosh, 1981; Foster, 2003). Here, we provide the first description of the RFPR Quarry B sauropod material, including the dorsal neural arches that potentially belong to CM 662. A complete list of sauropod specimens from both RFPR quarries is given in supplementary table 2 (available at https://doi.org/10.5531/sd.sp.36).

Much of the material from Quarry B, on which our study focuses, was initially cataloged as CM 1256, which was used as a general specimen number for prepared but unidentified material from the site (McIntosh, 1981). It is possible that this number was erroneously applied to the two dorsal neural arches that may belong to CM 662 as well. Most of the bones initially cataloged as CM 1256 have since been recataloged and given other specimen numbers (suppl. table 2, available at https://doi.org/10.5531/sd.sp.36; McIntosh, 1981), but some remained numbered as CM 1256 until recently. A few more of these specimens were recataloged as a result of the present reassessment.

There is significant difference in preservation among bones from RFPR Quarry B. Some are heavily deformed and crushed, whereas others are well preserved. A more detailed assessment of preservation is provided in the descriptions of the individual specimens below.

METHODS

Identification of the Material

Most specimens from RFPR Quarry B are fragmentary and incomplete. Other than Utterback's letters and rough sketch depicting the location of the two quarries, no documentation exists concerning the arrangement and articulation of bones. Some of the elements bear numbers that correspond to field numbers, but additional information could not be located at CM, and might never have been produced by Utterback. We therefore rely heavily on the attributions of elements to single specimens as reported by McIntosh (1981), with some modifications as outlined below. Given these issues, and the resulting incompleteness of the specimens, we refrain from including these fossils in a phylogenetic analysis. Instead, we apply an apomorphy-based identification where possible or detailed comparisons with existing Morrison Formation sauropod taxa if no apomorphy is known for any bone of a specific specimen. In so doing, we do not exclude the possibility that specimens that cannot be confidently identified at this point may eventually prove referable to presently unrecognized species.

The approach outlined above is relatively effective for Diplodocoidea thanks to recent revisions of the interrelationships of these sauropods and thus detailed knowledge of character distributions within the clade (Whitlock, 2011a; Mannion et al., 2012; Tschopp et al., 2015a; Tschopp and Mateus, 2017). On the contrary, the taxonomy of the early-branching macronarian *Camarasaurus* remains problematic. Four species are considered valid by most researchers (*C. supremus*, *C. grandis*, *C. lentus*,

and *C. lewisi*; McIntosh et al., 1996a, 1996b; Ikejiri et al., 2005; Woodruff and Foster, 2017); however, preliminary analyses indicate that more species could have been present (Tschopp et al., 2014), and that one—*Camarasaurus lewisi*—may even constitute a distinct genus, *Cathetosaurus*, as was originally proposed (Jensen, 1988; Mateus and Tschopp, 2013). Given that both character distributions and taxonomy within this clade remain to be resolved, we prefer to refer specimens that cannot be attributed to a particular species to Camarasauridae indet. instead of *Camarasaurus*.

A similar issue exists with *Haplocanthosaurus*. Two species are currently considered valid: *H. priscus* and *H. delfsi*. Very few phylogenetic analyses include both species (Calvo and Salgado, 1995; Gallina and Apesteguía, 2005; Mannion et al., 2019). In all but one analysis of Mannion et al. (2019; using an equal-weighting approach), the two species do not form a monophyletic clade (including a second analysis of Mannion et al., 2019, that used extended implied weighting). Both *Haplocanthosaurus* species have frequently been recovered within Diplodocoidea (Whitlock, 2011a; Mannion et al., 2012, 2019; Tschopp et al., 2015a), though they are also commonly positioned within Macronaria (Gallina and Apesteguía, 2005; Carballido et al., 2012; Royo-Torres et al., 2017). Of the few analyses that identify apomorphic features, none list any in the caudal vertebrae or chevrons. Given that the only specimen from RFPR referred to *Haplocanthosaurus* to date consists of two caudal vertebrae, a detailed systematic assessment of this (and other) material remains difficult (see also Foster and Wedel, 2014).

Terminology

The description of the RFPR bones follows the terminology for vertebral laminae and fossae proposed by Wilson (1999, 2012) and Wilson et al. (2011), respectively, with changes proposed by Tschopp and Mateus (2013b) and Carballido and Sander (2014). We prefer the directional terms *anterior* and *posterior* over *cranial* and *caudal*, respectively, following Wilson (2006). As in Tschopp and Mateus (2017), we describe the scapulocoracoid and the ischium as if they were oriented horizontally, the pubis as if oriented vertically, and the manus and pes as if the metapodials formed a straight line perpendicular to the axial series instead of being arched.

SYSTEMATIC PALEONTOLOGY

Sauropoda Marsh, 1878

Neosauropoda Bonaparte, 1986

Diplodocoidea Marsh, 1884

Flagellicaudata Harris and Dodson, 2004

Diplodocidae Marsh, 1884

Diplodocinae Marsh, 1884

Galeamopus Tschopp, Mateus, and Benson, 2015a

Galeamopus sp.

Referred Specimens: The specimens referable to *Galeamopus* from RFPR Quarry B comprise four nearly complete cervical vertebrae and fragments of a fifth (CM 36039), possibly two articulated dorsal vertebral arches (CM 36041, see above), and two caudal vertebrae (CM 36035). They may or may not be from a single individual. CM 36039 consists of four midcervical vertebrae and likely part of a fifth that is associated with the largest of the four elements (fig. 3; table 2). At least three of the four elements and the associated fragment appear to form a continuous series (fig. 3A–I). The fourth might not actually belong to the same taxon (fig. 3J–L; see below). The cervical vertebrae CM 36039 are identified as midcervical elements due to their centrum elongation and neural spine morphology. The three relatively complete, sequential elements most closely resemble cervical vertebrae 5–7 of

TABLE 2

Measurements of vertebrae referred to *Galeamopus* sp. from RFPR Quarry B (in mm)

	CM 36039				CM 36035	
	Cervical vertebra A[1]	Cervical vertebra B[2]	Cervical vertebra C[3]	Cervical vertebra D[4]	Midcaudal vertebra A[5]	Midcaudal vertebra B[6]
Centrum length	330	365	425	245	199	188
Centrum length without anterior condyle (functional length)	275	329	385	198		
Posterior cotyle dorsoventral height	83	93	91	96	119	103
Posterior cotyle transverse width	61	81		83	107	102
Neural arch dorsoventral height	200					
Neural spine dorsoventral height (without pedicel)	113					
Pedicel dorsoventral height	109					
Dorsoventral height (total)						201
Elongation index (sensu Wilson and Sereno, 1998)	3.98	3.92	4.67	2.55	1.86	1.84
Average elongation index (sensu Chure et al., 2010)	4.58	4.2		2.74	1.76	1.83

[1] Most complete, field number 213 (see fig. 3A–C).
[2] Lacking part of neural spine (see fig. 3D–F).
[3] In matrix with associated fragment, lacks part of neural spine (see fig. 3G–I).
[4] Shortest cervical vertebra, lacks part of neural spine (see fig. 3J–K).
[5] Lacking spine (not figured).
[6] Nearly complete (see fig. 5).

Galeamopus pabsti SMA 0011 (see description below). CM 36041 comprises two articulated dorsal vertebrae (fig. 4). Only the neural arches are preserved, so no meaningful measurements could be taken. These vertebrae were initially labeled as CM 1256, and subsequently relabeled as CM 662 (based on the whiter color of the latter number) and then CM 36041. According to McIntosh (1981), this specimen also includes a partial anterior caudal vertebra that could not be located in the CM collection in December 2017. It is possible that that specimen is actually the partially prepared posterior dorsal vertebra currently cataloged as CM 36282, which was not mentioned by McIntosh (1981). Specimen CM 36035 consists of two midcaudal vertebrae. One is complete (fig. 5) whereas the other lacks parts of the neural spine.

Description

Cervical Vertebrae: The cervical vertebrae CM 36039 have relatively elongate centra (table 2) with well-developed pleurocoels, which are subdivided into an anterior and a posterior pneumatic fossa by an oblique lamina. Posteroventral to the main pleurocoel there is an additional, distinct fossa. The ventral surface bears a midline keel that is not strongly developed and that is located only in the anterior half of the surface. There are no pneumatic openings lateral to the ventral keel. A ventral sulcus is present and formed in part by distinct posteroventral flanges. Close investigation of the median wall indicates that an opening in this wall was likely present but not recognized as an authentic feature and therefore filled during original preparation.

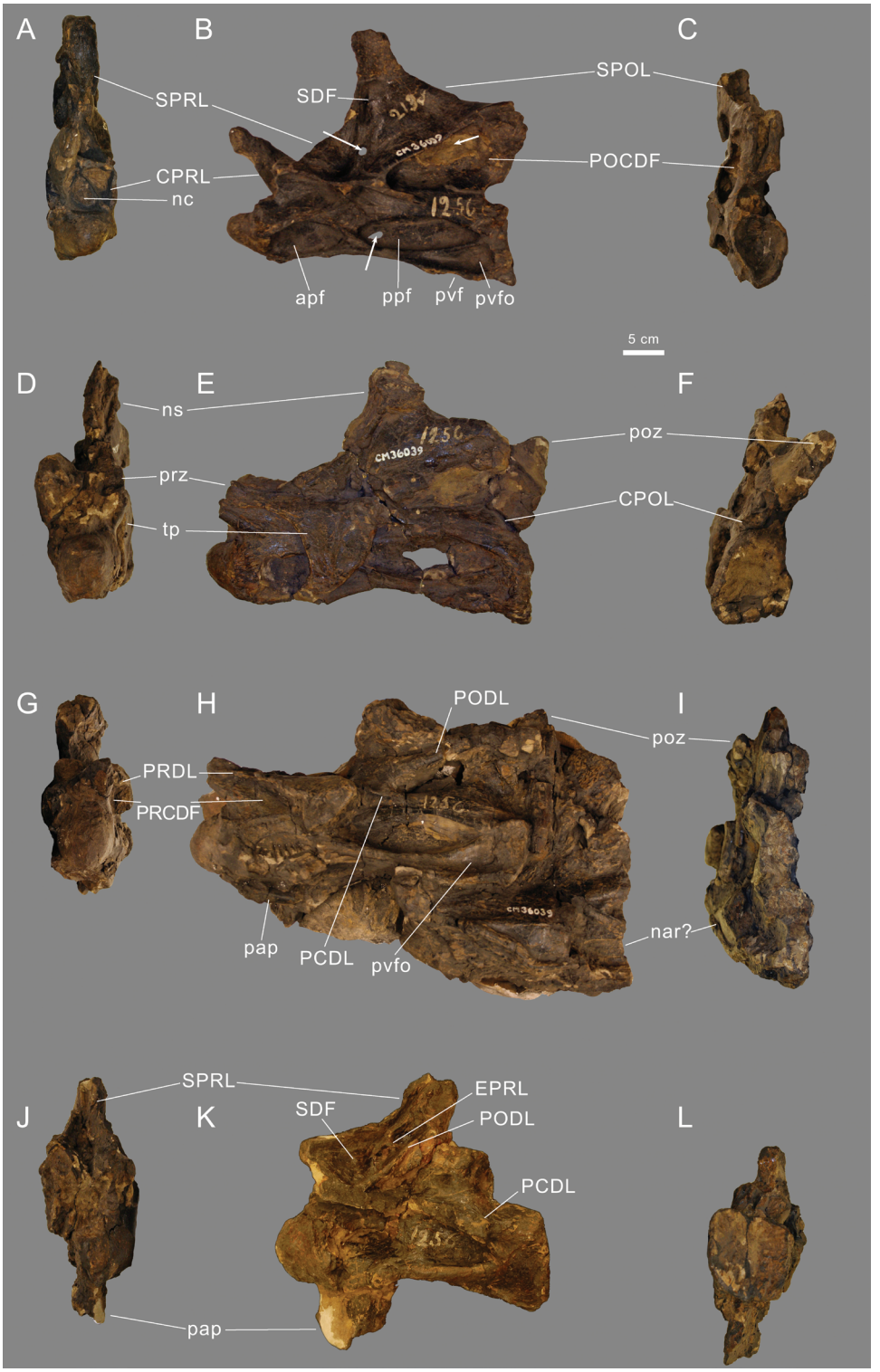
A
B
C
SPRL
SDF
SPOL
CPRL
nc
POCDF
apf
ppf
pvf
pvfo
5 cm
D
E
F
ns
poz
prz
CPOL
tp
G
H
I
PODL
poz
PRDL
PRCDF
pap
PCDL
pvfo
nar?
J
K
L
SPRL
EPRL
SDF
PODL
PCDL
pap

The neural spine is tall and vertically oriented. Spinal bifurcation can be observed in one vertebra of CM 36039, even though the spine is incomplete (fig. 3G–I). Elements with a complete neural spine are not bifurcated, indicating that the series represents the transition from single to bifid neural spines, which usually occurs among midcervical vertebrae (Wedel and Taylor, 2013; Tschopp et al., 2015a). The prezygapophyses are supported by centroprezygapophyseal laminae (CPRLs) that bifurcate dorsally. A pre-epipophysis occurs below the prezygapophyseal facets, which are mediolaterally convex. The transverse processes project laterally and do not bear any distinct, pointed posterior projection. There is a posteriorly facing vertical accessory lamina in the postzygapophyseal centrodiapophyseal fossa (POCDF). One vertebra has an opening in the spinodiapophyseal fossa (SDF), such that the left and right SDF communicate (fig. 3B). This opening is located somewhat anterior to the central portion of the fossa, but it is unclear whether this opening results from damage. The edges are rounded, but the bone here is extremely thin, making it difficult to determine whether the bone surface is complete. Indeed, interpretation of this feature remains contentious among the two of us (E.T. and M.C.L.) who have personally studied the specimen. E. Tschopp interprets the feature as a true opening, also based on the fact that *Galeamopus* generally has very strongly developed pneumaticity in cervical vertebrae, including additional openings connecting the left and right pleurocoels and the POCDF and the spinopostzygapophyseal fossa (SPOF) (Tschopp and Mateus, 2017). M. Lamanna instead interprets it as damage, partially based on the fact that no other sauropod specimen has yet been reported that has such an opening. CT scans of the vertebrae or new finds might help to solve the issue in future. Just dorsal to the opening, there is a distinct, dorsoventrally elongate subfossa. An additional opening occurs in the median wall of the POCDF, which communicates with the SPOF. The single neural spines are laterally expanded below the spine summit, and the lateral surface of the summit (above the SDF) is rugose. There is a prespinal lamina (PRSL) at the base of the spine that bifurcates dorsally, with the two branches connecting to the spinoprezygapophyseal laminae (SPRLs). The SPRL and the spinopostzygapophyseal lamina (SPOL) project anteriorly and posteriorly, respectively, and partially roof the spinoprezygapophyseal fossa (SPRF) and SPOF dorsally.

A fourth, partial cervical vertebra of CM 36039 (fig. 3J–L) has a shorter centrum than the other three (table 2) and pleurocoels that are more anteriorly restricted. The centrum is slightly curved in lateral view. It has well-developed parapophyses that project ventrolaterally. The posterior centrodiapophyseal lamina (PCDL) extends below the neural canal, but this is mostly due to the relatively long distance between the neural arch pedicels and the posterior edge of the centrum. The postzygodiapophy-

FIG. 3. Cervical vertebrae CM 36039, from RFPR Quarry B, referred to *Galeamopus* sp. Midcervical vertebrae in **A, D, G, J,** anterior, **B, E, H, K,** left lateral, and **C, F, I, L,** posterior views. Note the openings in the posterior pneumatic fossa, the SDF, and the POCDF in B (arrows). Scale bar applies to all vertebrae. These vertebrae were initially cataloged as CM 1256 and later recataloged as CM 36039. The number 213 corresponds to a field number. The mid- to posterior cervical vertebra in J–L may be referable to Camarasauridae indet. Abbreviations: **apf,** anterior pneumatic fossa; **CPOL,** centropostzygapophyseal lamina; **CPRL,** centroprezygapophyseal lamina; **EPRL,** epipophyseal-prezygapophyseal lamina; **nar,** neural arch; **nc,** neural canal; **ns,** neural spine; **pap,** parapophysis; **PCDL,** posterior centrodiapophyseal lamina; **POCDF,** postzygapophyseal centrodiapophyseal fossa; **PODL,** postzygodiapophyseal lamina; **poz,** postzygapophysis; **ppf,** posterior pneumatic fossa; **PRCDF,** prezygapophyseal centrodiapophyseal fossa; **PRDL,** prezygodiapophyseal lamina; **prz,** prezygapophysis; **pvf,** posteroventral flanges; **pvfo,** posteroventral fossa; **SDF,** spinodiapophyseal fossa; **SPOL,** spinopostzygapophyseal lamina; **SPRL,** spinoprezygapophyseal lamina; **tp,** transverse process. Photos by Andrew McAfee (A–J, L) and E.T. (K).

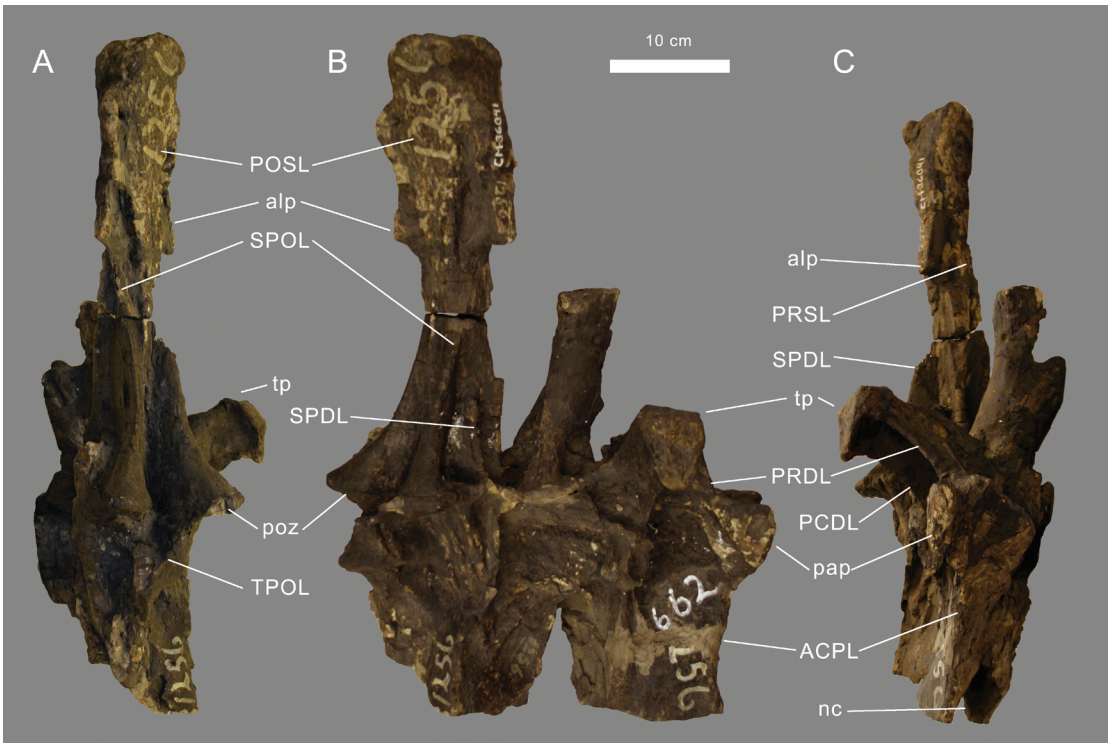

FIG. 4. Dorsal vertebral arches CM 36041 from RFPR Quarry B (?) referred to *Galeamopus* sp. Two articulated mid- to posterior neural arches in **A,** posterior; **B,** right lateral; and **C,** anterior views. Scale applies to all views. These vertebrae were initially cataloged as CM 1256, then numbered as CM 662 (possibly erroneously, see text), and finally recataloged as CM 36041. Abbreviations: **ACPL,** anterior centroparapophyseal lamina; **alp,** aliform process; **nc,** neural canal; **pap,** parapophysis; **PCDL,** posterior centrodiapophyseal lamina; **POSL,** postspinal lamina; **poz,** postzygapophysis; **PRDL,** prezygodiapophyseal lamina; **PRSL,** prespinal lamina; **SPDL,** spinodiapophyseal lamina; **SPOL,** spinopostzygapophyseal lamina; **tp,** transverse process; **TPOL,** interpostzygapophyseal lamina. Photos by Andrew McAfee.

seal lamina (PODL) is very steep and reaches close to the SPRL, resulting in an anteroposteriorly short SDF. The two laminae are connected by a short but distinct epipophyseal-prezygapophyseal lamina (EPRL).

Dorsal Vertebrae: The dorsal neural arches of CM 36041 bear only weak lateral lamination (fig. 4). The parapophysis lies nearly at the level of the prezygapophyses, slightly anteroventral to the prezygapophyseal facet. One anterior centroparapophyseal lamina (ACPL), two posterior centroparapophyseal laminae (PCPLs), and one PCDL can be identified. Two centropostzygapophyseal laminae (CPOL) extend dorsomedially and unite just below the hyposphene. An additional lamina extends from the hyposphene ventrolaterally to the PCDL. Two more laminae connect the postzygapophyses with the PCDL. The transverse process is almost horizontal, with a distinctly separated lateral articular surface. A dorsal bump or spur is not present. The articular surface is subtriangular with a horizontal dorsal margin, a nearly vertical anterior margin, and an oblique posteroventral edge. Above the transverse process, there is a distinct prezygodiapophyseal lamina (PRDL), a single spinodiapophyseal lamina (SPDL), and a PODL. In the more anterior of the two articulated vertebrae the PODL bifurcates posteriorly, but only on

FIG. 5. Midcaudal vertebra CM 36035 from RFPR Quarry B referred to *Galeamopus* sp. in **A,** anterior; **B,** left lateral; and **C,** posterior views. Note that the apex of the neural spine is damaged. Scale applies to all views. This vertebra was initially cataloged as CM 1256 and later recataloged as CM 36035. Abbreviations: **lr,** lateral ridge; **poz,** postzygapophysis; **prz,** prezygapophysis; **vlr,** ventrolateral ridge. Photos by Andrew McAfee (A, C) and E.T. (B).

the right side. The prezygapophyses are straight with the facets facing dorsomedially. The two facets form an angle of about 100° in anterior view. There is a distinct SPRL that connects almost to the facet. The postzygapophyses of the second vertebra are slightly concave and less inclined than the prezygapophyses of the first element. The hyposphene is very robust and widely expanded ventrally. Its posterior surface is relatively flat. The SPOL are not divided ventrally, and there is no separation into a medial and a lateral SPOL dorsally. The neural spine remains vertical at its base and has subparallel anterior and posterior margins in lateral view. There are distinct aliform processes that render the spine wider than long. The SPDL unites with the SPOL below these processes, whereas the SPRL connects to the aliform processes just above their ventralmost point. The aliform processes do not reach the width across the postzygapophyses, and do not extend to the spine summit, such that the spine tapers slightly at its dorsal end. The PRSL and postspinal lamina (POSL) are weakly developed at the base of the spine, but form a distinct, triangular, rugose scar that widens into a rounded end toward the summit. The spine summit is rounded in anterior and posterior view, without any indication of a notch. An indistinct, vertical groove that extends along the midline of both the PRSL and POSL might indicate that the scar starts to form in a lateral to medial direction.

Caudal Vertebrae: The caudal centra of CM 36035 are amphicoelous, with rounded articular surfaces in anterior and posterior view. The centra are relatively elongate, being 1.7–1.8 times as long as dorsoventrally high at their posterior cotyle (table 2). Both ventrolateral and dorsolateral ridges extend horizontally along the centrum. There is no ventral hollow, and the ventral surface is gently concave in lateral view. The neural arch pedicels occupy more than half of the centrum and are located above its central portion. The neural arch is relatively low. Neither the pre- nor the postzygapophyses exceed the centrum anteriorly or posteriorly, respectively, but the neural spine summit probably did overhang the posterior articular surface of the centrum (it is broken in both specimens). The neural spine is strongly inclined posteriorly and does not project much above the postzygapophyses.

Identification

McIntosh (1981) and Wedel (2001) referred the cervical vertebrae CM 36039 to *Camarasaurus*, but McIntosh later corrected himself in an email to M. Lamanna, changing his identification to *Diplodocus* (J.S. McIntosh, personal commun., 2005). Whereas an identification as *Camarasaurus* could actually be correct for the fourth, less elongate vertebra (fig. 3J–L; see below), the other three cervical vertebrae and the fragmentary vertebra are clearly diplodocine, and share apomorphic features with *Galeamopus* (a genus that was not known at the time of McIntosh's email). The presence of a posteroventral fossa on the lateral side, the dorsally bifurcated CPRL, and the convex prezygapophyses are all synapomorphies of Diplodocinae (Whitlock, 2011a; Tschopp et al., 2015a). Within Diplodocinae, the opening connecting the POCDF and the SPOF is currently known only in *Galeamopus* (Tschopp and Mateus, 2017). Additionally, the neural spines of CM 36039 are dorsoventrally very tall compared with all other known diplodocine genera. We therefore refer at least the three elongate cervical vertebrae and the associated fragment to *Galeamopus* sp.

The dorsal vertebrae CM 36041 were referred by McIntosh (1981) to *Diplodocus hayi*, probably in part because they were labeled as CM 662 in the past, and they could be the two dorsal neural arches that were never transferred to Cleveland and Houston (although this remains unclear; see Material). The species "*Diplodocus*" *hayi* has since been referred to the genus *Galeamopus* (Tschopp et al., 2015a). The combination of relatively short, horizontal transverse processes and weakly transversely expanded triangular aliform processes on the summit of the neural spine imply a referral to Diplodocinae (Tschopp et al., 2015a). The weak lamination of the neural arch pedicels and the vertical base of the neural spine also occur in *Galeamopus pabsti* (Tschopp and Mateus, 2017). However, because the genus comprises two distinct species (Tschopp and Mateus, 2017), and because it is possible that these neural arches were actually found associated with the holotype of *Galeamopus hayi* from RFPR Quarry A (HMNS 175; see Material), we here conservatively refer the vertebrae to *Galeamopus* sp.

The two caudal vertebrae CM 36035 were identified as *Apatosaurus* sp. by McIntosh (1981). However, their centrum elongation (fig. 6; suppl. table 3, available at https://doi.org/10.5531/sd.sp.36) is more pronounced than what is known for apatosaurine midcaudal vertebrae, reaching ratios only known from diplodocines among Morrison Formation sauropods (Tschopp et al., 2015a). Comparison with midcaudal vertebrae of *Galeamopus hayi* HMNS 175 show that the latter also have relatively low neural spines and longitudinal ridges on their lateral surfaces. *Diplodocus* midcaudal centra are usually more elongate with trapezoidal articular surfaces. *Barosaurus* midcaudal vertebrae are generally less elongate than are those of *Diplodocus*, but more elongate than those of *Galeamopus*, and have wider than tall articular surfaces (Tschopp et al., 2015a). *Supersaurus* has a similar elongation and lateral ridges, but generally taller neural spines than CM 36035 and *Galeamopus hayi* (Lovelace et al., 2007; Tschopp et al., 2015a). No other Morrison Formation diplodocine—including the second species within *Galeamopus*, *G. pabsti*—is currently known from midcaudal vertebrae.

We refer three cervical (and an associated fragment), two dorsal, and two caudal vertebrae from RFPR Quarry B to *Galeamopus* sp. Because of its less developed centrum elongation, the fourth and shortest cervical vertebra of CM 36039 (fig. 3J–L; table 2) could represent a mid- to posterior cervical vertebra of *Galeamopus*, although other features indicate a possible camarasaurid identification instead. These features include the anteriorly restricted pleurocoels and neural arch pedicels, and the small distance between the SPRL and PODL (fig. 3K), which occur in many specimens referred to *Camarasaurus* (e.g., McIntosh et al., 1996a) but not in diplodocids. We do not know the exact reasons for the initial attribution of this short vertebra

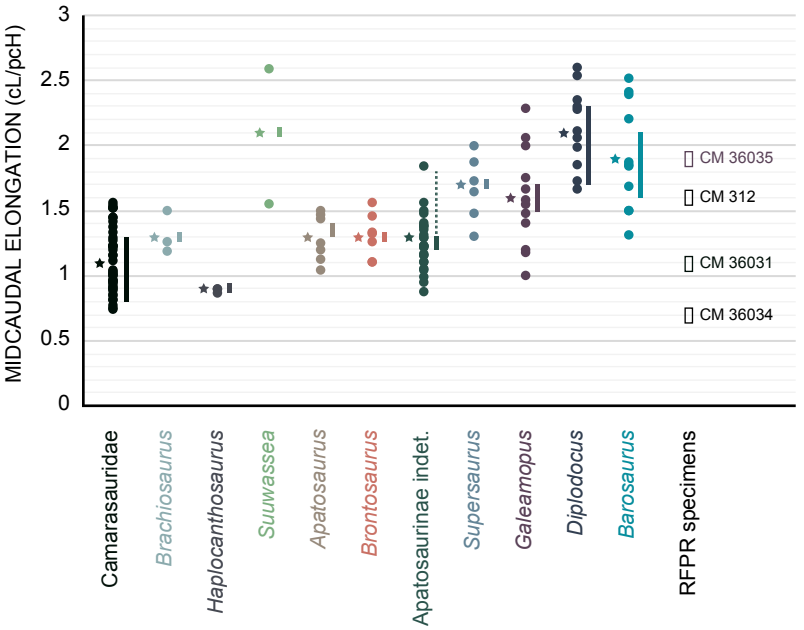

FIG. 6. Range of midcaudal centrum elongation in Morrison Formation sauropods. Ratio represents centrum length (cL) to posterior centrum height (pcH). Dots are ratios of single vertebrae, bars represent the range of means from individual specimens, and stars are the mean of the specimen means across the entire taxon. The dotted line in Apatosaurinae indet. indicates that the highest value (1.8) comes from a specimen represented by a single vertebra in this dataset (LACM 52844), whereas several other, more complete specimens all have values that range between 1.2 and 1.3 (represented by the continuous bar). The open rectangles represent ratios in specimens from RFPR (CM 312 and CM 36034 may be from a single individual, see text). Note the generally higher mean values of diplodocines (*Supersaurus*, *Galeamopus*, *Diplodocus*, *Barosaurus*) compared with apatosaurines (*Apatosaurus*, *Brontosaurus*, and indeterminate specimens) with the exception of LACM 52844. The RFPR specimens are colored as the taxon to which they are referred in the text, with the exception of CM 312 and CM 36034, which are referred to Neosauropoda indet.

with the other cervical vertebrae to a single specimen (CM 36039), but it may have been based on the field numbers. The most complete vertebra bears field number 213, and the others (including the shortest) bear 217–219 (see fig. 3 and suppl. table 1, available at https://doi.org/10.5531/sd.sp.36). Here, we opted to maintain this attribution, but with a note of caution that the specimen might include vertebrae of two different taxa, especially given that field number 213 also included some bones attributable to the camarasaurid CM 36019 (suppl. table 1), indicating that specimens of both a diplodocine and a camarasaurid were found intermingled.

Sauropoda Marsh, 1878

Neosauropoda Bonaparte, 1986

Diplodocoidea Marsh, 1884

Flagellicaudata Harris and Dodson, 2004

Diplodocidae Marsh, 1884

Diplodocinae Marsh, 1884

Diplodocinae indet.

Referred Specimens: A series of 38 middle to distal caudal vertebrae (CM 307), 37 of which were found articulated (Holland, 1906), can be

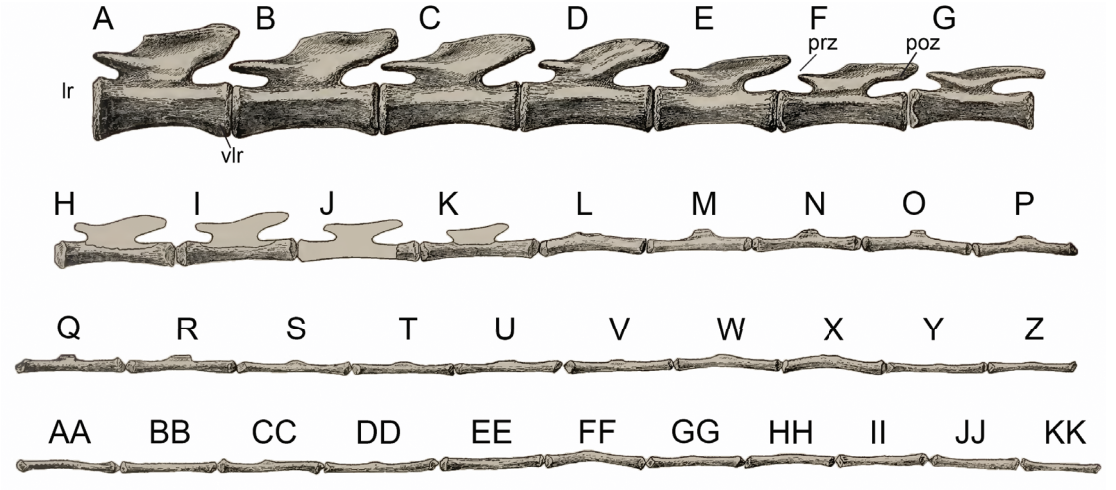

FIG. 7. Caudal vertebrae of Diplodocinae indet. CM 307 in left lateral view. The series can be divided into midcaudal vertebrae (A–F), posterior caudal vertebrae (G–K), and distal caudal vertebrae (L–KK), following the definition of Tschopp et al. (2015a). Abbreviations: **lr,** lateral ridge; **poz,** postzygapophysis; **prz,** prezygapophysis; **vlr,** ventrolateral ridge. Modified from Holland (1906); no scale provided in original figure, but see table 3 for detailed measurements.

referred to Diplodocinae indet. Most of the single vertebrae are relatively well preserved, but six elements were considerably reconstructed.

Description

Caudal Vertebrae: The 38 middle to posterior caudal vertebrae of CM 307 are currently mounted and on display together with the holotype (CM 84) and parts of the paratype (CM 94) specimens of *Diplodocus carnegii*, and interpreted as representing the serial positions 32 and 37 through 73. Most vertebrae of CM 307 were figured by Holland (1906: plate XXIX), and two distal caudal vertebrae were illustrated by Harris (2006: text-fig. 18C). The anteriormost preserved middle caudal vertebrae are relatively elongate, with a low but distinct neural arch (fig. 7; table 3). The first seven elements have amphiplatyan to amphicoelous centra (mounted as Cd 32 and Cd 37–42), with Cd 39 and 42 being clearly amphiplatyan. Caudal vertebrae 43 to 73 (as mounted) have generally biconvex centra, although two vertebrae (mounted as Cd 60 and 62) are anteriorly convex and posteriorly flat. The centra of the midcaudal elements have a gently arched ventral surface in lateral view and a longitudinal ridge on the dorsal half of their lateral surface. This ridge fades and eventually disappears through the series, such that the distalmost 30 elements no longer retain it. The neural arch base (almost) progressively shifts posteriorly in the seven anteriormost preserved caudal vertebrae, before coming to reside directly over the middle of the centrum and remaining there until the arch is completely lost in the last seven caudal vertebrae. It is gradually reduced along the series to be very indistinct in Cd 55 and more posterior vertebrae (as mounted). Where present, the prezygapophyses are short, and they only reach the anterior border of the centrum in the first three vertebrae. Postzygapophyses become indistinct and disappear after the sixth vertebra preserved in the series. The neural spine is directed posterodorsally and slightly overhangs the vertebral centrum posteriorly where it is preserved. The distalmost vertebrae are rodlike, with straight to slightly dorsally arched centra, forming the "whiplash" tail diagnostic of flagellicaudatan sauropods.

Identification

"Whiplash" tails occur in Flagellicaudata (Harris and Dodson, 2004) and some titanosaurs (Wilson et al., 1999). However, most dicraeosaurids have rather flat anterior and posterior articular surfaces on the posterior and distal caudal centra (Harris, 2006), and titanosaurs, dicraeosaurids, and apatosaurines have relatively short centra compared with diplodocines (Wilson et al., 1999; Tschopp et al., 2015a). Based on the extreme elongation of the distal caudal vertebrae of CM 307 (reaching a centrum length to posterior condyle height ratio of >10 in several elements; table 3), we herein refer this partial tail to Diplodocinae indet. Because the distal tails of most genera within this clade are not known, it is currently impossible to attribute CM 307 to a less inclusive taxon even though it is a fairly complete and informative specimen.

Sauropoda Marsh, 1878

Neosauropoda Bonaparte, 1986

Diplodocoidea Marsh, 1884

Flagellicaudata Harris and Dodson, 2004

Diplodocidae Marsh, 1884

Diplodocidae indet.

Referred Specimens: A single posterior dorsal vertebra (CM 36282) referable to Diplodocidae indet. is present among the material from RFPR Quarry B. This specimen was not mentioned by McIntosh (1981) and is only partly prepared. A single, nearly complete anterior caudal vertebra (CM 36033) can also be referred to Diplodocidae, as well as two right humeri (CM 28849 and CM 36026) and a single right metatarsal II (CM 36038). Both humeri and the metatarsal are well preserved and complete.

Description

Dorsal Vertebra: The partially preserved centrum of CM 36282 is too incomplete to yield any information on its external morphology. There seems to be some internal pneumaticity, but it remains unclear to what extent the vertebra was pneumatized and whether it was camerate or camellate (sensu Wedel et al., 2000). Ventrally the neural arch bears only weak lamination, so that the lateral surface of its pedicel is nearly flat. The parapophysis is located directly dorsal to the anterior margin of the pedicel, such that the ACPL is subvertical. There is a subtriangular, ventrally tapering, well-defined centrodiapophyseal fossa (CDF). The neural spine is strongly inclined anteriorly and does not bear a dorsal notch, indicating that CM 36282 is a posterior dorsal vertebra (Wedel and Taylor, 2013). The neural spine has subparallel anterior and posterior margins, and there are triangular aliform processes at its summit. The PRSL and POSL expand transversely toward the spine apex, but do not bifurcate as in *Apatosaurus* and *Brontosaurus* (e.g., AMNH FARB 550; E.T., personal obs., 2018). The zygapophyses are at about one third the height of the entire neural arch (table 4).

Caudal Vertebrae: The anterior caudal vertebra CM 36033 (fig. 8; table 5) has an amphicoelous centrum with a deeply concave anterior surface and a shallowly concave posterior face. There is a ventral keel, and foramina pierce both lateral and the ventral surfaces, but these openings are not set within a distinct pleurocoel. The transverse processes are simple rather than winglike, and this likely indicates a relatively posterior position in the anterior caudal series. The transverse processes project laterally, but their extremities are broken. They are supported by a single anterior centrodiapophyseal lamina (ACDL) and a PRDL, whereas the PODL and PCDL are absent or very reduced. The neural spine is slightly inclined posteriorly. Both the SPRL and SPOL extend onto the lateral surface of the spine and meet dorsally. The extension of the SPRL onto the lateral surface occurs only in the dorsal half of the spine. At the contact with the SPOL, the conjoined laminae form an aliform process. Both the PRSL and POSL are well developed and

TABLE 3

Measurements of the mid- to distal caudal vertebrae of Diplodocinae indet. CM 307 from RFPR Quarry B (in mm)

Vertebrae 2 to 38 (first column) are illustrated in figure 7.

Vertebra	Vertebra position (as mounted)	Centrum length (anteroposterior)	Posterior cotyle dorsoventral height	Posterior cotyle transverse width	Dorsoventral height (total)	Elongation index	Centrum morphology	Measured from
1	32	220	110	94	188	2.00	Amphicoelous	Right side
2	37	175	62	59	131	2.82	Amphicoelous	Right side
3	38	172	58	64	107	2.97	Amphicoelous	Left side
4	39	162	56	56	108	2.89	Amphiplatyan	Left side
5	40	152	50	47	97	3.04	Amphicoelous	Left side
6	41	155	44	41	75	3.52	Amphicoelous (slightly)	Left side
7	42	157	35	45	62	4.49	Amphiplatyan	Left side
8	43	167	30	55	55	5.57	Biconvex	Left side
9	44	156	17	45	55	9.18	Biconvex	Left side
10	45	139	24	39	45	5.79	Biconvex	Left side
11	46	148	25	32	33	5.92	Biconvex	Left side
12	47	127	27	33	31	4.70	Biconvex	Left side
13	48	125	26	29	28	4.81	Biconvex	Left side
14	49	131	16	29	31	8.19	Biconvex	Left side
15	50	132	15	25	28	8.80	Biconvex	Left side
16	51	132	12	23	20	11.00	Biconvex	Left side
17	52	139	14	27	18	9.93	Biconvex	Left side
18	53	134	13	23	21	10.31	Biconvex	Left side
19	54	138	19	17	22	7.26	Biconvex	Left side
20	55	144	10	19	14	14.40	Biconvex	Left side
21	56	124	13	19	13	9.54	Biconvex	Left side
22	57	137	15	17	14	9.13	Biconvex	Left side
23	58	131	20	15	20	6.55	Biconvex	Left side
24	59	135	18	14	16	7.50	Biconvex	Left side
25	60	124	15	13	18	8.27	Convex anterior, flat posterior	Left side
26	61	126	19	12	20	6.63	Biconvex	Left side
27	62	108	21	16	21	5.14	Convex anterior, flat posterior	Left side
28	63	127	17	12	18	7.47	Biconvex	Left side
29	64	117	19	15	22	6.16	Biconvex	Left side

Vertebra	Vertebra position (as mounted)	Centrum length (anteroposterior)	Posterior cotyle dorsoventral height	Posterior cotyle transverse width	Dorsoventral height (total)	Elongation index	Centrum morphology	Measured from
30	65	132	14	16	14	9.43	Biconvex	Left side
31	66	140	12	20	15	11.67	Biconvex	Left side
32	67	125	12	18	12	10.42	Biconvex	Left side
33	68	123	18	16	18	6.83	Biconvex	Left side
34	69	118	19	13	19	6.21	Biconvex	Left side
35	70	121	12	12	12	10.08	Biconvex	Left side
36	71	113	13	13	13	8.69	Biconvex	Left side
37	72	110	18	15	18	6.11	Biconvex	Left side
38	73	95	16	14	16	5.94	Biconvex	Left side

expand transversely the farther they project from the core of the spine. The anterior and posterior margins of the spine are subparallel in lateral view. The lateral margins are mostly parallel in anterior and posterior view, with a slight distal expansion where the SPOL and SPRL meet.

Humeri: The humerus CM 28849 is very stout, with a widely and symmetrically expanded proximal end that forms a rounded outline in anterior view (fig. 9A, B; table 6). The humeral head is not offset from the shaft posteriorly. There is a weak tubercle in the center of the concave proximal portion of the anterior side of the shaft (fig. 9A; unlike *Galeamopus pabsti*, in which this tubercle is located more laterally; Tschopp and Mateus, 2017). The deltopectoral crest is very well developed and terminates in a distinct distal end. The crest is concave laterally, and posterior to the crest there is a distinct, rugose, parallel ridge (fig. 9A). The distal end of the humerus is expanded, but less so than the proximal end. It is relatively flat mediolaterally on the anterior surface. The medial and lateral ridges on the anterior side are displaced toward the lateral side of the bone. Posteriorly, there is a distinct olecranon fossa between the condyles that extends proximally nearly to midshaft.

The humerus CM 36026 (fig. 9C, D) is slightly less stout and about 5% smaller than CM 28849 (table 6). It has a strongly expanded proximal end and a less expanded distal end. The proximal expansion is nearly symmetrical, with the medial corner slightly more expanded than the lateral. In anterior view, the proximal end is gently rounded. In contrast to that of CM 28849, the humeral head of CM 36026 is clearly offset from the shaft posteriorly. Like CM 28849, CM 36026 has a weak tubercle that is located in the center of the anterior concavity of the proximal part of the shaft, a deltopectoral crest with an abruptly terminating distal end, and a distinct, subparallel ridge posterior to this crest. Distally, the medial and lateral ridges are relatively strongly developed and located more laterally than medially. The olecranon fossa is shallower than in CM 28849, but this is possibly due to anteroposterior compression. The deltopectoral crest is also deformed by anteroposterior compression; otherwise, it would project significantly anteriorly.

Metatarsal II: CM 36038 (fig. 10) has a subrectangular proximal articular surface with slightly concave medial and lateral borders. The surface is anteroposteriorly longer than mediolaterally wide (table 7), and has distinct, rugose borders. It is convex anteroposteriorly and mediolaterally. Both the anterior and posterior margins are slightly medially inclined. The shaft is stout and twisted in a counterclockwise direction (when seen in proximal view), such that the anteroposterior axes of the proximal and distal articular surfaces are offset at an angle of approximately 30°. The anterior surface of the shaft

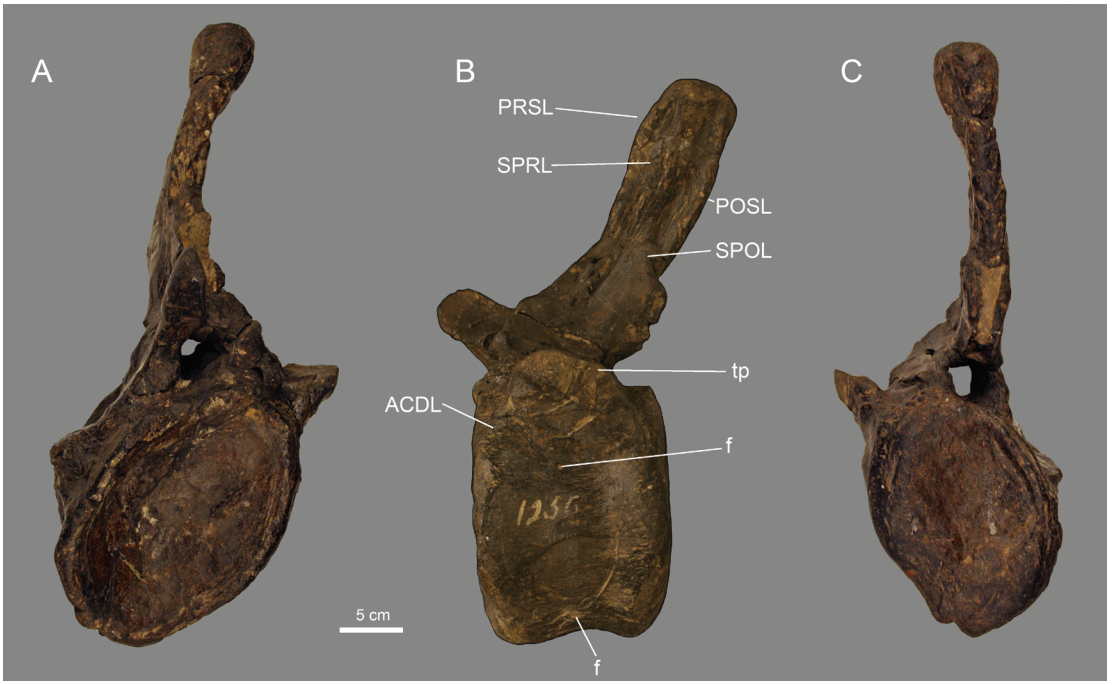

FIG. 8. Anterior caudal vertebra of Diplodocidae indet. CM 36033 in **A,** anterior; **B,** left lateral; and **C,** posterior views. Note the contact of the SPRL and SPOL on the dorsal part of the neural spine. Scale applies to all views. The vertebra was initially cataloged as CM 1256 and later recataloged as CM 36033. Abbreviations: **ACDL,** anterior centrodiapophyseal lamina; **f,** foramen; **POSL,** postspinal lamina; **PRSL,** prespinal lamina; **SPOL,** spinopostzygapophyseal lamina; **SPRL,** spinoprezygapophyseal lamina; **tp,** transverse process. Photos by Andrew McAfee (A, C) and E.T. (B).

is marked by a very distinct, rugose tuberosity on its distal half, more or less in the center of the shaft. The tuberosity is connected to the anterolateral corner of the distal articular surface by an oblique ridge. The lateral surface of the shaft is concave proximally and flattens more distally. The distal articular surface bears distinct condyles. The lateral condyle forms a rounded posterolateral process.

Identification

Dorsal vertebra CM 36282 is referred to *Apatosaurus* sp. in the CM database, but it is not mentioned in McIntosh's (1981) catalog, so it remains unclear who provided this identification. The weak lamination on the lateral surface of the neural arch pedicels is similar to that seen in *Galeamopus pabsti* (Tschopp and Mateus, 2017), but in the latter species, the transverse processes are generally located more dorsally with respect to neural arch height. A more ventral position of the transverse processes is known in apatosaurines as well as the diplodocine *Supersaurus vivianae* (Lovelace et al., 2007; Tschopp et al., 2015a). Because CM 36282 is still incompletely prepared, it is most conservative to refer this dorsal vertebra to Diplodocidae indet.

McIntosh (1981) referred the anterior caudal vertebra CM 36033 to *Apatosaurus*. This vertebra can be referred to Diplodocidae based on the contact of the SPRL and SPOL on the lateral surface of the neural spine (Wilson, 1999; Tschopp et al., 2015a). Within Diplodocidae, the lack of posterior diapophyseal laminae (PCDL and PODL) occurs in the diplodocines *Tornieria africana* and *Supersaurus vivianae*, as well as in apatosaurines

TABLE 4

Measurements of the posterior dorsal vertebra of Diplodocidae indet. CM 36282 from RFPR Quarry B (in mm; not figured)

Centrum length	170 (estimated)
Posterior cotyle dorsoventral height	180
Pedicel dorsoventral height	160
Neural arch dorsoventral height	470

(Tschopp et al., 2015a). Anterior caudal vertebrae of *Galeamopus hayi* were scored as if they had these laminae by Tschopp et al. (2015a), based on the mounted skeleton at HMNS. However, the mounted anterior caudal vertebrae are not from the type specimen, but instead were modelled after those of *Diplodocus carnegii* CM 94 (according to a label on exhibit at HMNS, 2010). Two undescribed, probable *Galeamopus* specimens (CMC VP 7573, WDC-GB) have anterior caudal vertebrae with weakly developed to absent posterior diapophyseal laminae, similar to CM 36033, *Tornieria*, and *Supersaurus*. Thus, several diplodocine genera seem to share this feature with apatosaurines, so we prefer to be conservative and refer CM 36033 to Diplodocidae indet.

Both humeri (CM 28849 and CM 36026) were identified as belonging to *Apatosaurus* sp. by McIntosh (1981). The symmetrically expanded proximal portions and the rounded proximal outlines in anterior view are synapomorphies of Diplodocoidea and Diplodocidae, respectively (Tschopp et al., 2015a). Within Diplodocidae, humeri as robust as CM 28849 and CM 36026 occur in apatosaurines and *Galeamopus* (fig. 11; suppl. table 4, available at https://doi.org/10.5531/sd.sp.36). We therefore conservatively refer these humeri to Diplodocidae indet., but note that neither displays the laterally positioned tubercle that was proposed as an autapomorphy of the species *Galeamopus pabsti* (Tschopp and Mateus, 2017). However, we cannot rule out referral to the second species of *Galeamopus*, *G. hayi*, which was found in RFPR Quarry A.

McIntosh (1981) referred metatarsal II CM 36038 to *Apatosaurus*. This metatarsal is clearly referable to Flagellicaudata because of the beveled proximal and distal articular surfaces and the presence of a rugose tuberosity on the anterolateral edge of the shaft, and to Diplodocidae based on the pronounced posterolateral process that does not occur in this form in dicraeosaurids (Harris, 2007; Tschopp et al., 2015a). However, it is impossible to confidently refer an isolated metatarsal to a specific genus within Diplodocidae. With a robusticity of 0.47 (sensu Tschopp et al., 2015a: C466), CM 36038 is less robust than any of the reported diplodocid metatarsals, the most similar being those of an indeterminate apatosaurine (SMA 0087; 0.55), *Diplodocus carnegii* CM 94 (0.52), and *D. hallorum* USNM 10865 (0.56) (Tschopp et al., 2015a). A ratio of <0.53 was found as autapomorphic of *D. carnegii* by Tschopp et al. (2015a), but an indeterminate, relatively complete diplodocine that generally shows more features resembling *Galeamopus* (CMC VP 7573; E.T., personal obs., 2017) has a ratio of 0.45. Few articulated pedes of diplodocine sauropods are known that could potentially confirm the genuine distribution of these ratios among species. We thus refer CM 36038 to Diplodocidae indet.

Sauropoda Marsh, 1878

Neosauropoda Bonaparte, 1986

Diplodocoidea Marsh, 1884

Flagellicaudata Harris and Dodson, 2004

Flagellicaudata indet.

Referred Specimens: A partial left scapula (CM 90276) and coracoid (CM 36025), the distal end of a left ischium (CM 28848), and two left

TABLE 5

Measurements of the anterior caudal vertebra of Diplodocidae indet. CM 36033 from RFPR Quarry B (in mm; see fig. 8)

Centrum length	140
Posterior cotyle dorsoventral height	175
Posterior cotyle transverse width	150
Dorsoventral height (total)	430
Neural spine maximum transverse width	46
Neural spine minimum transverse width	25
Neural spine anteroposterior length at summit	69
Neural arch dorsoventral height	258
Elongation index (sensu Wilson and Sereno, 1998)	0.80
Average elongation index (sensu Chure et al., 2010)	0.86

metatarsals (CM 90277) can be referred to Flagellicaudata indet. The scapula CM 90276 consists only of the scapular blade (preserved in two parts) and was therefore not measured. It was originally included in CM 36019, which is referred to the macronarian clade Camarasauridae below. Its proportionally large size compared with the other bones assigned to that specimen shows that it belongs to another sauropod individual, so it was recataloged during this study. The coracoid CM 36025 is well preserved. McIntosh (1981) identified the distal ischium CM 28848 as a right element, but the position of the rugose facet for articulation with the distal end of the contralateral ischium indicates that this bone is from the left side of the animal. The two left metatarsals (CM 90277) were originally included in CM 312, which is identified as Neosauropoda indet. below. Given that they are most likely from a different individual than the tail of that specimen, these two metatarsals have also been recataloged.

Description

Scapula: The left scapula CM 90276 (fig. 12) has a very straight blade, with only a slight ventral expansion at its posterior end, and a short dorsal process anterior to the otherwise unexpanded posterodorsal corner. The presence of such a dorsal process is unusual for diplodocoids, and it is therefore unclear whether this specimen might be pathologic. The central part of the blade is D-shaped in cross section, without any indication of a subtriangular process on the ventral edge. There is a rugose ridge on the medial surface.

Coracoid: The left coracoid CM 36025 has an open coracoid foramen (fig. 12), indicating that the animal to which it pertained was a juvenile (Schwarz et al., 2007). It has a rounded outline and is dorsoventrally taller than it is anteroposteriorly long (table 8). There is no significant expansion of the glenoid, and no clear notch and lip anterior to that structure. The entire bone is relatively flat, and the articulation with the scapula is straight.

Ischium: The ischium CM 28848 is in two pieces, one of which had originally been cataloged with the camarasaurid scapula CM 36029 (see below). Amy Henrici recently recognized that this fragment matched the broken end of CM 28848. Nonetheless, the specimen offers little morphological information. It has a subtriangular outline in distal view and bears a rugose articular surface for its right counterpart on its distomedial corner. The ischium is strongly expanded dorsoventrally, which would correspond to the mediolateral expansion in macronarians, in which the ischial shaft is twisted such that the long axis of its distal end is oriented mediolaterally. The newly recog-

FIG. 9. Right humeri of Diplodocidae indet. CM 28849 in **A,** anterior and **B,** medial views. CM 36026 in **C,** anterior and **D,** medial views. Note the rugose ridges parallel to the deltopectoral crests (arrows). Both specimens were initially included in CM 1256 and later recataloged. The numbers 72 (A) and 221 (C) are field numbers. Scale bar applies to both specimens. Abbreviations: **dpc,** deltopectoral crest; **lr,** lateral ridge; **mr,** medial ridge; **tub,** tubercle. Photos by E.T. (A, C) and Andrew McAfee (B, D).

nized second fragment is from the base of the shaft, and has an oval cross section and a muscle scar on the lateral side.

Metatarsals: The left metatarsal I of CM 90277 (fig. 13A–F) is relatively stout (table 9). Both the proximal and distal articular surfaces are not perpendicular to the shaft, but the proximal surface is more medially beveled than the distal. The proximal articular surface is wider mediolaterally than anteroposteriorly long. The anterior surface is mediolaterally concave and lacks foramina. The distal condyles are very distinct and the lateral condyle has a long posterolateral projection. The other preserved left metatarsal of CM 90277 is the third (fig. 13G–L). It has a subtriangular proximal articular surface and a slender shaft. In distal view, the mediolateral axis of the distal end is slightly twisted compared with the proximal end. It has relatively indistinct condyles, though the medial condyle extends considerably onto the anterior surface of the shaft. A short, weakly rugose crest marks the distalmost portion of the anterolateral edge of the shaft. A phalanx potentially belonging to the same pes (McIntosh, 1981) could not be located in the CM collection in 2017.

Identification

The weak distal expansion of the scapular blade CM 90276 indicates that it belongs to a flagellicaudatan (Tschopp et al., 2015a). The presence of a subtriangular process is variable within Diplodocidae (Tschopp et al., 2015a), and consequently a referral to a more specific taxon within Flagellicaudata is currently impossible. The only genus we can confidently exclude is *Supersaurus*, based on its autapomorphically expanded distal scapular blade (Lovelace et al., 2007; Tschopp et al., 2015a).

TABLE 6

Measurements of the right humeri referred to Diplodocidae indet. from RFPR Quarry B (in mm; see fig. 9)

	CM 28849	CM 36026
Proximodistal length	815	782
Proximal mediolateral width	433	383
Minimum shaft mediolateral width	160	170
Anteroposterior length of the shaft below the deltopectoral crest	100	78
Distal mediolateral width	320	284
Proximodistal length of the deltopectoral crest	375	355
Robustness index (sensu Wilson and Upchurch, 2003)	0.37	0.36

McIntosh (1981) referred the coracoid CM 36025 to *Camarasaurus*, but it lacks the glenoid notch and lip that are typically present in that taxon (Marsh, 1878; McIntosh et al., 1996a). The development of the notch in *Haplocanthosaurus* is similar to that in *Camarasaurus* (Hatcher, 1903). Apatosaurines generally have rectangular coracoids, with the exception of *Brontosaurus yahnahpin* (Marsh, 1881; Bakker, 1998; Tschopp et al., 2015a). The coracoid of *Suuwassea* has a more rounded outline and a weakly developed glenoid notch (Harris, 2007), similar to the condition in CM 36025. Nevertheless, this taxon seems to differ from the RFPR coracoid in having a more expanded glenoid (Harris, 2007), though the relatively flat ventral portion of CM 36025 could also be due to taphonomic compression. Although an attribution of the RFPR coracoid to Diplodocinae therefore seems likely, we opt to be more conservative and refer the bone only to Flagellicaudata indet.

The ischium CM 28848 was identified as *Apatosaurus* by McIntosh (1981). However, the distal ends of the ischia do not bear any features allowing referral to any taxon below Flagellicaudata, which can be diagnosed by triangular distal ends that form a V-shape in distal view when articulated. We therefore refer this specimen to Flagellicaudata indet.

McIntosh (1981) referred the metatarsals included in CM 312 (which are now cataloged as CM 90277) to *Camarasaurus*; this referral was most likely based on the caudal vertebrae of CM 312 rather than these metatarsals. Both metatarsals are clearly referable to Flagellicaudata because of the beveled proximal and distal articular surfaces of metatarsal I, the presence of a rugose tuberosity on the anterolateral edge of the shafts of both elements, and a posterolateral process in metatarsal I (Tschopp et al., 2015a). However, we cannot confidently refer these metatarsals to any recognized genus within Flagellicaudata. With a proximal width to proximodistal length ratio of 0.7, metatarsal I of CM 90277 is similar in this regard to dicraeosaurid and some diplodocine metatarsals, whereas the metatarsals of apatosaurines appear to be slightly stouter (Tschopp et al., 2015a). We therefore refer CM 90277 to Flagellicaudata indet., while noting that a referral to Apatosaurinae seems less plausible than an assignment to other flagellicaudatan taxa.

Sauropoda Marsh, 1878

Neosauropoda Bonaparte, 1986

Diplodocoidea Marsh, 1884

Diplodocoidea indet.

Referred Specimens: A partial dorsal centrum (CM 36042) can be referred to Diplodocoidea. Because it is so incomplete, no measurements were taken. A second, small piece of this bone was found among the material still cataloged as CM 1256 during this study; the two elements are now stored together.

FIG. 10. Right metatarsal II of Diplodocidae indet. CM 36038 in **A,** proximal; **B,** dorsal; **C,** medial; **D,** plantar; **E,** lateral; and **F,** distal views. The metatarsal was initially included in CM 1256 and later recataloged as CM 36038. Scale bar applies to all views. Abbreviations: **plp,** posterolateral process; **tub,** tuberculum.

Description

Dorsal Vertebra: The centrum is anteriorly flat and posteriorly concave and has a strongly concave ventral surface with two distinct longitudinal ridges. Only the ventral portions of the pleurocoels are preserved. They leave a thin median wall, and the rest of the centrum appears to be relatively solid rather than extensively pneumatized.

Identification

This dorsal centrum was identified as belonging to *Camarasaurus* by McIntosh (1981). However, the flat anterior end excludes an identification as *Camarasaurus* or any other macronarian because the dorsal centra of these sauropods are significantly opisthocoelous throughout the series (Carballido et al., 2012; Tschopp et al., 2015a). Within Diplodocoidea, at least *Haplocanthosaurus priscus* and *Brontosaurus excelsus* (YPM VP.001981) have transversely concave ventral surfaces, although not to the degree seen in CM 36042. We therefore conservatively refer this centrum to Diplodocoidea indet.

Sauropoda Marsh, 1878

Neosauropoda Bonaparte, 1986

Macronaria Wilson and Sereno, 1998

Camarasauridae Cope, 1877b

Camarasauridae indet.

Referred Specimens: Numerous specimens from RFPR Quarry B can be referred to Camarasauridae indet., including two (CM 21775 and CM 36019) that preserve apparently associated

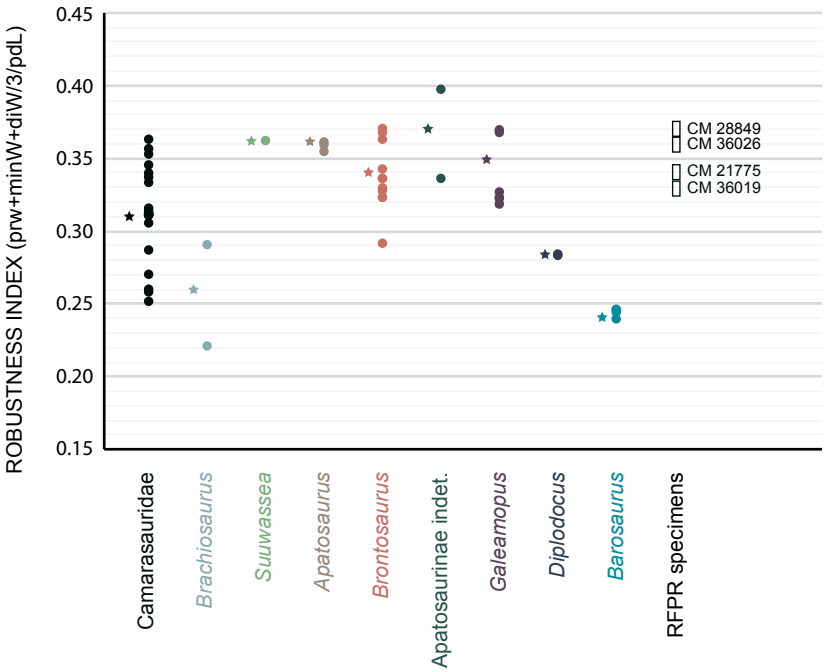

FIG. 11. Range of humeral robusticity indices (RI) in Morrison Formation sauropods. Ratio represents the mean of proximal, distal, and minimum shaft mediolateral widths (prW, diW, minW, respectively), divided by proximodistal length (pdL). Dots are ratios of single humeri and stars are the mean across the entire taxon. The open rectangles represent ratios in specimens from RFPR. Note that *Galeamopus* humeri have a more similar RI to apatosaurines (*Apatosaurus*, *Brontosaurus*, and indeterminate specimens) than to the other diplodocines *Diplodocus* and *Barosaurus*. The RFPR specimens CM 28849 and CM 36026 are referred to Diplodocidae indet., and CM 21775 and CM 36019 to Camarasauridae indet.

or articulated forelimb material that was thus cataloged together. We describe the articulated specimens CM 21775 and CM 36019 first, followed by the less complete specimens. The incomplete specimens referable to Camarasauridae indet. include a well-preserved left dentary (CM 36670), an anterior dorsal vertebra (CM 36040), two anterior caudal vertebrae (CM 36032), a series of 16 anterior to midcaudal vertebrae (CM 36031), and a series of 13 chevrons (CM 1253). Specimens CM 1253 and CM 36031 may belong to a single individual, according to McIntosh (1981). In addition, two partial scapulae (CM 36029, CM 36043), a right coracoid (CM 36027), two specimens with associated pubes and ischia (CM 28846, CM 36024), a pair of femora (CM 36021), a right tibia and fibula (CM 36020), and an isolated right fibula (CM 36022) can also be referred to Camarasauridae.

The partial right scapula CM 36029 included two fragments plus a more complete piece that nonetheless lacks a portion of the anterodorsal rim of the acromion and the distal half of the blade. The fracture with the remainder of the blade appears to be recent, so it is possible there are more fragments of this scapula among the material with the general number CM 1256 or the uncataloged RFPR material at CM; moreover, the distalmost portion of the blade may be the element that is currently cataloged as CM 36028 (see below). Due to the fragility of the material, the most complete piece of CM 36029 is visible only in medial view. CM 36043 is a nearly complete left scapula that lacks only a part of the dorsal margin

TABLE 7

Measurements of the right metatarsal II of Diplodocidae indet. CM 36038 from RFPR Quarry B (in mm; see fig. 10)

Proximodistal length	143
Proximal mediolateral width	61
Proximal anteroposterior height	116
Minimum mediolateral diameter of shaft	38
Distal mediolateral width	72
Distal anteroposterior height	66

TABLE 8

Measurements of the left coracoid of Flagellicaudata indet. CM 36025 from RFPR Quarry B (in mm; see fig. 12C–D)

Dorsoventral height	443
Anteroposterior length	300
Glenoid maximum diameter	105
Glenoid minimum diameter (perpendicular to maximum)	50

TABLE 9

Measurements of the left metatarsals I and III of Flagellicaudata indet. CM 90277 from RFPR Quarry B (in mm; see fig. 13)

	Metatarsal I	Metatarsal III
Proximodistal length	159	186
Proximal mediolateral width	112	60
Proximal anteroposterior height	107	88
Minimum mediolateral diameter of shaft	84	34
Minimum anteroposterior depth of shaft	45	40
Distal mediolateral width	146	69
Distal anteroposterior height	58	52

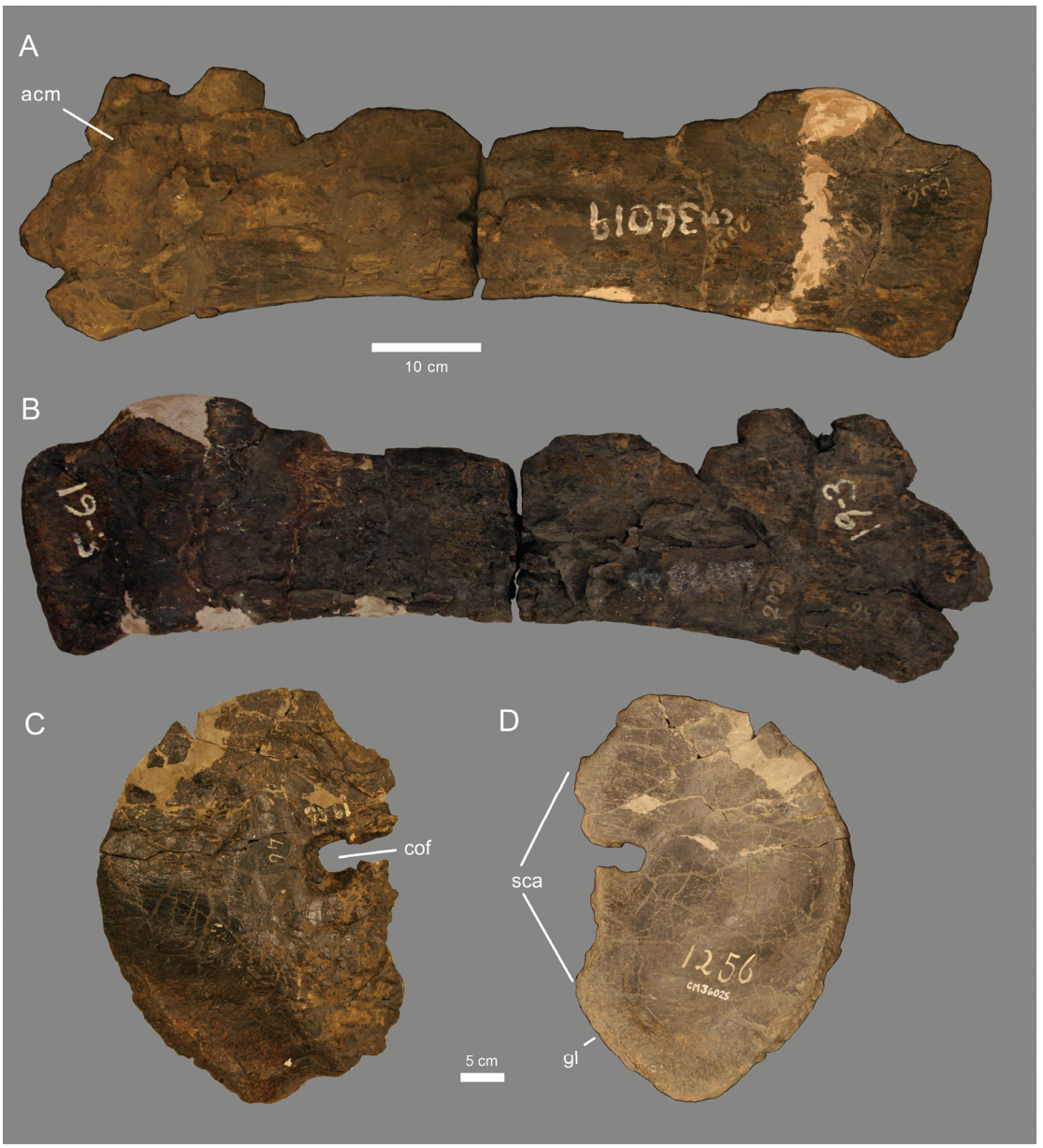

FIG. 12. Pectoral girdle elements of Flagellicaudata indet. Partial left scapula CM 90276 in **A,** lateral and **B,** medial views. Note the dorsal process toward the distal end. The specimen was initially included in CM 1256, later recataloged as CM 36019, and finally given its own catalog number CM 90276 during our reassessment (see text). There seem to be two field numbers associated with this scapula (193, 203). Left coracoid CM 36025 in **C,** lateral and **D,** medial views. Note the open coracoid foramen. The specimen was initially included in CM 1256 and later recataloged as CM 36025. Abbreviations: **acm,** acromion; **cof,** coracoid foramen; **gl,** glenoid; **sca,** scapular articular surface. Photos by E.T. (A, C) and Andrew McAfee (B, D).

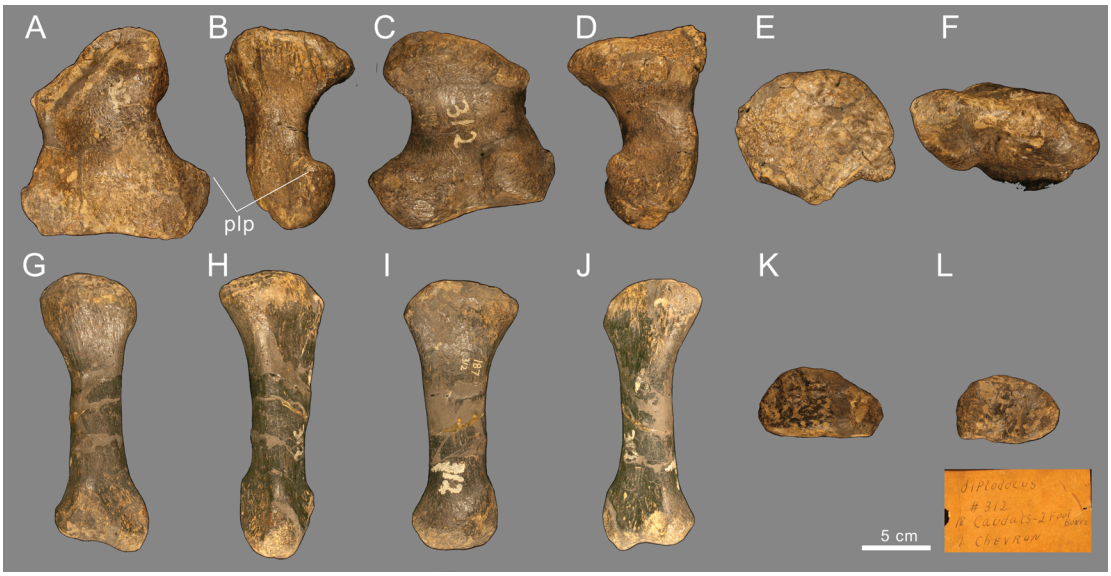

FIG. 13. Left metatarsals of Flagellicaudata indet. CM 90277 with original specimen collection tag. Metatarsal I in **A,** dorsal; **B,** lateral; **C,** plantar; **D,** medial; **E,** proximal; and **F,** distal views. Dorsal is upward in (E, F). Metatarsal III in **G,** dorsal; **H,** lateral; **I,** plantar, **J,** medial; **K,** proximal; and **L,** distal views. Dorsal is upward in (K, L). This specimen was initially cataloged as CM 312 and has been recataloged during this study as CM 90277. Scale bar applies to all views of both bones. Abbreviation: **plp,** posterolateral process. Photos by Enrica Sarotto.

of the distal blade and the anterodorsal portion of the acromion. The right coracoid CM 36027 is complete and well preserved. CM 28846 consists of a nearly complete right pubis and both ischia. CM 36024 comprises a right pubis and ischium, both of which are incomplete but otherwise well preserved. The tibia and fibula CM 36020 are complete, but the tibia has a heavily deformed cnemial crest, which makes it difficult to identify as either a right or left element. We here follow McIntosh (1981) in interpreting this as a right tibia, as its size fits well with the accompanying fibula, which is clearly from the right side. There is a considerable difference in size between the fibulae, indicating that there are at least two individuals represented among the camarasaurid hind limb material from RFPR.

Description

CM 21775: This specimen consists of dorsal ribs, both scapulae and coracoids, and the left sternal plate, humerus, ulna, and radius. The forelimb bones were originally included in CM's mounted skeleton of *Diplodocus carnegii*, before being replaced in 2006–2007 by scaled-up sculptures based on a well-preserved but smaller diplodocine right forelimb from the Morrison Formation of Cactus Park, Utah (BYU 681/4742 [humerus], BYU 681/4726 [radius], BYU 681/4708 [ulna]).

The dorsal rib shafts are subcircular in cross section. There is no indication of laminae on the posterior surface of the rib heads, as would be typical for diplodocines with the exception of *Galeamopus* (Tschopp et al., 2015a; Tschopp and Mateus, 2017).

The right scapula of CM 21775 is well preserved and nearly complete, lacking only part of the dorsal portion of the acromion and a small part of the base of the blade. The scapulae are large and have widely dorsoventrally expanded acromia and distal blades (table 10). The acromion has an abrupt ventral expansion and very rugose margins. The glenoid is medially beveled. There is a distinct tubercle with striated rugosi-

TABLE 10

Measurements of Camarasauridae indet. CM 21775 from RFPR Quarry B (in mm)
Asterisk indicates estimated measurement.

	Scapula, L[1]	Scapula, R[2]	Coracoid, L[3]	Coracoid, R[4]	Sternal plate, L[5]	Humerus, L[6]	Ulna, L[7]	Radius, L[8]
Proximodistal length	1270	1355*			552	1000	800	730
Acromion length (oblique)	680	690						
Acromion length (perpendicular)	680	680						
Minimum dorsoventral height distal blade	173	162						
Maximum dorsoventral height distal blade		450						
Dorsoventral height			570	512				
Anteroposterior length			430	406				
Glenoid maximum diameter			175	205				
Glenoid minimum diameter (perpendicular to maximum)			125	140				
Maximum mediolateral width					315			
Proximal mediolateral width						460	215	155
Minimum shaft mediolateral width						185	64	88
Distal mediolateral width						365	128	180
Proximodistal length deltopectoral crest						445		
Midshaft anteroposterior length						70		
Distal anteroposterior length								96
Robustness index (sensu Wilson and Upchurch, 2003)						0.34		

[1] See fig. 14A–B.
[2] Not figured.
[3] Not figured.
[4] See figure 14C–D.
[5] Not figured.
[6] See figure 15A–F.
[7] See figure 15G–J.
[8] See figure 15K–N.

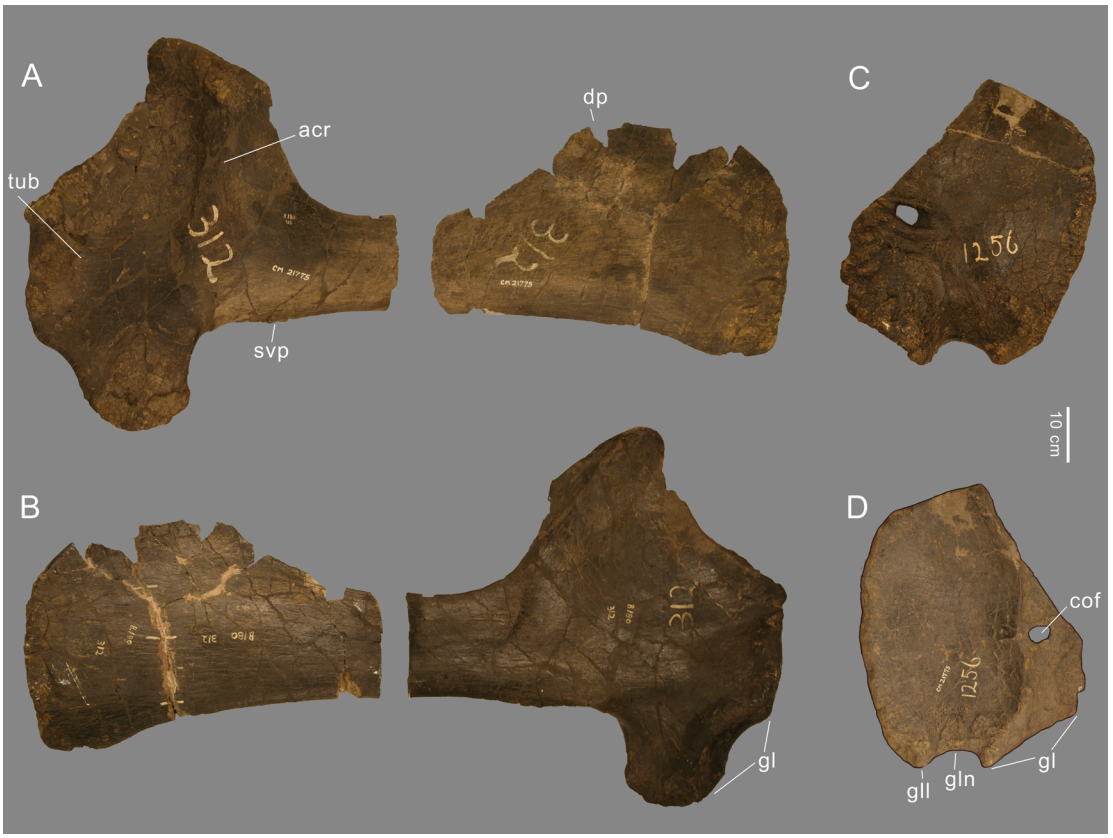

FIG. 14. Pectoral girdle bones of Camarasauridae indet. CM 21775. **A,** left scapula in lateral view; **B,** left scapula in medial view; **C,** right coracoid in lateral view; **D,** right coracoid in medial view. Abbreviations: **acr,** acromial ridge; **cof,** coracoid foramen; **dp,** dorsal process; **gl,** glenoid; **gll,** glenoid lip; **gln,** glenoid notch; **svp,** subtriangular ventral process; **tub,** tubercle. The scapula was first cataloged as CM 312, whereas the coracoid was initially cataloged as CM 1256. Photos by Andrew McAfee (A–C) and E.T. (D).

ties situated at about midheight of the acromion, toward its anterior margin (fig. 14). The striations are oriented subhorizontally. This tubercle probably indicates the position of the coracoid foramen, which enters the right coracoid laterally but extends through the coracoid-scapula articulation to exit the right scapulocoracoid on the scapular portion medially (see also the description of the coracoid below). The anterodorsal corner of the acromion forms nearly a right angle (this region is not preserved in the left scapula; fig. 14). There is a second, smaller tubercle positioned somewhat posteroventral to this corner on the lateral surface. The dorsal margin of the acromion was probably straight but is not completely preserved in either scapula. The acromial ridge is nearly perpendicular to the ridge that extends along the distal blade (fig. 14). The acromial ridge is marked posteriorly by a nearly vertical crest and more anteriorly by a slightly oblique crest. The surface between these crests is weakly concave and tapers dorsally in anteroposterior dimension. The area adjacent to the posterior edge of the acromial ridge is concave. The distal end of the blade is widely expanded and has a subtriangular ventral process and a strongly developed, rounded dorsal process close to the distal end (fig. 14), which is similar to that of *Camarasaurus grandis* YPM VP.001901 (Ostrom and McIn-

tosh, 1966), but more developed than that of *C. supremus* (AMNH FARB 5760/5761; Osborn and Mook, 1921).

The coracoids of CM 21775 are well preserved. They are subrectangular and dorsoventrally taller than anteroposteriorly long (fig. 14; table 10). The anterior margin expands mediolaterally from dorsal to ventral. The glenoid is rhomboid in shape and accompanied anteriorly by a shallow notch and a distinct, ventrally projecting lip that resembles that of *Camarasaurus* GMNH PV-101 (McIntosh et al., 1996a). The articular surface with the scapula is very rugose and has distinct medial and lateral margins. On the medial surface of the right coracoid, this margin is located anterior to the coracoid foramen, so that the foramen opens into the articular facet for the scapula medially (fig. 14). On the medial surface of the left coracoid, the foramen lies immediately anterior to the margin.

The left sternal plate of CM 21775 (table 10) lacks its posteromedial portion. It was oriented such that the thickened end would have pointed anteriorly and the smooth margin laterally, and the more anteroposteriorly concave surface would have faced dorsally. The sternal plate is dorsoventrally thick at its anterior end, the dorsal surface being more expanded than the ventral face. The smooth lateral border is nearly straight. The preserved portion of the medial border is gently curved, indicating that the complete sternal plate would have had a rather oval outline similar to those of *Camarasaurus supremus* (Osborn and Mook, 1921) and *Giraffatitan brancai* (Janensch, 1961) rather than the distinctly triangular contour present in most diplodocids (Tschopp and Mateus, 2012).

The left humerus of CM 21775 is complete (fig. 15A–F; table 10). It is slightly laterally expanded at its proximal end, but in general the mediolateral expansion is not as symmetrical as in flagellicaudatans (Tschopp et al., 2015a). The humeral head is centrally located and offset posteriorly from the shaft. The deltopectoral crest is very strongly developed and has a well-defined distal end. Posterior to the crest there is a well-developed bulge (fig. 15B). The anterior surface of the distal part of the shaft is very flat mediolaterally. The medial and lateral ridges are strongly developed and centrally located.

The left ulna of CM 21775 is stout and has a strongly expanded anteromedial process and a shorter anterolateral process (fig. 15G–J; table 10). The two processes meet at an acute angle where they would have received the proximal part of the radius. The proximal articular surface is roughly Y-shaped in proximal view (fig. 15I). A weak olecranon process is present, but it is not developed to the extent seen in derived macronarians such as titanosaurs (e.g., Poropat et al., 2015). The anterolateral process has a distinctly offset anterior tip that projects anteriorly. The ulnar shaft tapers distally to a position where there is an elevated, rugose area on its anterior surface for the attachment of the interosseous ligaments that would have connected the ulna to the radius in life. Further distally, the shaft curves considerably posteriorly, but it is unclear whether this is an authentic condition or a consequence of postmortem deformation. The distal end is expanded anteriorly and medially but not posteriorly.

The left radius of CM 21775 is slender and straight (fig. 15K–N; table 10). It has a subrectangular proximal articular surface with a mediolaterally oriented long axis. The shaft has subparallel medial and lateral margins. The posterior surface is marked by a long, continuous ridge that extends from the posteromedial corner of the proximal articular surface distolaterally until it reaches the midline of the shaft. From here, the ridge extends nearly straight distally to a position somewhat lateral to the center of the posterior edge of the distal articular surface. The ridge bears a distinct rugosity at midshaft. Distal to this rugosity, a second, parallel ridge arises and expands further distally into a wide, posteriorly projecting rugose area for the attachment of interosseous ligaments that would have connected the radius to the ulna (fig. 15L). The distal articular surface is ovoid, mediolaterally expanded, and anteroposteriorly longer medially

FIG. 15. Forelimb bones of Camarasauridae indet. CM 21775. Left humerus in **A,** medial; **B,** anterior; **C,** lateral; **D,** posterior; **E,** proximal; and **F,** distal views. Note the bulge posterior to the deltopectoral crest in (B). Left ulna in **G,** anterior; **H,** lateral; **I,** proximal; and **J,** distal views. Left radius in **K,** anterior; **L,** posterior; **M,** proximal; and **N,** distal views. Abbreviations: **amp,** anteromedial process; **dpc,** deltopectoral crest; **hh,** humeral head; **lr,** lateral ridge; **mr,** medial ridge; **rt,** tubercle for articulation with radius; **ut,** tubercle for articulation with ulna. Photos by Andrew McAfee.

than in its lateral half. The surface is slightly mediolaterally convex, but not distinctly beveled, as would be typical for *Galeamopus* (Tschopp and Mateus, 2017).

CM 36019: This specimen includes the nearly complete left forelimb (including a partial manus that was not mentioned by McIntosh, 1981) and the right scapula, coracoid, and humerus. A partial left scapula (in two pieces) that was initially cataloged as CM 36019 is much larger than the right scapula, the latter of which matches the relatively small size of the limb bones. Also, the morphology of the distal end of the larger scapula differs from that of the smaller element, with the former having a relatively unexpanded distal end compared with the minimum dorsoventral

TABLE 11

Measurements of Camarasauridae indet. CM 36019 from RFPR Quarry B (in mm)
Asterisk indicates estimated measurements.

	Scapula, R[1]	Coracoid, R[2]	Humerus, R[3]	Ulna, L[4]	Radius, L[5]	Carpal, L[6]	Mtc I, L[7]	Mtc III, L[8]	Mtc IV, L[9]
Proximodistal length	940 (incomplete)		770	546	525	48	212	235	252
Acromion length (oblique maximum diameter)	565								
Acromion length (perpendicular to distal blade)	550								
Minimum dorsoventral height of distal blade	130*								
Distal dorsoventral height of blade	205 (incomplete)								
Dorsoventral height		440							
Anteroposterior length		306							
Glenoid maximum diameter		119							
Glenoid minimum diameter (perpendicular to maximum)		88							
Proximal mediolateral width			350		125	154		45	52
Proximal anteroposterior length						103	63	82	72
Minimum shaft mediolateral width			145		68		49	30	36
Minimum shaft anteroposterior length							32	47	35
Distal mediolateral width			233		125		68	50	56
Distal anteroposterior length							52	69	59
Robustness index (sensu Wilson and Upchurch, 2003)			0.32						

[1] See figure 16A, 16D.
[2] See figure 16B–C.
[3] See figure 17A–D.
[4] See figure 17E–H.
[5] See figure 17I–L.
[6] See figure 18A–F.
[7] See figure 18G–L.
[8] See figure 18M–R.
[9] Not figured.

height of the blade. It is therefore unlikely that this larger scapula belongs to the same individual as the other bones cataloged as CM 36019, and the element has thus been recataloged as CM 90276 (see Flagellicaudata indet. above).

The right scapula of CM 36019 (fig. 16A, C) is severely deformed, particularly the distal blade, which lacks part of its dorsal margin. The bone is relatively small and has a widely dorsoventrally expanded acromion (table 11) that forms a right angle to the blade. The acromial ridge is located near the posterodorsal border of the acromion. The glenoid is slightly beveled medially, but it is unclear how much this may have been influenced by postmortem deformation. The articular surface with the coracoid is nearly straight. The preserved part of the distal blade shows that its distal end was expanded dorsally.

The right coracoid of CM 36019 (fig. 16B, D; table 11) is subrectangular, with generally rather rounded corners and a dorsal margin that is slightly anteroposteriorly shorter than the ventral margin. The anterior margin considerably expands mediolaterally from its dorsal to its ventral end. The scapular articular surface is straight. The coracoid foramen is not visible in medial view, but this structure is evident in lateral view, so its medial portion may have been filled during preparation. Anteroventral to the foramen, there is a rugose tubercle on the lateral surface (fig. 16B). The glenoid is strongly expanded mediolaterally, although the entire bone is compressed mediolaterally due to diagenesis. The articular surface for the humerus does not extend onto the lateral surface. It is anteriorly accompanied by a distinct notch.

The right humerus (fig. 17A–D) is complete, whereas the left lacks the proximal end and has a crushed posterior surface. The humerus is generally slender (table 11), and has a proximomedial corner that projects strongly medially, creating the typical, strongly asymmetrical proximal humeral outline of early-diverging macronarians such as *Camarasaurus* and brachiosaurids (Osborn and Mook, 1921; Gilmore, 1925; Janensch, 1961; McIntosh et al., 1996a, 1996b; Mannion et al., 2017). The proximal articular surface has a pronounced lateral corner, such that the lateral half of this surface is nearly horizontal when seen in anterior view. The tubercle in the anterior concavity is located in its center (fig. 17A). The deltopectoral crest expands considerably anteriorly toward its distal end and is posteriorly accompanied by a distinct ridge that extends subparallel to the crest. The medial and lateral ridges on the distal end of the anterior surface are well developed and lean somewhat laterally. They are located more laterally than medially, unlike the condition in CM 21775.

The left ulna of CM 36019 (fig. 17E–H; table 11) is heavily deformed, having a nearly sigmoidal shape in anterior view. However, the anteromedial process of the proximal articular surface is longer than the anterolateral process, and they probably met at an acute angle. The olecranon process is weakly developed. In medial view, the shaft tapers distally throughout most of its length, but has a considerably expanded posterodistal edge, like the ulna of CM 21775. The anterior surface bears distinct ridges for articulation with the radius (fig. 17F, G).

The left radius (fig. 17I–L; table 11) is crushed medially but otherwise little deformed. It has an ovoid proximal articular surface (fig. 17I), a straight shaft with the usual ridges, and a well-developed attachment scar for interosseous ligaments on its distal portion. The distal articular surface is heavily deformed but does not appear to be beveled.

One left carpal is preserved among the material cataloged as CM 36019 (fig. 18A–F). Given its proportions (table 11), it most likely represents the medial element of the original two carpal bones in the plesiomorphic neosauropod manus (Osborn, 1904; Bonnan, 2003; Tschopp et al., 2015b). It is subcircular in proximal view, slightly wider than anteroposteriorly long. The proximal articular surface is relatively flat. In anterior view, the carpal tapers medially where it would have articulated with metacarpal I. The nonarticular surfaces are highly rugose and pitted, with a distinct vertical ridge on the lateral side, as in *Camarasaurus* sp. SMA 0002 (Tschopp

FIG. 16. Pectoral girdle elements of Camarasauridae indet. CM 36019. **A,** right scapula in lateral view; **B,** right coracoid in lateral view; **C,** right coracoid in medial view; **D,** right scapula in medial view. The specimen was initially included in CM 1256 and later recataloged as CM 36019. The numbers 193, 203 (scapula), and 207 (coracoid) correspond to field numbers. Scale bar applies to both bones. Abbreviations: **acr,** acromial ridge; **ca,** coracoid articulation; **gl,** glenoid; **gln,** glenoid notch; **sca,** scapular articulation; **tub,** tubercle. Photos by E.T. (A, C) and Andrew McAfee (B, D).

et al., 2015b). The distal articular surface is more irregular for the articulation with the metacarpals.

The left metacarpal I (fig. 18G–L; table 11) is mediolaterally compressed in its proximal part. It has a distinctly concave proximal portion of the posterolateral surface for articulation with metacarpal II (fig. 18H, I) and a slightly beveled distal articular surface with two small but recognizable condyles. There is a well-developed anterior projection on the anterolateral edge, close to the distal articular surface (fig. 18G).

Metacarpal II or III (more likely III) of CM 36019 (fig. 18M–R) has a triangular proximal articular surface and is very slender (table 11). It has a mediolaterally compressed distal articular surface that is probably an artifact of diagenesis. The distal condyles have a clear intercondylar groove on the posterior surface of the bone (fig. 18O).

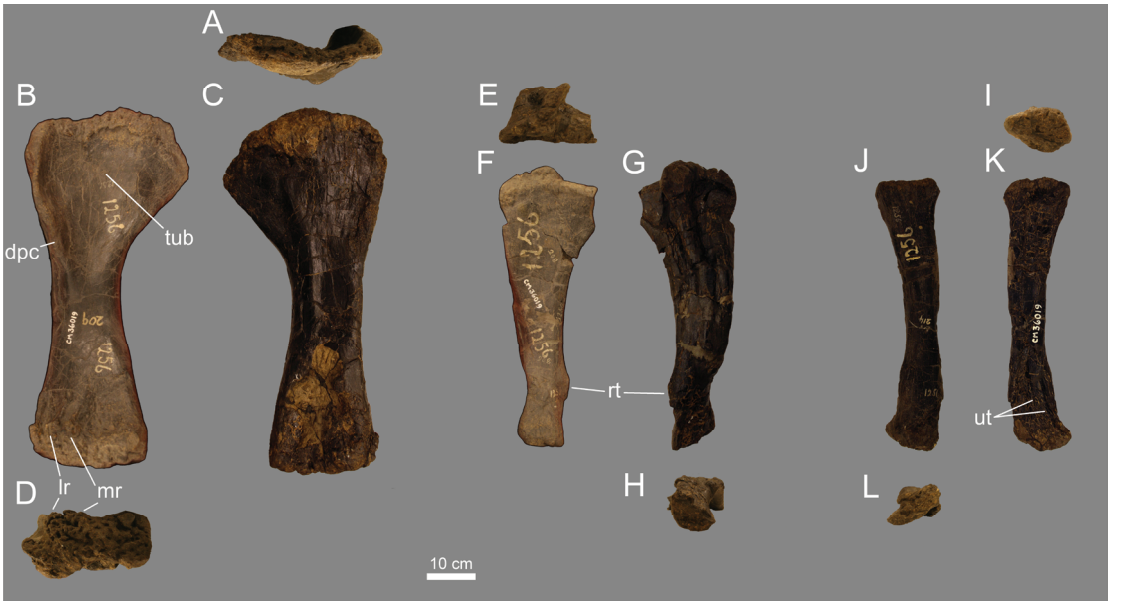

FIG. 17. Forelimb elements of Camarasauridae indet. CM 36019. Right humerus in **A,** proximal; **B,** anterior; **C,** posterior; and **D,** distal views. Left ulna in **E,** proximal; **F,** medial; **G,** lateral; and **H,** distal views. Left radius in **I,** proximal; **J,** anterior; **K,** posterior; and **L,** distal views. The specimen was initially included in CM 1256 and later recataloged as CM 36019. The numbers 209 (humerus), 208 (ulna), and 214 (radius) correspond to field numbers. Scale bar applies to all bones. Abbreviations: **dpc,** deltopectoral crest; **lr,** lateral ridge; **mr,** medial ridge; **rt,** tubercle for articulation with radius; **tub,** tubercle; **ut,** tubercle for articulation with ulna. Photos by Andrew McAfee (A, C–E, G–M) and E.T. (B, F).

Metacarpal III or IV (more likely IV) is in two pieces, with little to no missing material between the parts. The distal portion is diagenetically mediolaterally compressed. The proximal articular surface is triangular. The bone is longer than the probable metacarpal III of CM 36019, but about equally slender (table 11). The distal articular surface has a distinctly distally projecting, mediolaterally narrow lateral condyle.

Skull: A well-preserved left dentary (CM 36670) is the only cranial element present among the RFPR Quarry B material. It was initially cataloged as CM 312 and was referred to as such by Madsen et al. (1995). It was likely renumbered because there is no clear indication that would support an attribution to the same individual as the caudal vertebrae of CM 312 (see below).

The dentary CM 36670 (fig. 19; table 12) expands from posterior to anterior toward the symphysis but does not develop a chinlike ventral process as would be typical for flagellicaudatans (Whitlock, 2011a; Tschopp et al., 2015a). There is a poorly developed, obliquely oriented canal extending from posterodorsal to anteroventral along the lateral surface of the dentary, which was interpreted as a synapomorphy of *Camarasaurus* by Wilson and Sereno (1998) and Wilson (2002). The symphysis is dorsoventrally tall and ellipsoid, with subparallel anterior and posterior borders. The Meckelian canal is wide at the posterior end of the dentary, and tapers strongly to a point at about midlength, from where it continues as a weakly developed groove before widening slightly at the symphysis. There are 11 tooth positions, but no functional teeth are preserved and no replacement teeth are visible. The alveoli are generally large and subcircular but decrease slightly in diameter distally.

Dorsal Vertebrae: The centrum of the dorsal vertebra CM 36040 is strongly opisthocoelous

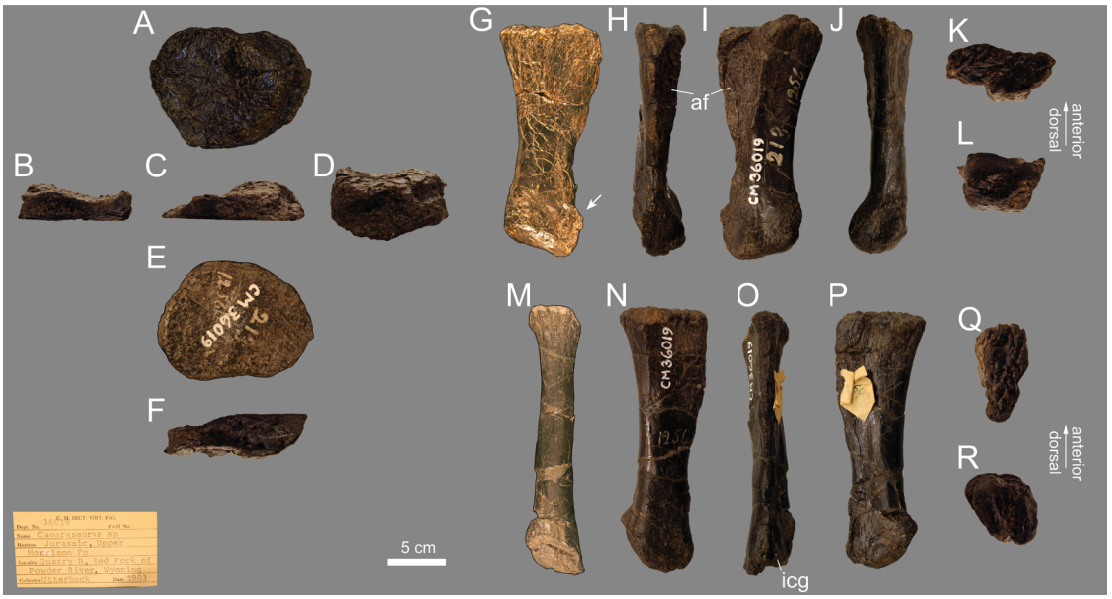

FIG. 18. Carpus and manus elements of Camarasauridae indet. CM 36019, with original specimen label. Large left carpal in **A,** distal; **B,** ?lateral; **C,** ?anterior; **D,** ?medial; **E,** proximal; and **F,** ?posterior views. The distal surface faces toward the top of panels B–D, and toward the bottom in F. Left metacarpal I in **G,** anterior; **H,** lateral; **I,** posterior (palmar); **J,** medial; **K,** proximal; and **L,** distal views. Note the distinct anterior projection toward the distal end (arrow in G). Left metacarpal ?III in **M,** anterior; **N,** lateral; **O,** posterior (palmar); **P,** medial; **Q,** proximal; and **R,** distal views. The specimen was initially included in CM 1256 and later recataloged as CM 36019. The number 213 is a field number. It is unclear what the sheet attached to metacarpal ?III may represent. Scale bar applies to all bones. Abbreviations: **af,** articular facet; **icg,** intercondylar groove. Photos by Andrew McAfee (A–D, F, H–M, O–S) and E.T. (E, G, N).

(fig. 20) and wider transversely than tall dorsoventrally (table 13). The ventral surface is transversely wide and convex. A small pleurocoel pierces the anterodorsal portion of the lateral surface of the centrum. The right pleurocoel is divided into dorsal and ventral subfossae by a horizontal lamina. Anterior to the pleurocoel, the parapophyses project ventrolaterally. They are connected posteriorly to the PCPL and dorsally to the paradiapophyseal lamina (PPDL), which might represent a captured ACDL (see Wilson, 2012, for an explanation of the concept of lamina capture).

The base of the neural arch is formed by strong CPRL and CPOL and laminar but well-developed PPDL and PCDL. The PPDL and PCDL unite at the ventral edge of the transverse process and enclose a very deep, subtriangular CDF. The prezygapophyseal centrodiapophyseal fossa (PRCDF) is particularly deep posteromedial to the CPRL, and bears two distinctly delimited, suboval subfossae below the transverse process. The prezygapophyses are connected medially by the interprezygapophyseal lamina (TPRL), which is widely V-shaped in anterior view and supported ventrally by a short single interprezygapophyseal lamina (sTPRL; sensu Carballido and Sander, 2014) that extends ventrally from the TPRL along the vertebral midline toward the roof of the neural canal but fades before reaching this opening. The prezygapophyseal facets are large, mediolaterally wider than anteroposteriorly long, and suboval in outline. They are weakly mediolaterally convex. Lateral to the prezygapophyseal facet is a distinct tuberosity that projects slightly anteriorly from the

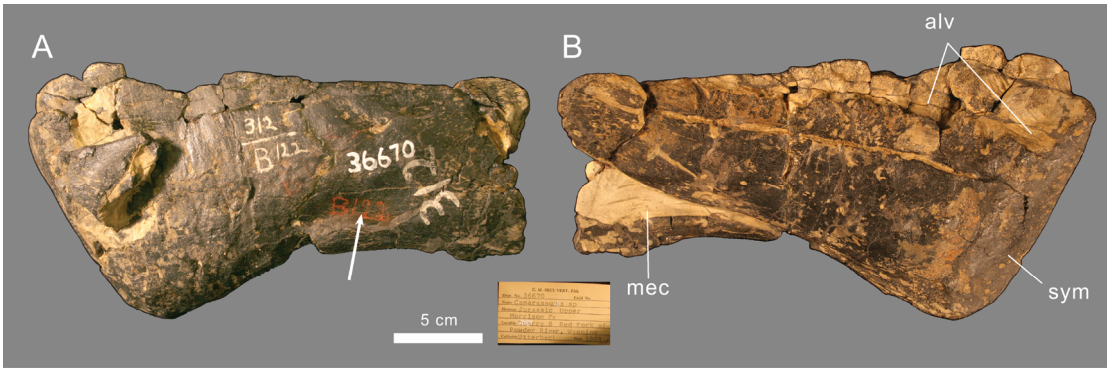

FIG. 19. Left dentary of Camarasauridae indet. CM 36670 in lateral (A) and medial (B) views, with original specimen label. Note the canal on the lateral surface that was interpreted as an autapomorphy of *Camarasaurus* (arrow; see text). The dentary was initially cataloged as CM 312 and later recataloged as CM 36670. The number B122 likely represents a field number. Scale bar applies to both views. Abbreviations: **alv,** alveoli; **mec,** Meckelian canal; **sym,** symphysis. Photos by Enrica Sarotto.

PRDL. The SPRL and PRDL are distinct. The transverse processes are very wide anteroposteriorly but lack their lateral extremities. In addition to the PPDL, PCDL, and PRDL, the transverse processes are connected to the PODL. There is no SPDL, which is probably due to the anterior position of this vertebra within the dorsal series. The SPRL are angled posteriorly, enclosing a relatively distinct subfossa within the SDF. The neural spine is bifurcated, with apparently strongly diverging but probably dorsoventrally low metapophyses (their ends are broken off, so their original dorsal extent can only be estimated). There is no median tubercle within the rather U-shaped notch between the metapophyses, which has traditionally been interpreted to be typical of *Camarasaurus* (McIntosh, 1990a, 1990b). The postzygapophyses are ellipsoid with the long axis oriented mediolaterally. There is a weak epipophysis but no indication of an interpostzygapophyseal lamina (TPOL).

Caudal Vertebrae: Both anterior caudal vertebrae of CM 36032 are strongly anteroposteriorly compressed. One is nearly complete and most likely represents the first caudal vertebra (fig. 21A–D), based on the fact that there are no articular facets for chevrons. The second element is damaged and strongly reconstructed, and so provides little morphological information.

The first caudal vertebra of CM 36032 (fig. 21A–D) has a centrum that is transversely very wide and dorsoventrally tall (table 14). The centrum is amphicoelous and subcircular in anterior and posterior view. Neither pneumatic nor blind fossae or foramina are present on the lateral and ventral surfaces. The ventral surface is convex but lacks a keel. There are no distinct chevron facets. The transverse processes are subtriangular in anterior view, with a dorsoventrally tall lateral end and a concave anterior surface due to the presence of weak ACDL and PRDL. The lateral end of the transverse process is subtriangular in lateral view, with the tip pointing dorsally and slightly anteriorly. It therefore does not have the more rectangular wing shape typical of Diplodocimorpha (Whitlock, 2011a). The neural arch occupies the entire length of the centrum. It is curved in lateral view, with the pedicels leaning slightly anteriorly and the spine summit inclined posteriorly. The prezygapophyses overhang the centrum, whereas the postzygapophyses do not. Indistinct SPRLs follow the anterior edge of the neural spine, diminishing dorsally. The SPOLs are distinct, project posteriorly at the base of the spine, and fade dorsally. There is no contact between the SPRL and SPOL on the lateral surface of the neural spine. The spine summit is greatly expanded transversely, in a rounded fash-

TABLE 12

Measurements of left dentary of Camarasauridae indet. CM 36670 from RFPR Quarry B (in mm; see fig. 19)

Dorsoventral height of symphysis	142
Anteroposterior length of symphysis	41
Number of teeth/alveoli	11

TABLE 13

Measurements of anterior dorsal vertebra of Camarasauridae indet. CM 36040 from RFPR Quarry B (in mm; see fig. 20)

Centrum length	290
Centrum length without anterior condyle	200
Posterior cotyle dorsoventral height	185
Posterior cotyle transverse width	265
Transverse process mediolateral length (as preserved)	350
Neural arch pedicel dorsoventral height	170

TABLE 14

Measurements of caudal vertebrae referred to Camarasauridae indet. from RFPR Quarry B (in mm)
Measurements with asterisk estimated; measurements with dagger indicate that the vertebra in question is incomplete in the measured dimension).

	CM 36032	**CM 36031**		
	Caudal vertebra 1[1]	Anteriormost caudal vertebra[2]	Anterior caudal vertebra[3]	Midcaudal vertebra[4]
Centrum length	104	133	140	138
Posterior cotyle dorsoventral height	275*	205	188	133
Posterior cotyle transverse width	306	167	154	116
Dorsoventral height (total)	535	455	305†	244
Neural spine maximum transverse width	105	72	38†	21
Neural spine minimum transverse width	39	38	35†	24
Neural spine anteroposterior length at summit	66	101	61†	82
Neural arch dorsoventral height	295	250	127†	109
Elongation Index (sensu Wilson and Sereno, 1998)	0.38	0.64	0.74	1.04
Average Elongation Index (sensu Chure et al., 2010)	0.36	0.72	0.82	1.11

[1] Element with anteroposteriorly compressed centrum (see fig. 21A–D).
[2] Element with dorsoventrally tall transverse process (not figured).
[3] Nearly complete (see fig. 21F–H).
[4] Bears old, handwritten label 862 (see fig. 21I–L).

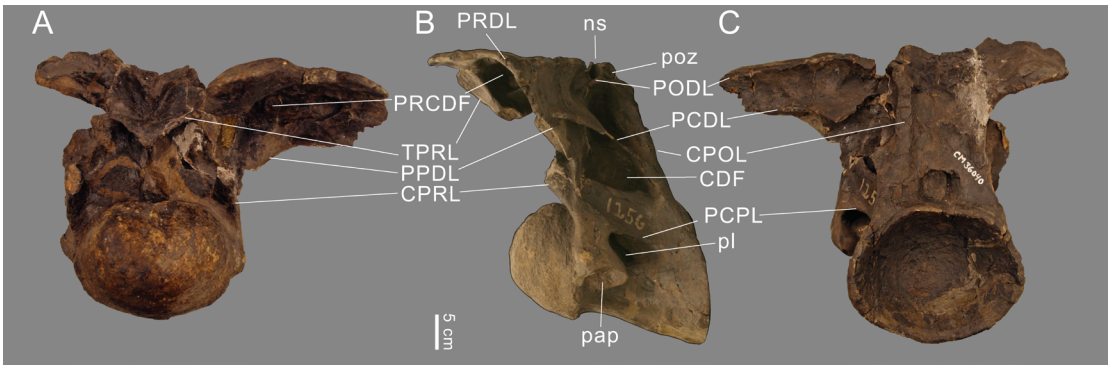

FIG. 20. Anterior dorsal vertebra of Camarasauridae indet. CM 36040 in **A,** anterior; **B,** left lateral; and **C,** posterior views. Scale bar applies to all views. The specimen was initially cataloged as CM 1256 and later recataloged as CM 36040. Abbreviations: **CDF,** centrodiapophyseal fossa; **CPOL,** centropostzygapophyseal lamina; **CPRL,** centroprezygapophyseal lamina; **ns,** neural spine; **pap,** parapophysis; **PCDL,** posterior centrodiapophyseal lamina; **PCPL,** posterior centroparapophyseal lamina; **pl,** pleurocoel; **PODL,** postzygodiapophyseal lamina; **poz,** postzygapophyses; **PPDL,** paradiapophyseal lamina; **PRCDF,** prezygapophyseal centrodiapophyseal fossa; **PRDL,** prezygodiapophyseal lamina; **TPRL,** interprezygapophyseal lamina.

ion. The expansion is restricted to the dorsalmost third of the spine.

The 16 caudal vertebrae of CM 36031 can be divided into nine anterior elements (six with well-developed transverse processes, three with reduced transverse processes), and seven midcaudal vertebrae without transverse processes (following the definition of Mannion et al., 2013). The anterior caudal vertebrae of CM 36031 have rounded centra (fig. 21F–H) that are higher than wide and relatively short (table 14). As in CM 36032, there is no indication of pneumaticity. The ventral surfaces of the anteriormost elements of CM 36031 are concave, with distinct ridges connecting the anterior and posterior chevron facets. In more posterior vertebrae, the ventral surface becomes flat. Transverse processes are triangular in axial view in the anteriormost elements, and none of the laminae supporting the processes are well developed. The processes are expanded anteroposteriorly and ventrally at their lateral end. The neural arch pedicels are restricted to the anterior part of the centrum and are angled anteriorly. Both the pre- and postzygapophyses overhang the centrum anteriorly and posteriorly, respectively. There is a hyposphenal ridge ventromedial to the postzygapophyses. The area anterior to the postzygapophyseal facets is rather flat. The dorsal portion of the neural spine is bulbous. Three anterior caudal vertebrae, which would represent the transition from bulbous to parallel distal ends, are broken, so we cannot say whether this transition was gradual or abrupt. The SPOL is distinct but not significantly posteriorly extended as it is in some *Camarasaurus* specimens (e.g., SMA 0002; E.T., personal obs.). The PRSL projects anteriorly.

The midcaudal vertebrae of CM 36031 (fig. 21I–L; the vertebrae without transverse processes but retaining well-developed zygapophyses; Mannion et al., 2013) are relatively short, with a centrum that is dorsoventrally higher than transversely wide and that has a horizontal ridge along the lateral surface. There are no distinct openings on the lateral or ventral surfaces. The articular facets for the chevrons are distinct both anteriorly and posteriorly, but the posterior facets are more developed. These facets render the surface between them concave, but these concavities diminish toward the center, where the surface becomes transversely flat. The neural arch pedicels are located more anteriorly than posteriorly, but the neural arch as a whole,

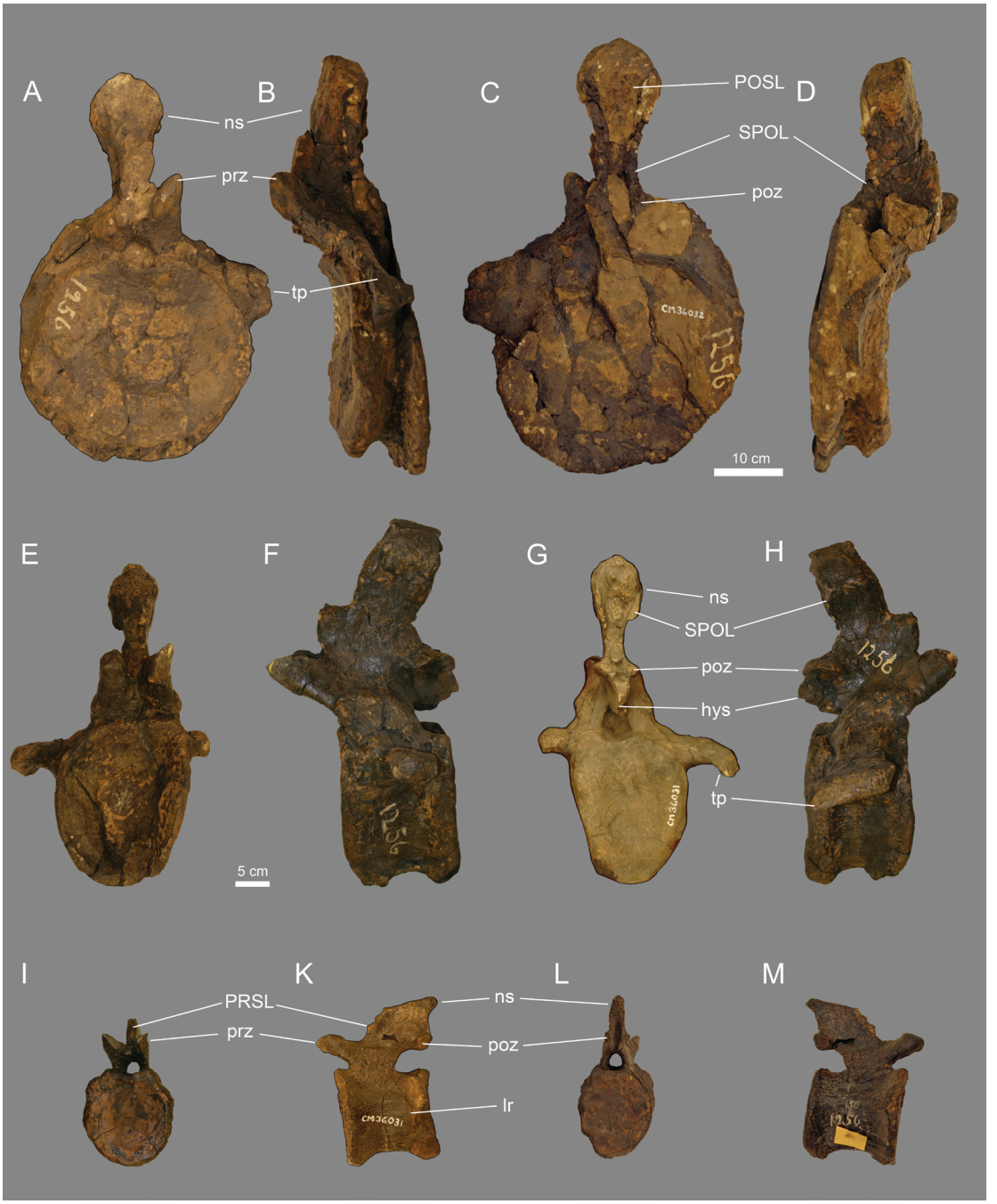
A
B
C
D
ns
prz
tp
POSL
SPOL
poz
10 cm
E
F
G
H
5 cm
ns
SPOL
poz
hys
tp
I
K
L
M
PRSL
prz
ns
poz
lr

including the neural spine, is situated directly above the centrum and surpasses it both anteriorly and posteriorly. The lateral surface of the pedicels is rugose. The neural spine (where complete) is low and anteroposteriorly elongate. Prezygapophyseal facets are mediolaterally convex. Weak SPRLs remain on the anterolateral edge of the spine, so that there is no contact with the SPOLs. Between the SPRL, there is a well-developed PRSL with anteriorly projecting spurs at midheight of the spine. The postzygapophyseal facets are concave and separate from one another; they are not connected by any lamina or hyposphenal ridge. The neural spine overhangs the postzygapophyses posteriorly and tapers slightly posterodorsally.

Chevrons: The chevrons CM 1253 (fig. 22) are from the anteriormost portion of the tail. The anteriormost elements are proximodistally long, decreasing considerably in length from the sixth or seventh preserved element toward the posterior (table 15). None of the chevrons has a bridged hemal canal (which would be typical for anterior chevrons of diplodocids; McIntosh, 1990a, 1990b), although in some elements, the articular facets for the caudal vertebrae are nearly in contact on the midline. The articular surfaces are subdivided into two facets that articulate with the caudal vertebrae located anteriorly and posteriorly, respectively, but these facets are not as distinctly separated as in *Camarasaurus lewisi* (BYU 9047; Jensen, 1988; McIntosh et al., 1996b). The anteriormost chevrons have distal shafts with a subcircular cross section that curve considerably posteriorly below the hemal canal. The anteroposterior length of the distal shaft increases gradually along the sequence. The distal end of the shaft tapers in more anterior chevrons, but in the last preserved elements of the series (around the 10th to 12th preserved chevrons; fig. 22E, F) it expands transversely, especially posteriorly. A short, rodlike element with a large proximal articular facet possibly represents one half of the first chevron in the series (fig. 22A, B).

Pectoral Girdle: The partial right scapula CM 36029 has a widely expanded acromion (table 16) and appears to have an S-shaped articular surface with the coracoid in lateral view. It is not clear whether the acromion was pierced by a foramen as in the scapulae of *Camarasaurus supremus* (Osborn and Mook, 1921) as well as in other specimens referred to this genus (e.g., SMA 0002). The glenoid is beveled medially. There is a subtriangular process on the anteriormost portion of the ventral edge of the scapular blade. The medial surface itself does not bear a rugosity or scar, unlike the condition in CM 36030 (see below). The cross section of the scapular blade is D-shaped.

Two additional pieces were originally cataloged under the same number (CM 36029). The large piece is the base of the shaft of an ischium, as indicated by its oval instead of D-shaped cross section and the presence of a muscle scar close to the lateral side. This piece matched the broken end of the left ischium CM 28848, which we referred to Flagellicaudata (see above), and is thus removed from CM 36029. The second, smaller fragment cataloged as CM 36029 preserves two rounded, somewhat concave articular

FIG. 21. Caudal vertebrae of Camarasauridae indet. Anterior caudal vertebra CM 36032 (A–D), anterior caudal vertebra of CM 36031 (E–H), and midcaudal vertebra of CM 36031 (I–M) in anterior (A, E, I), left lateral (B, F, K), posterior (C, G, L) and right lateral (D, H, M) views. The figured caudal vertebra CM 36032 is likely the first in the caudal series. Note the bulbous expansion of the neural spine summits in the anterior caudal vertebrae. The 10 cm scale bar applies to all views of CM 36032, whereas the 5 cm scale bar applies to both bones and all views of CM 36031. Both specimens were initially cataloged as CM 1256 and later recataloged as CM 36032 (A–D) and 36031 (E–M). The caudal vertebrae CM 36031 and the chevrons CM 1253 (fig. 22) might pertain to a single individual. Abbreviations: **hys,** hyposphenal ridge; **lr,** lateral ridge; **ns,** neural spine; **POSL,** postspinal lamina; **poz,** postzygapophyses; **PRSL,** prespinal lamina; **prz,** prezygapophyses; **SPOL,** spinopostzygapophyseal lamina; **tp,** transverse process. Photos by E.T. (A, G) and Andrew McAfee (B–F, H–M).

FIG. 22. Chevrons of CM 1253. Probable first chevron, ?right half, in **A,** lateral and **B,** medial views. Anterior chevron in **C,** right lateral and **D,** posterior views. Middle chevron in **E,** anterior and **F,** posterior views; note the transverse expansion of the distal end of the shaft (arrows). The caudal vertebrae CM 36031 and the chevrons CM 1253 might pertain to a single individual. Scale bar applies to all chevrons. Photos by E.T.

surfaces that are in contact with one another. This piece might be a portion of the coracoid that articulated with the scapula of CM 36029, in which case the articular surfaces may represent the glenoid and the scapular facet, respectively.

The acromial ridge of the largely complete left scapula CM 36043 forms a right angle with the distal blade (fig. 23A, B). The glenoid surface is not beveled. There is a subtriangular process on the ventral edge, very close to the glenoid and anterior to the acromial ridge. The surface posterior to the acromial ridge is concave, which occurs in many diplodocids (Upchurch et al., 2004; Tschopp et al., 2015a) but has also been recovered as a synapomorphy of Camarasauromorpha (Mannion et al., 2017). The distal blade is D-shaped and widely expanded distally (table 16), both ventrally and dorsally. Because the dorsal edge is incompletely preserved, it is unclear whether a separate dorsal process was present. The distal expansion reaches nearly as high as the acromion and has a rounded dorsal corner and an angular ventral corner.

The right coracoid CM 36027 (fig. 23C, D; table 16) is subquadrangular in shape, with a widened, relatively rounded anterodorsal corner. The coracoid foramen is fully enclosed by bone. The anterior margin of the coracoid remains about equally thick throughout its extent. The scapular facet is sigmoidal in lateral view. The glenoid is widely expanded mediolaterally and bordered anteriorly by a shallow but distinct and relatively long notch. There is no distinct glenoid lip.

Pelvic Girdle: The right pubis of CM 28846 has a very wide shaft and an elongate ischial articular surface that extends nearly to midlength (fig. 24; table 17). There is no ambiens process. The ischia of CM 28846 have bladelike distal shafts, with a small, rugose ridge at the base (fig. 24). The shafts articulate medially.

The pubis of CM 36024 (fig. 25; table 17) is relatively stout. The ischial articular surface extends distally to slightly beyond midshaft. As in CM 28846, and in contrast to flagellicaudatans (Tschopp et al., 2015a), there is no distinct ambiens process. The ischium of CM 36024 is relatively slender and lacks the distal part of the shaft. There is a weakly developed scar on the lateral surface. The distal shaft is too incomplete to provide useful morphological information.

TABLE 15

Measurements of chevrons of Camarasauridae indet. CM 1253 from RFPR Quarry B
Chevrons labeled A–M in anterior to posterior sequence; in mm.

	A (single)[1]	**B**[2]	**C**	**D**	**E**	**F**	**G**	**H**	**I**	**J**	**K**	**L**[3]	**M**
Field number	85		88	87	78	76	66	69	68	64	77	42	
Proximodistal length	153	345	377	390	360	375		315	283	246	234	217	169
Proximal transverse width		132	141	145	106	117	115	120	124		102	107	75
Proximodistal depth of cleft		115	108	108	109	90	84	83	62	60	86	85	70

[1] See figure 22A–B.
[2] See figure 22C–D.
[3] See figure 22E–F.

TABLE 16

Measurements of pectoral girdle elements referred to Camarasauridae indet. from RFPR Quarry B (in mm)
Asterisk indicates estimated measurements.

	CM 36029	**CM 36043**	**CM 36027**
	Scapula, R[1]	Scapula, L[2]	Coracoid, R[3]
Anteroposterior length	760 (preserved length)	1252	435
Acromion height (oblique, from ventralmost to dorsalmost point)		570	
Dorsoventral height of acromion (perpendicular to scapular blade)	710	510*	
Minimum dorsoventral height of scapular blade	170*	182	
Maximum dorsoventral height of scapular blade		462	
Dorsoventral height			555
Glenoid maximum diameter			145
Glenoid minimum diameter (perpendicular to maximum)			105

[1] Not figured.
[2] See figure 23A–B.
[3] See figure 23C–D.

Hind Limb: The femora CM 36021 are relatively short and stout (fig. 26; table 18), with an elevated femoral head. They have a lateral bulge on the proximal part of the lateral surface of the shaft, but are not medially deflected proximally as would be typical for titanosauriforms (Wilson, 2002; D'Emic, 2012). The fourth trochanter of CM 36021 is located on the medial edge of the posterior surface and does not curve toward the center of the shaft distally. Its medial surface is concave. A ridge extends along the anterolateral edge of the shaft close to the distal end, as in the camarasaurid TMP2007.003.0003 (E.T., personal obs., 2017). The lateral epicondyle of the distal articular surface is distinctly expanded laterally, similar to the state in *Camarasaurus supremus* AMNH FARB 5765 (Osborn and Mook, 1921: fig. 109).

The tibia and fibula CM 36020 (fig. 27A–D) are anteroposteriorly compressed and deformed. The cnemial crest of the tibia is heavily distorted. There is additional preparation damage, mostly punctures and gouges. The posterior surface of the tibia is badly crushed.

The tibia (fig. 27A, B; table 18) has an ellipsoid, anteroposteriorly elongate proximal articu-

FIG. 23. Pectoral girdle elements of Camarasauridae indet. A, B) left scapula CM 36043 in **A,** lateral and **B,** medial views. The scapula was initially cataloged as CM 1256 and later recataloged as CM 36043. Right coracoid CM 36027 in **C,** lateral and **D,** medial views. The coracoid was initially cataloged as CM 1256 and later recataloged as CM 36027. The number 206 (in C) corresponds to the field number. Abbreviations: **acr,** acromial ridge; **cof,** coracoid foramen; **gl,** glenoid; **gln,** glenoid notch; **sca,** scapular articular surface; **vp,** ventral process. Photos by E.T. (A, D) and Andrew McAfee (B, C).

FIG. 24. Right pubis and ischium (arranged as if articulated) of Camarasauridae indet. CM 28846 in **A,** medial and **B,** lateral views. Note the absence of a distinct, anteriorly protruding ambiens process (arrow, B). Abbreviations: **ac,** acetabular surface; **is,** ischium; **of,** obturator foramen; **pu,** pubis. Photos by Andrew McAfee (ischium) and E.T. (pubis).

lar surface. The cnemial crest initially projects anterolaterally, then curves laterally. The shaft is somewhat twisted, but deformation hinders any interpretation of the degree of this twist. The distal end is stepped for the articulation with the astragalus and has distinctly expanded anterior margins toward the medial side. No important morphological details can be observed from the damaged posterior surface, other than the possible presence of a relatively narrow crest on the posterolateral corner that extends proximally from the distal surface for about 200 mm.

The right fibula of CM 36020 (fig. 27C, D) has an anteroposteriorly long proximal end (table 18) and tapers from that region until midshaft. The rugosities of the proximal surface extend onto the lateral surface for 40–60 mm, forming a marked, steplike transition with the smooth surface of the shaft. On the proximal portion of the medial surface, there is a distinct, triangular tibial scar with a striated rugosity that tapers distally and extends over slightly less than one third the total length of the fibula. The distal end of the triangular scar is considerably expanded medially compared with the longitudinal axis of the shaft, but there does not seem to be a significant, corresponding deflection in the proximal shaft (but this might also be due to diagenetic deformation). The insertion for the m. iliofibularis (the fibular trochanter) is located on the proximal half of the lateral surface of the shaft and is oval in shape. The proximalmost portion of this trochanter is marked by a groove that extends distally along its midline until about half its proximodistal length. The distal end of the fibula is expanded significantly anteriorly and slightly less so posteriorly.

TABLE 17

Measurements of pelvic girdle elements referred to Camarasauridae indet. from RFPR Quarry B (in mm)

	CM 28846			CM 36024
	Pubis, R[1]	Ischium, L[2]	Ischium, R[3]	Pubis, R[4]
Proximodistal length	850	975	970	835
Length of puboischial articular surface	420			

[1] See figure 24.
[2] Not figured.
[3] See figure 24.
[4] See figure 25.

TABLE 18

Measurements of hind limb elements referred to Camarasauridae indet. from RFPR Quarry B (in mm)

	CM 36021		CM 36020		CM 36022
	Femur, L[1]	Femur, R[2]	Tibia, R[3]	Fibula, R[4]	Fibula, R[5]
Proximodistal length	1315	1320	709	718	910
Proximal mediolateral width	500	470	107	38	
Proximal anteroposterior length		165	252	168	225
Minimum shaft mediolateral width	223	230	115	77	62
Minimum shaft anteroposterior length		100	68	45	
Distal mediolateral width	435	405	208	53	98
Distal anteroposterior length	265	255	96	168	165
Proximodistal length from femoral head to distal end of fourth trochanter		685			
Proximodistal length of triangular scar					285
Proximodistal distance from proximal surface to distal end of trochanter					435

[1] See figure 26.
[2] Not figured.
[3] See figure 27A–B.
[4] See figure 27C–D.
[5] See figure 27E–F.

The right fibula CM 36022 (fig. 27E, F) is very similar to, though substantially larger than, that of CM 36020. It has an equally developed triangular tibial scar on the proximal portion of the medial side that occupies nearly one third the length of the shaft (table 18). Also as in CM 36020, the trochanter has a concave surface and is located proximal to midshaft. The medial surface distal to the tibial scar is anteroposteriorly concave. The distal end of the fibula is expanded mediolaterally and anteriorly and bears a short vertical ridge on the anterior surface just proximal to the distal end. The distal surface is slightly beveled, extending further distally on the posterior than on the anterior side.

Identification

McIntosh (1981) and Wilhite (2003) identified CM 21775 as *Camarasaurus*. The specimen can be excluded from Diplodocoidea due to its asymmetrically expanded proximal half of the

FIG. 25. Right pubis of Camarasauridae indet. CM 36024. **A,** proximal; **B,** lateral; **C,** medial; and **D,** distal views. Scale bar applies to all views. Abbreviation: **ace,** acetabular margin. Photos by Andrew McAfee.

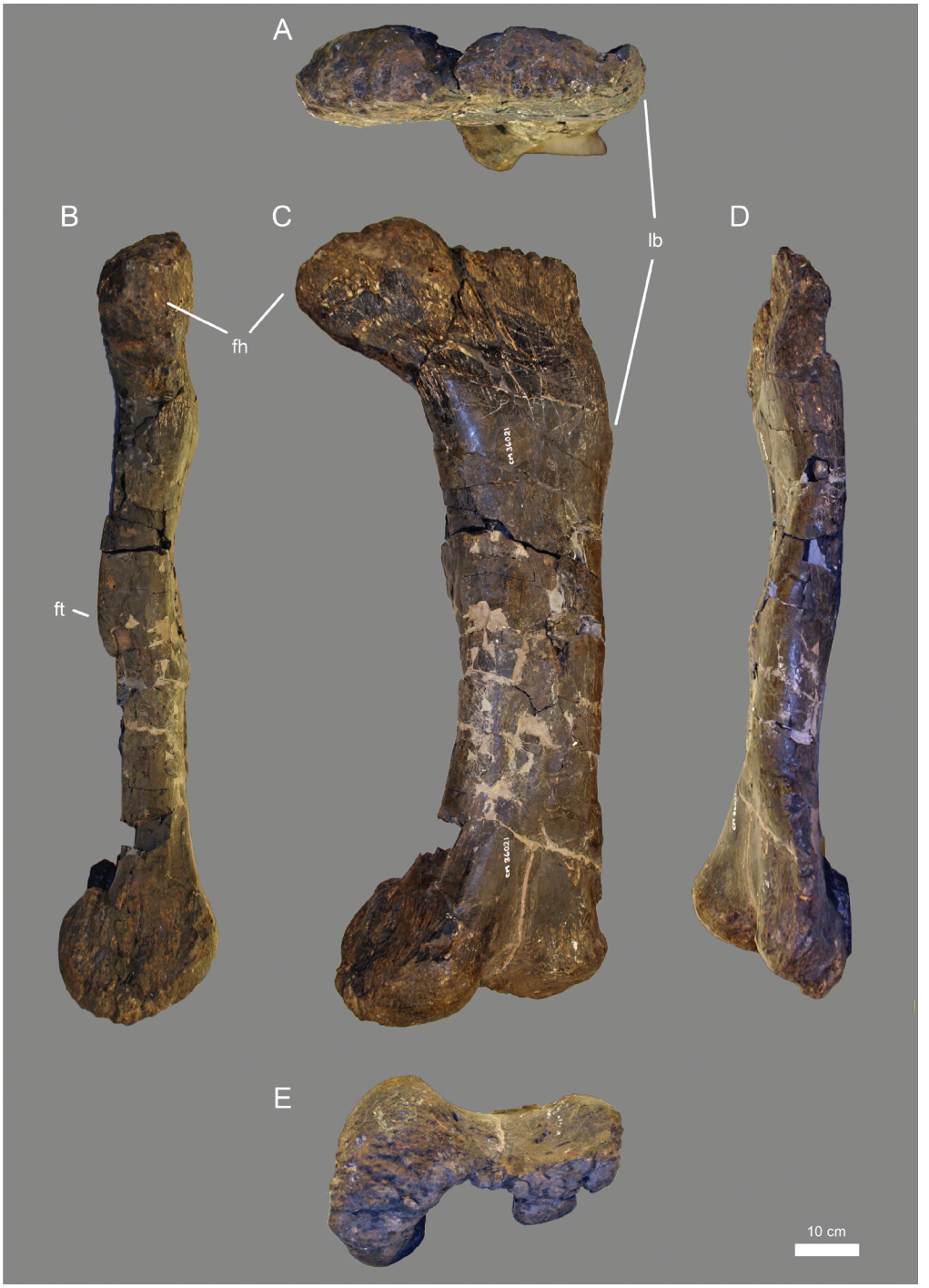

FIG. 26. Left femur of Camarasauridae indet. CM 36021. **A,** proximal; **B,** medial; **C,** anterior; **D,** lateral; and **E,** distal views. Scale bar applies to all views. Abbreviations: **fh,** femoral head; **ft,** fourth trochanter; **lb,** lateral bulge. Photos by Andrew McAfee.

FIG. 27. Hind limb elements of Camarasauridae indet. CM 36020 (A–D) and CM 36022 (E, F). Right tibia of CM 36020 in **A,** anterior and **B,** posterior views. Right fibula of CM 36020 in **C,** medial and **D,** lateral views. Right fibula of CM 36022 in **E,** medial and **F,** lateral views. The bones were initially cataloged as CM 1256 and later recataloged as CM 36020 (A–D) and CM 36022 (E, F). The numbers 215 and 216 correspond to field numbers. Scale bar applies to all bones/views. Abbreviations: **cc,** cnemial crest; **fit,** fibular trochanter; **tis,** tibial scar. Photos by E.T. (A–E) and Andrew McAfee (F).

humerus. It can be included in Camarasauromorpha based on the concave area posterior to the acromial ridge of the scapula, and excluded from Brachiosauridae based on the presence of a notch anterior to the glenoid on the coracoid (Mannion et al., 2017). The widely expanded distal blade of the scapula with a dorsal projection and the rectangular coracoid are most similar to *Camarasaurus grandis* YPM VP.001901 (Marsh, 1878) and *Lourinhasaurus alenquerensis* (Mocho et al., 2014) but different from *Camarasaurus supremus* AMNH FARB 5760/5761. Hence, we refer CM 21775 to Camarasauridae indet.

CM 36019 was identified as *Camarasaurus* by McIntosh (1981). The specimen is clearly macronarian due to its asymmetrical proximal humerus and its long metacarpals relative to radius length (metacarpal IV to radius proximodistal length ratio is 0.48 in CM 36019, diplodocoids have relatively shorter metacarpals; Wilson, 2002; Tschopp et al., 2015a, 2015b). The notch anterior to the glenoid on the coracoid excludes the specimen from Brachiosauridae (Mannion et al., 2017). Within Camarasauridae, the slenderness of metacarpal III (proximodistal length/distal mediolateral width = 4.7) most closely resembles the camarasaurids FMNH P25120 (5.1; Bonnan, 2001) and SMA 0002 (4.3; Tschopp et al., 2015b). However, CM 36019 differs from FMNH P25120 in having a relatively shorter metacarpal I compared with metacarpal IV (0.8 versus 1.0; Bonnan, 2001), and from SMA 0002 by the relatively shorter metacarpals compared with radius length (0.48 versus 0.56; Tschopp et al., 2015b). The scapula does not seem to bear the distinct dorsal projection that is present in *Camarasaurus grandis* YPM VP.001901 (Marsh, 1878), *Lourinhasaurus alenquerensis* (Mocho et al., 2014), and CM 21775, although this could be partly obscured by damage to the dorsal margin of the scapular blade in CM 36019. The potentially generically distinct *Camarasaurus lewisi* (Jensen, 1988;

McIntosh et al., 1996b; Mateus and Tschopp, 2013) has a more gracile humerus (BYU 9047 has a robusticity index of 0.26 compared with 0.32 in CM 36019; McIntosh et al., 1996b) and a slightly higher ulna to humerus length ratio (0.76 in BYU 9047, 0.71 in CM 36019; McIntosh et al., 1996b). However, no feature exists that would allow an unambiguous attribution to a species or genus within Camarasauridae, so we refer CM 36019 to Camarasauridae indet.

McIntosh (1981) and Madsen et al. (1995) identified the dentary CM 36670 as referable to *Camarasaurus*. This referral is supported by the presence of the canal on the lateral surface, which was proposed to be a synapomorphy of the genus (Wilson and Sereno, 1998; Wilson, 2002). However, no dentary is known for *C. lewisi* and *Lourinhasaurus alenquerensis*, so the distribution of this groove among Camarasauridae remains uncertain. We thus prefer to refer CM 36670 to Camarasauridae indet. until a systematic revision of the clade resolves character distributions and phylogenetic relationships at lower taxonomic levels.

The dorsal vertebra CM 36040 was referred to *Camarasaurus* by McIntosh (1981). The morphology of the bifurcated neural spine, with its wide, U-shaped notch without a median tubercle, clearly identifies the vertebra as that of a camarasaurid to the exclusion of *C. lewisi*, which has a more V-shaped notch (Jensen, 1988; McIntosh et al., 1996b). However, other than excluding an attribution to *C. lewisi*, it remains impossible to refer CM 36040 to a particular species or genus based on autapomorphies, so we assign the specimen to Camarasauridae indet.

McIntosh (1981) referred the caudal vertebrae CM 36032 and CM 36031 and the chevrons CM 1253 to *Camarasaurus*. The absence of pneumatic features in the vertebrae excludes them from Flagellicaudata (Tschopp et al., 2015a), and the presence of a lateral ridge excludes a referral to Titanosauriformes (Mannion et al., 2017). Among the known non-flagellicaudatan, non-titanosauriform taxa from the Morrison Formation, Camarasauridae is the only clade with a distinct and abrupt dorsal expansion of the caudal neural spines (Ikejiri et al., 2005). This expansion occurs in several species of *Camarasaurus* (Ikejiri et al., 2005) and also to some extent in *Lourinhasaurus alenquerensis* (Mocho et al., 2014). In *Camarasaurus*, Ikejiri et al. (2005) proposed that a gradual versus abrupt change from expanded to unexpanded neural spines distinguishes the species *C. lentus* and *C. grandis*. However, because the transition occurs within the three elements that lack neural spines, it is impossible to assess in CM 36031, the only camarasaurid specimen from RFPR with an extended series of anterior to midcaudal vertebrae. Therefore, we herein refer the caudal vertebrae of CM 36031 and CM 36032 to Camarasauridae indet.

The chevrons CM 1253 are more difficult to identify. Although the proximally open hemal canal that extends to near midlength of the chevron is most similar to camarasaurids among Morrison Formation sauropods, these features occur in many other sauropod taxa as well. However, based on McIntosh's (1981) interpretation that CM 1253 might belong to the same individual as CM 36031, we tentatively refer the former specimen to Camarasauridae indet. as well.

The pectoral girdle elements CM 36029, CM 36043, and CM 36027 were referred to *Camarasaurus* by McIntosh (1981). Only a few features of these bones have been recognized as synapomorphies of neosauropod clades in the past. However, the acromion of CM 36029 is considerably higher compared with the minimum dorsoventral height of the blade (4.2) than in any diplodocoid (2.1–3.7), and is instead at the higher end of the range within Macronaria (3.1–4.7) (Tschopp, unpubl. data). CM 36029 and CM 36043 are both distinguishable from brachiosaurids in the perpendicular arrangement of the acromial ridge and the distal blade (Tidwell et al., 1999; Schwarz et al., 2007). Finally, the widely expanded distal blade of CM 36043 also excludes a referral to Flagellicaudata. Excluding all of these possibilities, the most plausible referral for both scapulae is Camarasauridae indet.

The shallow but distinct glenoid notch supports a referral of the coracoid CM 36027 to either *Haplocanthosaurus* or Camarasauridae (Tschopp et al., 2015a; Mannion et al., 2017). CM 36027 can be distinguished from *Haplocanthosaurus* by its more rectangular outline (Hatcher, 1903), leaving a referral to Camarasauridae as the most plausible identification. Within this clade, the relatively indistinct glenoid lip anterior to the notch differs from the condition in GMNH-PV 101, which was referred to *C. grandis* by McIntosh et al. (1996a).

McIntosh (1981) listed CM 28846 and CM 36024 as *Camarasaurus*. The absence of a prominent ambiens process in the pubes and the bladelike distal ends of the ischia exclude a referral of this material to Flagellicaudata. The elongate puboischial contact is typical of macronarian sauropods. Within Macronaria, brachiosaurids generally have a less expanded anterior body of the pubis compared with camarasaurids and CM 28846 and CM 36024 (Janensch, 1961; Mannion et al., 2013; Mocho et al., 2016). We therefore refer CM 28846 and CM 36024 to Camarasauridae indet.

McIntosh (1981) referred the hind limb specimens CM 36021, CM 36020, and CM 36022 to *Camarasaurus*. Among sauropod femora, a lateral bulge occurs only in diplodocids and macronarians (Tschopp et al., 2015a). Within Macronaria, a medial deflection of the proximal end of the femur is often found in the sister clade of Camarasauridae or *Camarasaurus* (e.g., Wilson, 2002; D'Emic, 2012). The robusticity index (sensu Wilson and Upchurch, 2003) of 0.29 in CM 36021 is higher than in any diplodocid reported by Tschopp et al. (2015a), and similar to values found in the camarasaurids CM 11338 (0.30; Bonnan, 2001), OMNH 1794 (0.29; Wilhite, 2003), and *Lourinhasaurus* MIGM 4931 (0.28; Mocho et al., 2014). Finally, the strong dorsolateral expansion of the femoral head, the lateral extension of the lateral epicondyle, and the longitudinal ridge along the anterolateral margin of the distal shaft have not been observed in diplodocid sauropods. Within Camarasauridae, no unambiguous femoral features that would distinguish any particular genus or species are known. Therefore, we refer CM 36021 to Camarasauridae indet.

CM 36020 and CM 36022 can be referred to Camarasauridae based on the elongate, triangular scar on the proximomedial surface of the fibula, which was identified as an autapomorphic feature of the genus *Camarasaurus* by Wilson (2002), but that also occurs in *Lourinhasaurus alenquerensis* (Mocho et al., 2014). On this basis, we refer these specimens to Camarasauridae indet.

Sauropoda Marsh, 1878

Neosauropoda Bonaparte, 1986

Neosauropoda indet.

Referred Specimens: Several specimens from RFPR Quarry B cannot be identified to a clade more specific than Neosauropoda. These include a specimen that consists of associated caudal vertebrae, chevrons, and a partial ischium (CM 312), which will be described first. Two additional specimens that consist of midcaudal vertebrae (CM 36034, CM 36036) can be referred only to Neosauropoda, and these likely represent different portions of the same tail as CM 312 (see below). Two partial scapulae (CM 36028, CM 36030) do not preserve any characters that allow an identification beyond Neosauropoda, as is also the case for a nearly complete right ischium (CM 28847) and a right tibia (CM 36023).

The specimen CM 312 (figs. 28, 29) initially included several bones that have since been recataloged, most likely because they could not be unambiguously attributed to the same individual as the caudal vertebrae (see above and suppl. table 2, available at https://doi.org/10.5531/sd.sp.36). Only the caudal vertebrae, chevrons, and the distal end of an ischium (fig. 28) can be assigned to a single individual (following McIntosh, 1981). A series of dorsal ribs cataloged as CM 312 most likely belongs to another individual (McIntosh, 1981), but

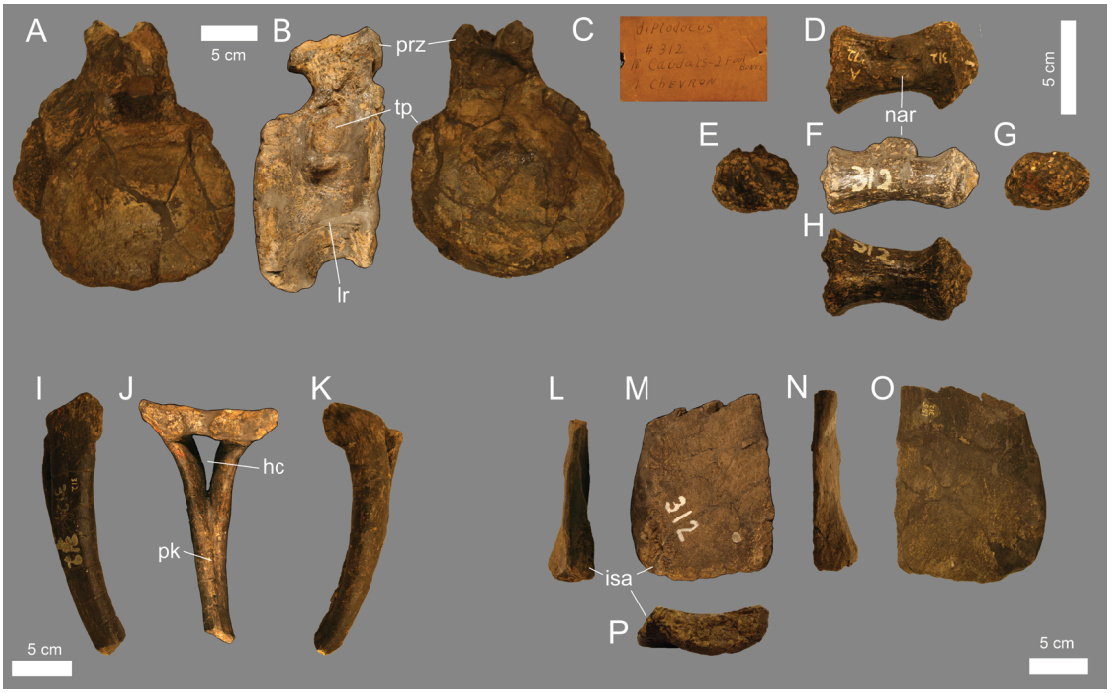

FIG. 28. Caudal vertebrae, chevron, and partial ischium of Neosauropoda indet. CM 312, with original specimen collection tag. Partial anterior caudal vertebra lacking the neural spine in **A,** posterior; **B,** right lateral; and **C,** anterior views. Partial posterior caudal vertebra lacking part of the neural arch in **D,** dorsal; **E,** anterior; **F,** left lateral; **G,** posterior; and **H,** ventral views. Partial anterior chevron lacking the distal end of the shaft in **I,** left lateral; **J,** posterior; and **K,** right lateral views. Distal end of right ischium in **L,** medial; **M,** dorsal; **N,** lateral; **O,** ventral; and **P,** distal views; proximal toward the top in L–P. Scale bars are different for the four bones. Abbreviations: **hc,** hemal canal; **isa,** ischial articular surface; **lr,** lateral ridge; **nar,** neural arch; **pk,** posterior keel; **prz,** prezygapophysis; **tp,** transverse process. Photos by Andrew McAfee (A, C–E, G–I, K, L, N–P) and E.T. (B, F, J, M).

these were not recataloged because we could not confidently assess their identity or association. They are described at the end of this section. Two left metatarsals (I and III or IV) initially cataloged as CM 312 that cannot be confidently referred to the same individual specimen as the tail (McIntosh, 1981), and are likely from a different taxon, were recataloged as CM 90277 (see above). CM 36034 includes one nearly complete anterior midcaudal vertebra and a second vertebra of similar serial position that lacks nearly all the neural spine (field number 179; fig. 30). CM 36036 is a single midcaudal vertebra that lacks most of the neural spine. Morphological features of both CM 36034 and CM 36036 indicate that they are likely from different portions of the same tail as CM 312. CM 36028 is the incompletely preserved distal end of a right scapular blade. It may be the distal end of CM 36029, but if so, there would be pieces missing between the two preserved portions (which might be included in the uncataloged material or the fragments still numbered as CM 1256). CM 36030 is a partial left scapula that is poorly preserved (only the distal scapular blade remains) and observable only on the medial side. The proximal end of the right tibia CM 36023 is compressed and anteroposteriorly flattened. Its anterior surface is severely crushed.

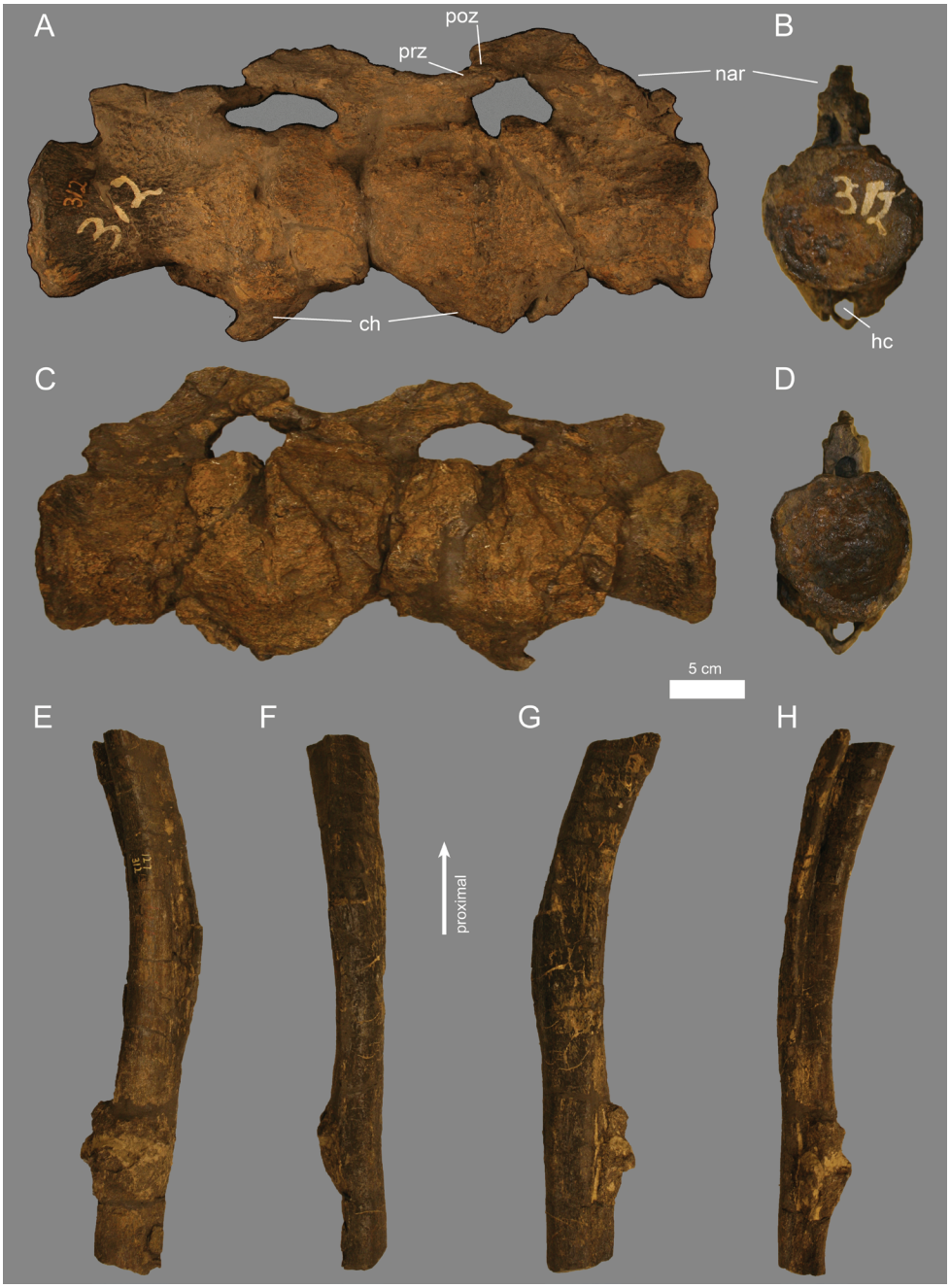

FIG. 29. Pathological bones of Neosauropoda indet. CM 312. Three fused midcaudal vertebrae and two fused chevrons in **A,** right lateral; **B,** anterior; **C,** left lateral; and **D,** posterior views. Left dorsal rib in **E,** anterior; **F,** lateral; **G,** posterior; and **H,** medial views. Note the bulbous bony outgrowths along the articulations between the vertebral centra (A, C), and at the distal end of the preserved portion of the rib (E–H). Scale applies to both elements. The number 127 on the dorsal rib represents a field number. Abbreviations: **ch,** chevron; **hc,** hemal canal; **nar,** neural arch; **poz,** postzygapophysis; **prz,** prezygapophysis. Photos by Andrew McAfee (B–H) and E.T. (A).

TABLE 19

Measurements of selected elements (in mm) of Neosauropoda indet. CM 312 from RFPR Quarry B

	Anterior caudal vertebra[1]	Midcaudal vertebra[2]	Posterior caudal vertebra[3]	Distal caudal vertebra[4]
Centrum length	123	148	100	81
Posterior cotyle height	125	90	34	31
Posterior cotyle width	135	68	55	47
Dorsoventral height (total)		147	59	33
Elongation Index (sensu Wilson and Sereno, 1998)	0.98	1.64	2.94	2.61
Average elongation index (sensu Chure et al., 2010)	0.95	1.87	2.25	2.08

[1] See figure 28A–C.
[2] Field number 177; not figured.
[3] Not figured.
[4] Field number 172; figure 28D–H.

Description

CM 312: Two anterior caudal vertebrae are relatively short anteroposteriorly and have anterior and posterior intercentral articular surfaces that are widely expanded transversely (fig. 28A–C; table 19). The centra are strongly amphicoelous and have well-developed lateral ridges ventral to the transverse processes (fig. 28B), resulting in deeply concave ventrolateral sides. A single ventral ridge connects the distinct posterior chevron facets with the margin of the anterior cotyle, which lacks chevron facets. A very similar arrangement occurs in other caudal vertebrae among the RFPR Quarry B material (CM 36034, CM 36036), which would also fit in general size and morphology into a continuous, combined caudal series with CM 312, indicating that these specimens all belong to a single individual (see below). The transverse processes lie completely on the centrum, and are anteroposteriorly short knobs that are somewhat inclined anteriorly (fig. 28B). The neural arch pedicels are located more anteriorly than posteriorly, but the neural arches themselves are too incomplete to determine whether they were shifted anteriorly in their entirety. The prezygapophyses project anterior to the anterior rim of the centrum.

Midcaudal vertebrae (defined as those that lack transverse processes but that retain well-developed zygapophyses, following Mannion et al., 2013; Tschopp et al., 2015a) have amphicoelous centra that are hourglass shaped in ventral view (table 19). There is no ventral hollow, nor are there longitudinal ridges on the lateral sides of the centrum, similar to the midcaudal vertebrae of an undescribed skeleton generally regarded as that of *Haplocanthosaurus* (FHPR 1106; J. Foster, personal commun., 2019). The neural arch pedicel occupies about two thirds of the dorsal surface of the centrum. The neural arch is very low dorsoventrally and overhangs the centrum both anteriorly and posteriorly. The neural spine becomes strongly posteriorly inclined in mid- to posterior elements. Three midcaudal vertebrae are fused (fig. 29A–D). The fusion also includes the chevrons and to a lesser extent the zygapophyses, which remain identifiable in all cases. This pathology likely represents a case of Diffuse Idiopathic Skeletal Hyperostosis (DISH) and was described and figured by Rothschild and Berman (1991: fig. 1A).

Posterior caudal vertebrae of CM 312 (fig. 28D–H) become procoelous, with a distinctly convex posterior articular surface in some but not all elements along the series. The articular

surfaces are strongly pitted and rugose, indicating that intervertebral soft tissue might have partly ossified in this specimen (fig. 28E, G). The neural arch is located above the middle of the centrum. The zygapophyses tend to be relatively more elongate than in more anteriorly positioned vertebrae. The posteriormost preserved caudal vertebrae are strongly dorsoventrally compressed. The neural arch is damaged in all elements, with only the pedicels preserved. The centra are relatively short, with rounded articular surfaces in anterior and posterior view.

The only preserved chevron, other than those that are fused to the pathologic series of caudal vertebrae, has a bridged hemal canal and transversely wide articular facets that are slightly curved posteriorly toward their lateral ends (fig. 28I–K). No distinct subdivision into anterior and posterior articular facets occurs, as would be diagnostic for *Camarasaurus lewisi* (McIntosh et al., 1996b). The shaft is incomplete. It has a subcircular cross section with indications of a posterior keel extending along the midline (fig. 28J), but the keel itself is missing.

The distal end of a right ischium cataloged as CM 312 (fig. 28L–P) has an unexpanded, bladelike morphology, unlike the condition in diplodocids in which this part of the bone is triangular (McIntosh, 1990a, 1990b). There is also a distinct articular surface for its left counterpart on the distal end of the medial edge, which is slightly expanded compared with the more anterior portion of the edge (fig. 28L, M, P).

The cross sections of the dorsal ribs cataloged with CM 312 range in shape from rounded to rather planklike, and thus probably represent a nearly complete series. None of the preserved rib heads bears oblique laminae on the posterior surface that would support a referral to a diplodocine other than *Galeamopus* (Tschopp et al., 2015a; Tschopp and Mateus, 2017). The distal end of one rib (field number 156) has irregularly expanded, rugose edges, resembling elements identified as sternal ribs in *Brontosaurus excelsus* and other diplodocid species (Marsh, 1896; Tschopp and Mateus, 2013a, 2017). Another rib (field number 127) has a strongly rugose, bulbous bony outgrowth along the shaft (fig. 29E–H), indicating a healed break during the lifetime of the animal (Foth et al., 2015).

Caudal Vertebrae: The vertebral centra of CM 36034 are relatively anteroposteriorly short and dorsoventrally tall (fig. 30; table 20). The centra are amphicoelous, with horizontal ventrolateral ridges and strongly developed posterior chevron facets. Distinct ventral ridges extend from the facets anteriorly, but unite at the midline to form a ventral keel that reaches the anterior articular surface. The neural canal is not oriented perpendicular to the articular facets of the centrum, but instead is anterodorsally inclined when the articular surfaces are oriented vertically, similar to the condition in *Haplocanthosaurus* (Hatcher, 1903; Foster and Wedel, 2014). The neural arch pedicels are located more on the anterior half of the centrum, but the complete neural arch extends over the entire centrum. The prezygapophyses are short. The postzygapophyses are so poorly preserved that they offer no useful morphological information. The neural spine is anteroposteriorly longer than transversely wide and does not significantly expand transversely toward the summit. There is no contact between the SPRL and SPOL on its lateral surface, as would be typical for diplodocids (Tschopp et al., 2015a); rather, the condition in CM 36034 is similar to that in the probable *Haplocanthosaurus* skeleton FHPR 1106 (J. Foster, personal commun., 2019). The POSL becomes more pronounced and projects posteriorly toward the summit.

The centrum of CM 36036 is amphicoelous with subcircular articular surfaces, relatively short anteroposteriorly (table 20), and lacks ridges or hollows. The neural arch occupies most of the length of the centrum and is located dorsal to its anteroposterior midline in lateral view. The small preserved portion of the neural spine offers little morphological information other than the presence of SPRLs that extend along its anterolateral edges. The posterior portion of the centrum is irregularly expanded in all directions,

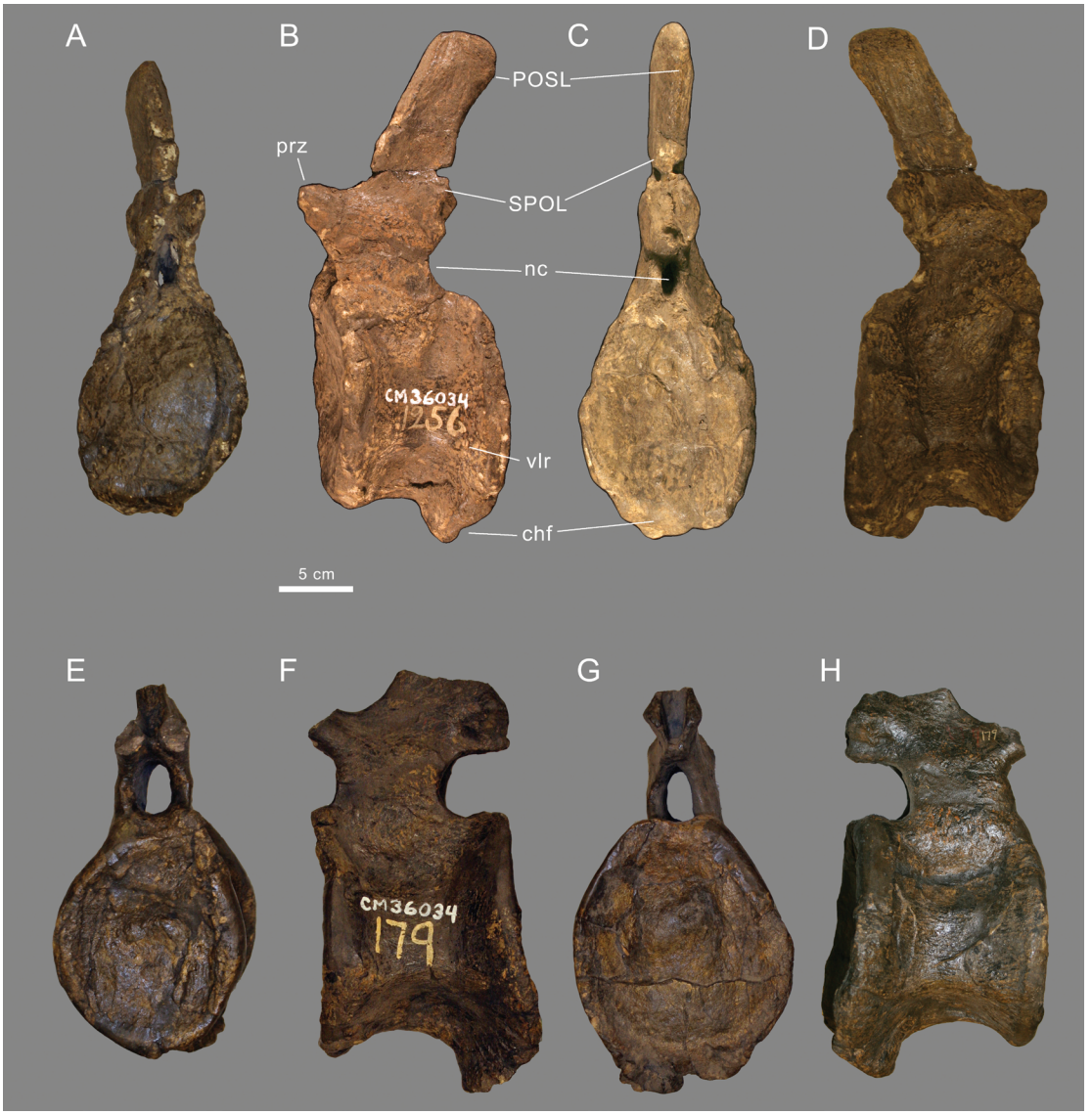

FIG. 30. Anterior midcaudal vertebrae of Neosauropoda indet. CM 36034 in **A, E,** anterior; **B, F,** left lateral; **C, G,** posterior; and **D, H,** right lateral views. Note the strongly developed chevron facets and the inclination of the neural canal. The specimen was initially cataloged as CM 1256 and later recataloged as CM 36034. The number 179 corresponds to the field number. Scale bar applies to both bones and all views. Abbreviations: **chf,** chevron facet; **nc,** neural canal; **POSL,** postspinal lamina; **prz,** prezygapophysis; **SPOL,** spinopostzygapophyseal lamina; **vlr,** ventrolateral ridge. Photos by Andrew McAfee (A, D–H) and Enrica Sarotto (B, C).

TABLE 20

Measurements of midcaudal vertebrae referred to Neosauropoda indet. from RFPR Quarry B (in mm)
Measurements with dagger indicate that the vertebra in question is incomplete in the measured dimension.

	CM 36034[1]	CM 36034[2]	CM 36036[3]
Centrum length	115	136	135
Posterior cotyle dorsoventral height	163	172 (155 without chevron facets)	92
Posterior cotyle transverse width	117	132	91
Dorsoventral height (total)	352	253†	129†
Neural spine maximum transverse width	26	–	–
Neural spine minimum transverse width	18	20	–
Neural spine anteroposterior length at summit	51	–	–
Neural arch dorsoventral height	190	84†	33†
Elongation index (sensu Wilson and Sereno, 1998)	0.71	0.74 (not counting chevron facets)	1.47
Average elongation index (sensu Chure et al., 2010)	0.82	0.80	1.48

[1] Near-complete element; see figure 30A–D.
[2] Incomplete element; field number 179; see figure 30E–H.
[3] Not figured.

TABLE 21

Measurements of scapulae referred to Neosauropoda indet. from RFPR Quarry B (in mm)

	CM 36028	**CM 36030**
	Scapula, R	Scapula, L
Preserved anteroposterior length		900
Preserved maximum dorsoventral height of posterior of scapular blade	345	340
Preserved minimum dorsoventral height of scapular blade	210	184

forming rugose margins around the posterior articular surface, indicating the presence of DISH. Manual articulation with the fused midcaudal vertebrae of CM 312 that are affected by DISH as well shows that the vertebra CM 36036 is a near-perfect match and thus most likely belongs to the same individual.

Scapulae: The distal end of the scapula CM 36028 is only slightly expanded ventrally and has an angular posteroventral corner. The posterodorsal corner is rounded. It is unclear whether an additional, separate dorsal process was present close to the distal end of the blade, which would allow a referral to Camarasauridae. The blade has a D-shaped cross section. Given its incompleteness, it remains unclear whether the distal expansion was twice as wide as the minimum blade width (table 21), which would exclude a referral to Diplodocidae (Tschopp et al., 2015a).

In the scapula CM 36030, there is some indication of a small subtriangular process on the ventral edge, close to the proximal end of the blade. A rugose, slightly curved ridge occurs on the dorsal half of the medial surface, at a slightly more distal position on the blade compared with

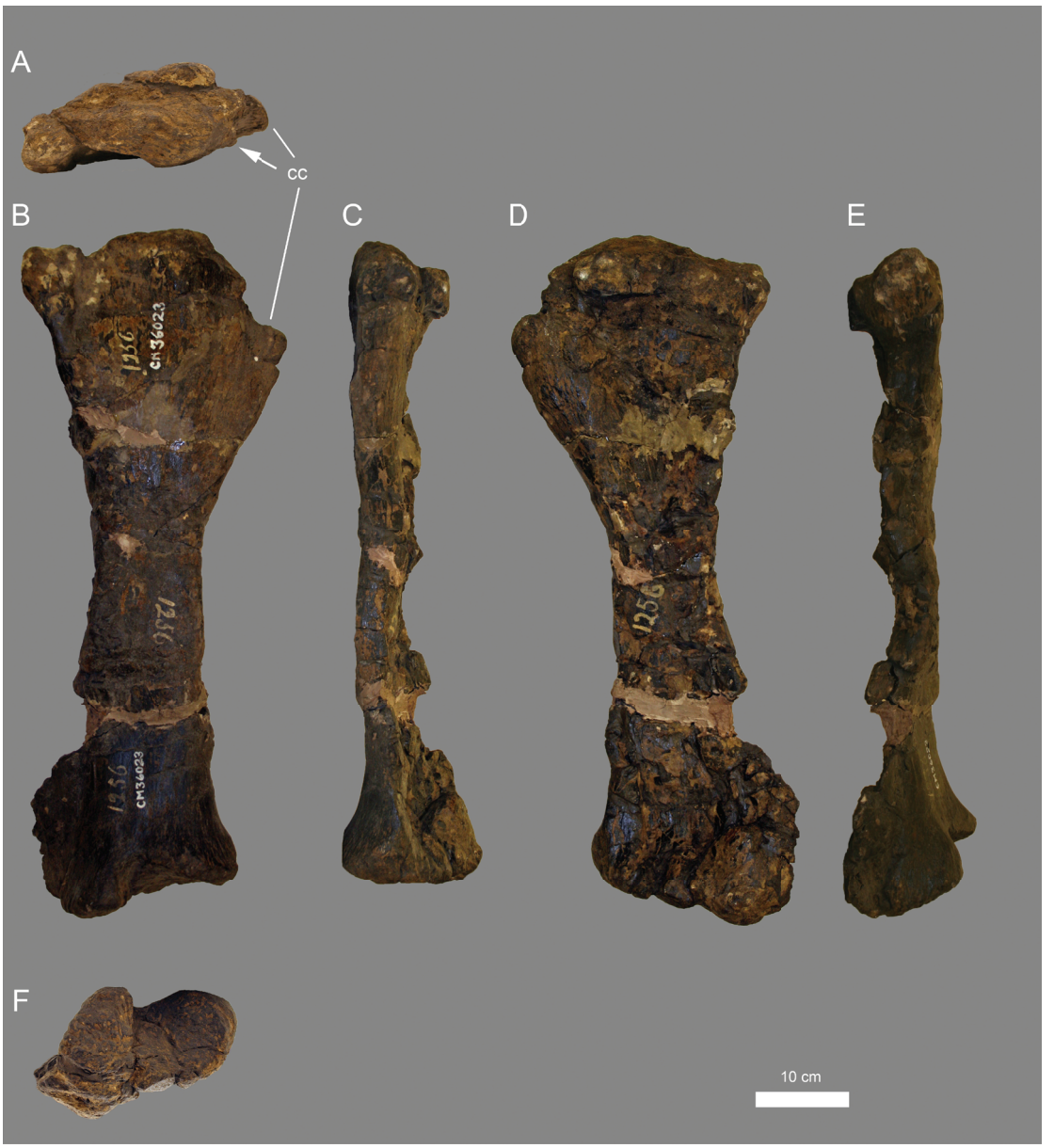

FIG. 31. Right tibia of Neosauropoda indet. CM 36023 in **A,** proximal, **B,** posterior, **C,** medial, **D,** anterior, **E,** lateral, and **F,** distal views. Note the second cnemial crest (arrow in A). The specimen was initially cataloged as CM 1256 and later recataloged as CM 36023. Scale bar applies to all views. Abbreviations: **cc,** cnemial crest. Photos by Andrew McAfee.

TABLE 22

Measurements of the neosauropod right tibia CM 36023 from RFPR Quarry B (in mm; see fig. 31)
Several measurements were not taken because they would be misleading due to deformation.

Proximodistal length	710
Minimum shaft mediolateral width	112

the subtriangular process. The blade appears D-shaped in cross section. The distal blade is ventrally and dorsally expanded, and probably exceeded twice the minimum blade breadth (table 21). It remains unclear whether a separate dorsal process was present.

Ischium: The distal end of the ischium CM 28847 is bladelike, with an articular facet for the contralateral ischium on the narrow medial side. Measurements are not meaningful because a piece of the proximal part of the shaft is missing. The preserved portion of the base of the shaft does not bear any indication of the presence of a rugose ridge on the lateral margin.

Tibia: The rounded outline of the proximal articular surface of the tibia CM 36023 (fig. 31) indicates that it probably would have been subcircular in contour prior to diagenetic deformation. There is a small but distinct fibular tubercle posterior to the cnemial crest, which projects into a short second cnemial crest (sensu Bonaparte et al., 2000; fig. 31A). The cnemial crest is rounded and arises slightly distal to the proximal articular surface.

Identification

The caudal series and ischium CM 312 were referred to *Camarasaurus* by McIntosh (1981). This interpretation was most likely based on the bladelike distal end of the ischium, which articulated with its counterpart at the thin medial margin, a feature typical of that genus (McIntosh and Williams, 1988; McIntosh, 1990a, 1990b). However, the strong development of the posterior chevron facets resembles *Haplocanthosaurus* (Hatcher, 1903; McIntosh and Williams, 1988) more closely than any other known Morrison Formation sauropod. Also, a bladelike distal ischium occurs in *Camarasaurus* and *Haplocanthosaurus priscus* (Hatcher, 1903; McIntosh and Williams, 1988). However, the caudal vertebrae seem to be more elongate than typical camarasaurid or *Haplocanthosaurus* elements (fig. 6; suppl. table 3, available at https://doi.org/10.5531/sd.sp.36), although they approach the condition in the undescribed skeleton FHPR 1106, a probable specimen of *Haplocanthosaurus*. The caudal vertebrae of CM 312 also differ from those of other Jurassic non-neosauropod taxa such as turiasaurs and mamenchisaurids in having amphicoelous centra and less anteroposteriorly expanded spine summits, respectively (Sekiya, 2011; Royo-Torres et al., 2017). We therefore conservatively refer CM 312 to Neosauropoda indet., noting that this specimen shares several (but not all) features with caudal series referred to *Haplocanthosaurus*. Thus, we also cannot exclude the possibility that CM 312 represents a previously unknown species.

The anterior midcaudal vertebrae CM 36034 were referred to *Haplocanthosaurus* by McIntosh (1981), an assignment that was subsequently questioned by Foster and Wedel (2014), who argued that caudal vertebrae of this taxon are of low diagnostic value. We agree with Foster and Wedel (2014) concerning the limited diagnostic utility of *Haplocanthosaurus* caudal vertebrae, although the very strongly developed posterior chevron facets are rarely seen in other Morrison Formation sauropods, as is the simple architecture of the neural spines. The inclination of the anterior caudal neural arch with respect to the articular surfaces is also very similar to that seen in anterior caudal vertebrae of MWC 8028 (Wedel et al., 2018), a specimen referred to *Haplocanthosaurus* sp. by Foster and Wedel (2014).

Interestingly, the development of the chevron facets in caudal vertebrae of CM 312 is similar to that observed in CM 36034; moreover, in both specimens, these facets are anteriorly accompanied by ridges that converge to form a midline ventral keel in the anterior half of the centrum, indicating that they are referable to the same taxon. Since no other overlapping, similar material is known from RFPR Quarry B, it seems likely that these two specimens (as well as CM 36036) are part of a single individual.

Although the caudal vertebrae of CM 36034 are generally very similar to those of *Haplocanthosaurus*, their short prezygapophyses differ from those in the known species *H. priscus* and *H. delfsi* (Hatcher, 1903; McIntosh and Williams, 1988; though the length of the CM 36034 prezygapophyses might have been slightly taphonomically distorted or even abbreviated by weathering). We therefore conservatively refer CM 36034 only to Neosauropoda indet. following our interpretation of CM 312.

Although CM 36036 was previously identified as *Camarasaurus* (McIntosh, 1981), we refer this midcaudal vertebra to Neosauropoda indet. based on the same arguments presented for CM 312. This also reflects the interpretation that these two specimens (and possibly CM 36034 as well) most likely pertain to a single individual (see above).

McIntosh (1981) referred the scapulae CM 36028 and CM 36030 to *Camarasaurus*. However, due to their incompleteness, these bones do not preserve any features that are currently regarded as apomorphies of particular sauropod genera. A D-shaped scapular blade was recovered as a synapomorphy of *Jobaria* + Neosauropoda by Wilson (2002). *Jobaria* has a relatively short, stout scapular blade with a widely expanded posterior end and a ventral extension (Sereno et al., 1999) that contrasts the straighter ventral edge of CM 36028. Within Neosauropoda, we can also likely exclude a referral of CM 36028 to *Haplocanthosaurus* because, like *Jobaria*, this genus has a wide, expanded posteroventral corner of the scapular blade (Hatcher, 1903; McIntosh and Williams, 1988). On the other hand, CM 36030 has a subequally expanded distal blade, as in *Jobaria*, *Haplocanthosaurus*, and camarasaurids. A referral of CM 36030 to diplodocoids more derived than *Haplocanthosaurus* can probably be discounted because of their narrower scapular blades (see, e.g., *Apatosaurus louisae* CM 3018 or *Galeamopus pabsti* SMA 0011; Gilmore, 1936; Tschopp and Mateus, 2017). The ridge on the medial surface of CM 36030 also occurs on the flagellicaudatan scapula CM 90276 but not on the camarasaurid scapula CM 36029. A broader survey of sauropod scapulae would be needed to ascertain whether this feature is diagnostic to a particular taxonomic level. We therefore refer CM 36028 and CM 36030 to Neosauropoda indet.

McIntosh (1981) referred the ischium CM 28847 to *Camarasaurus*, likely based on its unexpanded, bladelike distal end. However, bladelike distal ischia are more widespread within sauropods, having been found as a synapomorphy of *Jobaria* + Neosauropoda by Wilson (2002). Because the ischium of *Jobaria* is generally more slender than CM 28847, we refer the latter to Neosauropoda indet.

McIntosh (1981) referred the tibia CM 36023 to *Camarasaurus*. The presence of a second cnemial crest is a local autapomorphy of the genus *Galeamopus* within Diplodocidae (Tschopp and Mateus, 2017), but this condition also occurs in at least some specimens of *Camarasaurus* (Ostrom and McIntosh, 1966). The robustness of CM 36023 (minimum shaft width to proximodistal length ratio = 0.16) also does not allow us to distinguish between the two genera: *Galeamopus pabsti* SMA 0011 has a ratio of 0.16 (Tschopp and Mateus, 2017), whereas *Camarasaurus* ranges from 0.13 to 0.17 (McIntosh et al., 1996a; Tschopp, unpubl. data). Although we can exclude other diplodocid taxa due to the presence of the second cnemial crest in CM 36023, and *Haplocanthosaurus* because tibiae of this taxon are much more robust (USNM 4275 has a ratio of 0.22; McIntosh and Williams, 1988), we prefer to be conservative and refer CM 36023 only to Neosauropoda indet.

Sauropoda Marsh, 1878

Sauropoda indet.

Referred Specimens: The catalog number CM 1256 initially encompassed most of the unprepared, unidentified material from RFPR Quarry B. This number currently includes vertebral fragments—among them a right prezygapophysis of a dorsal vertebra (possibly belonging to CM 36040; E.T., personal obs., 2017) and the apex of a caudal neural spine, both likely from a camarasaurid—as well as several pieces of dorsal ribs. Two very slender, rod-like bones (in five parts, collectively) probably represent sternal ribs, being similar to bones of Morphotype C sensu Tschopp and Mateus (2013a). There are also three chevrons with bridged hemal canals that might belong to the same individual as CM 312 (and, by extension CM 36034 and CM 36036), a portion of a scapula or coracoid that preserves parts of the glenoid, and two sternal plates. Additional, unidentifiable pieces include fragments of appendicular bones. During our study, a few elements were identified to belong to recataloged specimens. It is possible that the same is true for other fragments, but the near total absence of field notes hampers such referrals.

A few fragments, most likely of dorsal ribs, remain uncataloged, and cannot be referred to a specific taxon with certainty. A note within the box containing these fragments indicates that they most likely belong to CM 1255 or CM 1256. CM 1255 is from a different site (Quarry N of the Freezeout Hills, Wyoming), whereas CM 1256 was a "catchall" number for material from RFPR Quarry B (see above).

DISCUSSION

Sauropod Systematics and Diversity at RFPR

In extant terrestrial ecosystems, large herbivores tend to coexist through resource partitioning (Dodson, 1975; Whitlock, 2011b; Button et al., 2014), and it seems likely that this was also the case in the Mesozoic. Four major groups are represented in the Morrison Formation sauropod fauna: Flagellicaudata, non-flagellicaudatan Diplodocoidea, and the macronarian clades Camarasauridae and Brachiosauridae. Among these Morrison sauropod clades, niche partitioning has been demonstrated among flagellicaudatans, camarasaurids, and brachiosaurids based on tooth morphology, tooth wear, and neck posture (Calvo, 1994; Fiorillo, 1998; Upchurch and Barrett, 2000) and snout and general skull shape (Whitlock, 2011b; Button et al., 2014). More recently, tooth replacement rates were used to infer niche partitioning among the diplodocids *Apatosaurus* and *Diplodocus* (McHugh, 2018). Because the skull and teeth of the non-flagellicaudatan diplodocoid *Haplocanthosaurus* remain unknown, these analyses could not incorporate this genus. However, the strongly divergent vertebral anatomy of *Haplocanthosaurus* versus that of diplodocids, camarasaurids, and brachiosaurids, with its very weakly developed pneumatization (Wedel, 2001, 2003; Foster and Wedel, 2014), implies that this genus had a lifestyle that differed from that of macronarians or other diplodocoids. Additionally, *Haplocanthosaurus* may have been temporally segregated from many other Morrison sauropod genera, as currently known specimens are generally interpreted to come from stratigraphically low layers of this formation (Foster 2003; Foster and Wedel, 2014; see above, however for a discussion of the difficulties of long-distance temporal correlation within the Morrison Formation).

Species- and often even genus-level referrals of the RFPR Quarry B material are hampered by the incompleteness of most of the specimens and the lack of apomorphic features at these lower taxonomic levels in many sauropod clades. Genus-level referrals were possible only within Flagellicaudata, which has received detailed taxonomic and systematic treatment within the last few years (Whitlock, 2011a, 2011c; Mannion et al., 2012; Tschopp and Mateus, 2013b, 2016, 2017; Gallina et al., 2014, 2019; Schwarz-Wings and Böhm, 2014; Rauhut et al., 2015; Salgado et al., 2015; Tschopp et al., 2015a, 2018b; McPhee

et al., 2016; Melstrom et al., 2016; Hanik et al., 2017; Woodruff et al., 2018; Xu et al., 2018). However, our taxonomic reassessment of the RFPR material shows that there is no clear evidence for the presence at the site of more than one genus within any of the major Morrison Formation sauropod clades.

Within Flagellicaudata, and more specifically Diplodocidae, certain previous referrals were incorrect. These erroneous identifications likely resulted from the less complete state of knowledge of diplodocid taxonomic and anatomical diversity at the time they were made. A great deal of taxonomic revision has taken place and a number of new diplodocid genera have been described since the RFPR material was studied by McIntosh (1981): *Supersaurus* was erected by Jensen (1985), *Kaatedocus* by Tschopp and Mateus (2013b), *Leinkupal* by Gallina et al. (2014), and *Galeamopus* by Tschopp et al. (2015a), whereas *Tornieria* was found to be valid by Remes (2006), and *Brontosaurus* by Tschopp et al. (2015a). Prior to 1985, only *Barosaurus*, *Diplodocus*, and *Apatosaurus* were considered valid genera within Diplodocidae, with the first two being comparatively gracile animals and the latter very robust (McIntosh, 1990a, 1990b). This relatively clear difference at the time probably led researchers to attribute all robust diplodocid bones to *Apatosaurus* and more gracile elements to *Diplodocus* or *Barosaurus*. With the more recent recognition of a much higher taxonomic diversity of diplodocines in the Morrison Formation, these earlier referrals have become questionable, especially because some recently recognized genera such as *Supersaurus* and *Galeamopus* have morphologies intermediate between those of the derived diplodocines *Barosaurus* and *Diplodocus* and the apatosaurine *Apatosaurus* (Lovelace et al., 2007; Tschopp and Mateus, 2017). Of particular interest in this case is *Galeamopus*, because the holotype of the type species was found at RFPR Quarry A (Holland, 1924; Foster, 2003; Tschopp et al., 2015a; Tschopp and Mateus, 2017). *Galeamopus* combines the presence of clearly diplodocine, relatively gracile presacral vertebrae with anterior caudal vertebrae that are less pneumatic than those of more derived members of the clade and robust limbs similar to those of apatosaurines (McIntosh, 1990a; Tschopp et al., 2015a; Tschopp and Mateus, 2017).

Some cervical, dorsal, and caudal vertebrae from RFPR Quarry B are referable to *Galeamopus*. Among these specimens, some show characteristics that were proposed to be autapomorphic of the species *Galeamopus pabsti* (e.g., the opening connecting the POCDF and SPOF in cervical vertebrae; Tschopp and Mateus, 2017), whereas the humeri referred to Diplodocidae indet. lack proposed autapomorphies of this species (e.g., the laterally situated tubercle on the proximal portion of the anterior surface of the humerus; Tschopp and Mateus, 2017). It remains possible that some of these morphological differences represent individual variation rather than species-level autapomorphies, and that proposed "autapomorphic" features of *G. pabsti* might actually be synapomorphies at a higher taxonomic level. In the case of the opening connecting the POCDF and SPOF, at least a distinct concavity occurs in the same position in the cervical vertebrae of *G. hayi* (HMNS 175; E.T., personal obs., 2010), and it may be possible that a putative opening remained unrecognized as an authentic morphological feature and was erroneously restored and filled during preparation. Additional information and more specimens will be needed to understand the variability of these features below the genus level. The other flagellicaudatan bones that we identify as Flagellicaudata indet., Diplodocidae indet., or Diplodocinae indet. lack apomorphic features that would unambiguously imply referral to *Galeamopus*; however, such an identification also cannot be ruled out for any of these RFPR specimens. The stout diplodocid right humeri CM 28849 and CM 36026 indicate a minimum of two flagellicaudatan individuals represented at RFPR Quarry B (see below). Given that, within Diplodocidae, equally stout humeri occur only in Apatosaurinae and the diplodocine *Galeamopus* (fig. 11) and that there is no strong evidence supporting the presence of apatosaurines based on

the 49 recovered vertebrae (the most abundant flagellicaudatan bones at RFPR Quarry B), it seems plausible to assume that *Galeamopus* is the only flagellicaudatan genus present at the site. However, although we think it safe to make this assumption for more large-scale paleoecological and paleobiogeographical studies, we prefer to be conservative in the detailed taxonomic assignments of individual specimens, awaiting the identification of additional apomorphic features or the discovery of more information regarding the attribution of bones to particular sauropod individuals in the quarry.

Camarasaurids include the most complete specimens from RFPR Quarry B (CM 21775, CM 36019), as well as several additional, less complete fossils. Some morphological features differ among the specimens referred to this clade herein. These differences include the ridge on the medial surface of the scapular blade and another ridge close to the lateral edge of the ischial blade, as well as the presence of a subtriangular ventral process and a rounded dorsal process on the scapular blade. The ridges most likely represent attachment sites for muscles, the variability of which may be taxonomic, ontogenetic, or even sexually dimorphic in nature. The presence of a subtriangular ventral process at the base of the scapular blade has been shown to be highly variable in both diplodocoids (Tschopp et al., 2015a) and macronarians (Mateus et al., 2011; Mocho et al., 2014). The dorsal process on the distal portion of the scapular blade is variably developed within Camarasauridae (Marsh, 1878; Osborn and Mook, 1921; Ikejiri et al., 2005; Mocho et al., 2014), but without a detailed revision of the taxonomy of this group, it is impossible to know if this feature is diagnostic for any particular species. Indeed, distinguishing species within Camarasauridae is currently difficult to impossible due to the dearth of potentially diagnostic features at lower taxonomic levels (Woodruff and Foster, 2017). In sum, there is evidence for only one (and less likely two) camarasaurid species at RFPR Quarry B.

Among the indeterminate neosauropod material from the quarry, there are specimens that share selected features with both macronarians and the non-flagellicaudatan diplodocoid *Haplocanthosaurus*. However, the most complete of these specimens (CM 312), as well as material previously referred to *Haplocanthosaurus* (CM 36034, which likely belongs to the same tail as CM 312 and CM 36036, see above), also bear features that distinguish them from described specimens of the known genera, instead resembling the undescribed possible *Haplocanthosaurus* specimen FHPR 1106 in these regards. As is the case for Camarasauridae, *Haplocanthosaurus* is in dire need of revision; indeed, in some phylogenetic analyses, the two species referred to this genus do not form a monophyletic clade (e.g., Gallina and Apesteguía, 2005). These systematic difficulties disallow any referral of these specimens below Neosauropoda indet., but it is clear that a third taxon besides *Galeamopus* and a camarasaurid is present among the material from RFPR Quarry B.

According to our reassessment, only one of the genera previously reported from the RFPR quarries (*Apatosaurus*, *Camarasaurus*, *Diplodocus*, *Galeamopus*, and *Haplocanthosaurus*) can be confirmed. All the flagellicaudatan material likely belongs to *Galeamopus* instead of *Apatosaurus* or *Diplodocus*. *Camarasaurus* and/or *Haplocanthosaurus* may be present, but current knowledge of neosauropod trait distribution and low-level taxonomy does not allow referral of the incomplete specimens from RFPR Quarry B to either of these genera. In sum, there is evidence for one diplodocid (*Galeamopus*), one camarasaurid, and a third neosauropod taxon of unclear affinities (possibly *Haplocanthosaurus*) at the site.

Material clearly referable to Flagellicaudata from RFPR Quarry B is mostly nonoverlapping, with the only duplicated elements being the two right humeri. The minimum number of flagellicaudatan individuals at the site is therefore two, with one being slightly larger than the other (based on the 5% difference in humerus length; see table 6). Regarding the vertebrae

referred to *Galeamopus*, size comparisons with two other diplodocine (most likely *Galeamopus*) specimens from Montana that preserve associated cervical, dorsal, and caudal vertebral series (CMC VP 7573; WDC-GB; Tschopp, unpubl. data) indicate that the *Galeamopus* vertebrae from RFPR Quarry B all scale to approximately the same body size. Given that there is no overlap in elements, these vertebrae may therefore all be from a single individual. Camarasaurid bones are more numerous than those of diplodocoids, and based on the occurrence of three right scapulae and coracoids, we can estimate the minimum number of camarasaurid individuals in RPFR Quarry B to be three—one rather small individual and two larger ones. There is no overlapping material among the specimens referable to Neosauropoda indet., suggesting that a single individual was present at RFPR Quarry B. In total, we estimate the minimum number of preserved sauropod individuals to be six (plus one theropod; McIntosh, 1981; Foster, 2003), one fewer than estimated by Foster (2003).

Geographical Segregation within the Morrison Formation?

Geographical segregation among Morrison Formation sauropods has been postulated as one of several potential explanations for their high diversity (Tschopp and Mateus, 2017; Maltese et al., 2018; Whitlock et al., 2018). Geographical differences in taxon distributions within the Morrison Formation have been found in mammals (Foster et al., 2006), turtles and semiaquatic crocodyliforms (Foster and McMullen, 2017), and stegosaurs (Maidment et al., 2018). A trend indicating geographical segregation among flagellicaudatan sauropods has been proposed as well (Tschopp and Mateus, 2017; Maltese et al., 2018). However, a recent, detailed paleobiogeographic analysis shows a rather complex pattern with a generally high number of sauropod genera shared among different geographical regions and low local endemism (Whitlock et al., 2018). Our taxonomic reassessment of the RFPR fauna sheds new light on this issue.

Diversity at RFPR Quarry B seems to have been slightly lower than previously thought, with only three instead of four taxa being present: *Galeamopus*, a camarasaurid, and an indeterminate neosauropod. Both *Diplodocus* and *Apatosaurus*, which were reported from the site in the past (McIntosh, 1981; Foster, 2003), are most likely absent, and the presence of *Haplocanthosaurus* remains dubious (see also Foster and Wedel, 2014). *Diplodocus* and *Apatosaurus* were identified by Whitlock et al. (2018) as two of the five Morrison Formation sauropod genera that occur in all four of the subregions defined in their study. However, these authors also noted that they relied on previous referrals, and that misidentifications are therefore among "the biggest concerns," specifically citing *Galeamopus* as an example of potentially hidden taxonomic diversity (Whitlock et al., 2018: 11). Our findings underscore these concerns and call for additional systematic reassessments of historic collections from the Morrison Formation, especially those from Montana and northern Wyoming that allegedly include *Diplodocus* and/or *Apatosaurus*. If these historic identifications of specimens from the northern Morrison Formation as *Diplodocus* or *Apatosaurus* cannot be confirmed, the general connectivity of flagellicaudatan genera among geographical regions within the formation would be lower, and local endemism (according to Whitlock et al., 2018, already most pronounced in the north) may be higher as a result. To date, the northernmost specimen referred to *Diplodocus* or *Apatosaurus* in Wyoming and Montana that has been described and systematically assessed in detail is the apatosaurine NSMT-PV 20375 from Thermopolis, Wyoming (Upchurch et al., 2004). NSMT-PV 20375 was initially referred to *Apatosaurus ajax* (Upchurch et al., 2004), but the specimen could not be assigned to the two apatosaurine genera that were considered valid by Tschopp et al. (2015a). However, it remains the north-

ernmost well-supported occurrence of Apatosaurinae as a whole.

Clearly, geographical segregation was not equally developed among different Morrison Formation sauropod taxa, even those within Flagellicaudata. Although all three genera identified as locally endemic to the northern region by Whitlock et al. (2018; *Dyslocosaurus*, *Kaatedocus*, and *Suuwassea*, each of which is currently known from only a single locality) are flagellicaudatans (Tschopp et al., 2015a), and even if *Diplodocus* and *Apatosaurus* turn out to have been absent from the north, *Barosaurus* would remain potentially present in all geographical regions, and *Galeamopus* and *Supersaurus* in at least two of these (Lovelace et al., 2007; Tschopp et al., 2015a, 2018b; Tschopp and Mateus, 2017; Whitlock et al., 2018). Given that the holotype of the diplodocine *Barosaurus lentus* (the only *Barosaurus* species currently considered valid; McIntosh, 2005; Tschopp et al., 2015a) is from northern South Dakota (Marsh, 1890; Lull, 1919), the presence of *Barosaurus* in Whitlock et al.'s (2018) northern subregion cannot be disputed. Additional *Barosaurus* specimens are known from Dinosaur National Monument (McIntosh, 2005; Tschopp et al., 2015a), which is part of the western subregion as defined by Whitlock et al. (2018). The northern and western subregions are not directly connected (see Whitlock et al., 2018: fig. 1), so presence of *Barosaurus* in the intervening eastern region seems legitimate as well. *Barosaurus* is also reported from the southern subregion, from an unclear locality in Oklahoma (Stovall's Pit 5 according to Turner and Peterson, 1999; Stovall's Pit 6 according to Foster, 2003; Stovall's Pit 1 according to the Paleobiology Database, from where Whitlock et al., 2018, extracted their data). In Stovall's (1938) initial taxonomic assessment of Pit 1, all sauropod bones were referred to *Brontosaurus excelsus*. A revision of the fauna of the Stovall pits by Hunt and Lucas (1987) also did not mention *Barosaurus*, although these authors noted that a caudal series referred to *Diplodocus* in an unpublished 1940 report by Stovall and Shead appeared to differ from that of *D. carnegii*. Turner and Peterson (1999) and Foster (2003) mentioned *Barosaurus* from Stovall's Pit 5 or Pit 6, respectively, without a detailed taxonomic assessment. The partial tail mentioned by Hunt and Lucas (1987) is from Stovall's Pit 5, and most of the specimens listed as *Barosaurus* in the online database of the Sam Noble Museum (OMNH 1961–1963, 1971, 2150, 4026, 10240, 10246, 10295, and 10340) are indeed caudal vertebrae, with some additional specimens including a cervical vertebra (OMNH 2052) and an astragalus (OMNH 10337). Given that cervical and caudal vertebrae are among the most diagnostic elements in flagellicaudatans (Tschopp et al., 2015a), such a referral could be possible; however, restudy of this material is needed to definitively assess its taxonomic assignment. Nonetheless, even if these specimens proved to belong to a different genus, *Barosaurus* would remain one of the most wide-ranging sauropod genera within the Morrison Formation, especially among flagellicaudatans. Similar geographic ranges have been reported for macronarian genera (Woodruff and Foster, 2017; Maltese et al., 2018).

Indeed, macronarian genera generally seem to be more widespread within the Morrison Formation than their flagellicaudatan counterparts (Woodruff and Foster, 2017; Maltese et al., 2018; Whitlock et al., 2018). Although this may reflect the differing evolutionary histories of these two sauropod groups or greater specialization in Flagellicaudata than Macronaria, it may also represent the fact that the latter clade has not yet received the same level of detailed phylogenetic and systematic treatment as diplodocids, and as a result our understanding of species- and even genus-level diversity is not uniform among Morrison Formation sauropods. Preliminary data from *Camarasaurus* suggests that there may be more valid species than currently recognized, and that some of these might even represent one or more distinct genera (Mateus and Tschopp, 2013; Tschopp et al., 2014). On the other hand, a

recent study of brachiosaurid material suggested that *Brachiosaurus altithorax* is the only species of this clade in the Morrison Formation (D'Emic and Carrano, in press). It is therefore possible that at least camarasaurid species were as geographically segregated as are those of flagellicaudatans, but that the data are currently not sufficient to discern localized, species-level biogeographic patterns among Morrison Formation sauropods. Additional difficulties arise from the sedimentary history of the Morrison Formation depositional basin.

Because the Sundance Sea regressed to the north, it is highly likely that the base of the Morrison Formation, which represents terrestrial sediments deposited after regression occurred, is time transgressive, and the sediments in the north may well be younger than those in the south. Sedimentology (Turner and Peterson, 2004), General Circulation Models (Sellwood and Valdes, 2008), ecosystem modeling (Noto and Grossman, 2010), and palynology (Hotton and Baghai-Riding, 2010) suggest that the climate of the southern Morrison basin was semiarid, whereas that in northern parts of the basin was seasonally wet. On the other hand, plant macrofossils indicate that wet conditions occurred at least locally throughout much of the Morrison depositional basin (Tidwell et al., 1998; Gee et al., 2014); similarly, dinosaur distribution patterns indicate a more mosaic type of environment, with interspersed patches of savannalike and more forested habitats (Whitlock et al., 2018). Given that the temporal resolution and stratigraphic correlation among different sites within the Morrison Formation remains tentative, it is also possible that some of these seemingly conflicting data represent climatic fluctuations through time. In short, it is presently unclear whether the geographical segregation observed in sauropod and other Morrison Formation dinosaur faunas is due to temporal differences (i.e., the southern and northern faunas are not contemporaneous), differing environmental requirements among taxa, or some combination of these factors.

CONCLUSION

Detailed description and taxonomic reassessment of historic sauropod material from the Upper Jurassic Morrison Formation site known as Red Fork of the Powder River Quarry B, excavated by W.H. Utterback for the Carnegie Museum in 1902 and 1903, reveal that diplodocid specimens previously referred to *Diplodocus* and *Apatosaurus* actually belong to the recently recognized genus *Galeamopus*. The other genera traditionally recognized from the site, *Camarasaurus* and *Haplocanthosaurus*, cannot be unambiguously identified based on autapomorphies, so we refer the material in question to either Camarasauridae indet. or Neosauropoda indet. At least three distinct sauropod taxa are represented by a minimum of six individuals (two flagellicaudatans, three camarasaurids, and one indeterminate neosauropod) in the material from Red Fork of the Powder River Quarry B. These finds add to earlier studies proposing that flagellicaudatan sauropods, with the possible exception of *Barosaurus*, were more regionally restricted within the Morrison Formation than were macronarians. Our reassessment also highlights the need for a thorough systematic and taxonomic revision of the genera *Diplodocus* and *Apatosaurus*, as well as the non-flagellicaudatan diplodocoid and camarasaurid sauropod genera from the Morrison Formation.

ACKNOWLEDGMENTS

We thank Amy Henrici, Dan Pickering, Case Miller, Linsly Church (CM); and Enrica Sarotto (New York) for their help in the collections in Pittsburgh. Comparative data were collected on previous collection visits thanks to Dan Brinkman, Marilyn Fox, and Jacques Gauthier (YPM); Jessica Lippincott, Bill Wahl, Levi Shinkle, and Burkhard Pohl (WDC); Glenn Storrs (CMC); Kirby Siber, Thomas Bolliger, and Rani Ukil (SMA); Brandon Strilisky (TMP); Daniela Schwarz (M.B.R.), Bob Masek, Tyler Keillor, and Paul Sereno (University of Chicago); and Brooks

Britt and Rod Scheetz (BYU). Mick Ellison (AMNH); Andrew McAfee, Alyssa McNece, and Hannah Smith (CM); and Enrica Sarotto assisted with photography and figure production. The unpublished letters between Utterback and Hatcher and the quarry sketch, plus an emergency on-location camera and additional information on the history of CM specimens from RFPR, were provided by Henrici. John Foster and John Whitlock provided very useful reviews that increased the value of this paper and inspired new collaborative projects. We also want to thank Dan Chure, who donated the chevron from CM 662 (now HMNS 175) back to the Carnegie Museum, and who oversees the J.S. McIntosh Archive together with Brooks Britt and Rod Scheetz at BYU, where the notebooks, photos, and correspondence are stored. This archive was paramount in resolving some of the historic questions regarding the RFPR sites.

E. Tschopp has been supported by Theodore Roosevelt Memorial Fund and Division of Paleontology Postdoctoral Fellowships of the American Museum of Natural History, New York. Additional support was provided by the Macaulay Family endowment and the Gingrich Fund to Mark Norell and the Division of Paleontology, American Museum of Natural History. Support for previous collection visits by E. Tschopp was provided through his Ph.D. fellowship from the Fundaçao para a Ciência e a Tecnologia (Ministério da Ciência, Tecnologia e Ensino Superior, Portugal), a Volkswagen Foundation Postdoctoral Fellowship within the framework of the "*Europasaurus*-Projekt," and a Karl Hirsch Memorial Grant from the Western Interior Paleontological Society.

REFERENCES

Bakker, R.T. 1998. Dinosaur mid-life crisis; the Jurassic-Cretaceous transition in Wyoming and Colorado. Bulletin of the New Mexico Museum of Natural History and Science 14: 67–77.

Bonaparte, J.F. 1986. The early radiation and phylogenetic relationships of the Jurassic sauropod dinosaurs, based on vertebral anatomy. *In* K. Padian (editor), The beginning of the age of dinosaurs: 247–258. Cambridge: Cambridge University Press.

Bonaparte, J.F., W. Heinrich, and R. Wild. 2000. Review of *Janenschia* Wild, with the description of a new sauropod from the Tendaguru beds of Tanzania and a discussion on the systematic value of procoelous caudal vertebrae in the Sauropoda. Palaeontographica Abteilung A 256: 25–76.

Bonnan, M.F. 2001. The evolution and functional morphology of sauropod dinosaur locomotion. Ph.D. dissertation, Northern Illinois University, Dekalb, Illinois.

Bonnan, M.F. 2003. The evolution of manus shape in sauropod dinosaurs: implications for functional morphology, forelimb orientation, and phylogeny. Journal of Vertebrate Paleontology 23: 595–613.

Brinkman, P.D. 2010. The second Jurassic dinosaur rush. Museums and paleontology at the turn of the 20th century. Chicago: University of Chicago Press, 345 pp.

Brown, B. 1935. Sinclair dinosaur expedition, 1934. Natural History 36: 2–15.

Button, D.J., E.J. Rayfield, and P.M. Barrett. 2014. Cranial biomechanics underpins high sauropod diversity in resource-poor environments. Proceedings of the Royal Society of London B, Biological Sciences 281: 20142114.

Calvo, J.O. 1994. Jaw mechanics in sauropod dinosaurs. Gaia 10: 183–193.

Calvo, J.O., and L. Salgado. 1995. *Rebbachisaurus tessonei* sp. nov. A new sauropod from the Albian-Cenomanian of Argentina; new evidence on the origin of the Diplodocidae. Gaia 11: 13–33.

Carballido, J.L., and P.M. Sander. 2014. Postcranial axial skeleton of *Europasaurus holgeri* (Dinosauria, Sauropoda) from the Upper Jurassic of Germany: implications for sauropod ontogeny and phylogenetic relationships of basal Macronaria. Journal of Systematic Palaeontology 12: 335–387.

Carballido, J.L., L. Salgado, D. Pol, J.I. Canudo, and A. Garrido. 2012. A new basal rebbachisaurid (Sauropoda, Diplodocoidea) from the Early Cretaceous of the Neuquén Basin; evolution and biogeography of the group. Historical Biology 24: 631–654.

Cope, E.D. 1877a. On a dinosaurian from the Trias of Utah. Proceedings of the American Philosophical Society 16: 579–584.

Cope, E.D. 1877b. On *Amphicoelias*, a genus of saurians from the Dakota Epoch of Colorado. Proceedings of the American Philosophical Society 17: 242–246.

D'Emic, M.D. 2012. The early evolution of titanosauriform sauropod dinosaurs. Zoological Journal of the Linnean Society 166: 624–671.

D'Emic, M.D., and M.T. Carrano. In press. Redescription of brachiosaurid sauropod dinosaur material from the Upper Jurassic Morrison Formation, Colorado, USA. The Anatomical Record.

Demko, T.M., B.S. Currie, and K.A. Nicoll. 2004. Regional paleoclimatic and stratigraphic implications of paleosols and fluvial/overbank architecture in the Morrison Formation (Upper Jurassic), Western Interior, USA. Sedimentary Geology 167: 115–135.

Dodson, P. 1975. Taxonomic implications of relative growth in lambeosaurine hadrosaurs. Systematic Biology 24: 37–54.

Dunagan, S.P. 1999. A North American freshwater sponge (*Eospongilla morrisonensis* new genus and species) from the Morrison Formation (Upper Jurassic), Colorado. Journal of Paleontology 73: 389–393.

Dunagan, S.P., and C.E. Turner. 2004. Regional paleohydrologic and paleoclimatic settings of wetland/lacustrine depositional systems in the Morrison Formation (Upper Jurassic), Western Interior, USA. Sedimentary Geology 167: 269–296.

Erickson, B.R. 2014. History of the Poison Creek expeditions 1976–1990 with description of *Haplocanthosaurus* post cranials and a subadult diplodocid skull. Science Museum of Minnesota Monograph 8: 1–33.

Fiorillo, A.R. 1998. Dental micro wear patterns of the sauropod dinosaurs *Camarasaurus* and *Diplodocus*: Evidence for resource partitioning in the Late Jurassic of North America. Historical Biology 13: 1–16.

Foster, J.R. 2003. Paleoecological analysis of the vertebrate fauna of the Morrison Formation (Upper Jurassic), Rocky Mountain region, USA. New Mexico Museum of Natural History and Science Bulletin 23: 1–72.

Foster, J.R., and S.K. McMullen. 2017. Paleobiogeographic distribution of Testudinata and neosuchian Crocodyliformes in the Morrison Formation (Upper Jurassic) of North America: evidence of habitat zonation? Palaeogeography, Palaeoclimatology, Palaeoecology 468: 208–215.

Foster, J.R., and M.J. Wedel. 2014. *Haplocanthosaurus* (Saurischia: Sauropoda) from the lower Morrison Formation (Upper Jurassic) near Snowmass, Colorado. Volumina Jurassica 12: 197–210.

Foster, J.R., K.C. Trujillo, S.K. Madsen, and J.E. Martin. 2006. The Late Jurassic mammal *Docodon*, from the Morrison Formation of the Black Hills, Wyoming: implications for abundance and biogeography of the genus. New Mexico Museum of Natural History and Science Bulletin 36: 165–169.

Foth, C., et al. 2015. New insights into the lifestyle of *Allosaurus* (Dinosauria: Theropoda) based on another specimen with multiple pathologies. PeerJ 3: e940.

Gallina, P.A., and S. Apesteguía. 2005. *Cathartesaura anaerobica* gen. et sp. nov., a new rebbachisaurid (Dinosauria, Sauropoda) from the Huincul Formation (Upper Cretaceous), Río Negro, Argentina. Revista del Museo Argentino de Ciencias Naturales Nueva Serie 7: 153–166.

Gallina, P.A., S. Apesteguía, A. Haluza, and J.I. Canale. 2014. A diplodocid sauropod survivor from the Early Cretaceous of South America. PLoS ONE 9: e97128.

Gallina, P.A., S. Apesteguía, J.I. Canale, and A. Haluza. 2019. A new long-spined dinosaur from Patagonia sheds light on sauropod defense system. Scientific Reports 9: 1392.

Gee, C.T., R.D. Dayvault, R.A. Stockey, and W.D. Tidwell. 2014. Greater palaeobiodiversity in conifer seed cones in the Upper Jurassic Morrison Formation of Utah, USA. Palaeobiodiversity and Palaeoenvironments 94: 363–375.

Gilmore, C.W. 1925. A nearly complete articulated skeleton of *Camarasaurus*, a saurischian dinosaur from the Dinosaur National Monument, Utah. Memoirs of the Carnegie Museum 10: 347–384.

Gilmore, C.W. 1936. Osteology of *Apatosaurus*: with special reference to specimens in the Carnegie Museum. Memoirs of the Carnegie Museum 11: 175–300.

Hanik, G.M., M.C. Lamanna, and J.A. Whitlock. 2017. A juvenile specimen of *Barosaurus* Marsh, 1890 (Sauropoda: Diplodocidae) from the Upper Jurassic Morrison Formation of Dinosaur National Monument, Utah, USA. Annals of Carnegie Museum 84: 253–263.

Harris, J.D. 2006. The axial skeleton of the dinosaur *Suuwassea emilieae* (Sauropoda: Flagellicaudata) from the Upper Jurassic Morrison Formation of Montana, USA. Palaeontology 49: 1091–1121.

Harris, J.D. 2007. The appendicular skeleton of *Suuwassea emilieae* (Sauropoda: Flagellicaudata) from the Upper Jurassic Morrison Formation of Montana (USA). Geobios 40: 501–522.

Harris, J.D., and P. Dodson. 2004. A new diplodocoid sauropod dinosaur from the Upper Jurassic Morri-

son Formation of Montana, USA. Acta Palaeontologica Polonica 49: 197–210.

Hatcher, J.B. 1901. *Diplodocus* (Marsh): its osteology, taxonomy, and probable habits, with a restoration of the skeleton. Memoirs of the Carnegie Museum 1: 1–61.

Hatcher, J.B. 1902. Structure of the forelimb and manus of *Brontosaurus*. Annals of the Carnegie Museum 1: 356–376.

Hatcher, J.B. 1903. Osteology of *Haplocanthosaurus*, with description of a new species and remarks on the probable habits of the Sauropoda and the age and origin of the *Atlantosaurus* beds: Additional remarks on *Diplodocus*. Memoirs of the Carnegie Museum 2: 1–72.

Holland, W.J. 1906. The osteology of *Diplodocus* Marsh. Memoirs of the Carnegie Museum 2: 225–264.

Holland, W.J. 1924. The skull of *Diplodocus*. Memoirs of the Carnegie Museum 9: 378–403.

Hotton, C.L., and N.L. Baghai-Riding. 2010. Palynological evidence for conifer dominance within a heterogeneous landscape in the Late Jurassic Morrison Formation, USA. *In* C.T. Gee (editor), Plants in Mesozoic time: morphological innovations, phylogeny, ecosystems: 295–328. Bloomington: Indiana University Press.

Hunt, A.P., and S.G. Lucas. 1987. J.W. Stovall and the Mesozoic of the Cimarron Valley, Oklahoma and New Mexico. New Mexico Geological Society Guidebook 38: 139–151.

Ikejiri, T., V. Tidwell, and D.L. Trexler. 2005. New adult specimens of *Camarasaurus lentus* highlight ontogenetic variation within the species. *In* V. Tidwell and K. Carpenter (editors), Thunder-lizards: the sauropodomorph dinosaurs: 154–179. Bloomington: Indiana University Press.

Janensch, W. 1961. Die Gliedmassen und Gliedmassengürtel der Sauropoden der Tendaguru-Schichten. Palaeontographica-Supplementbände 177–235.

Jennings, D.S., and S.T. Hasiotis. 2006. Paleoenvironmental and stratigraphic implications of authigenic clay distributions in Morrison Formation deposits, Bighorn Basin, Wyoming. New Mexico Museum of Natural History and Science Bulletin 36: 25–34.

Jensen, J.A. 1985. Three new sauropod dinosaurs from the Upper Jurassic of Colorado. Great Basin Naturalist 45: 697–709.

Jensen, J.A. 1988. A fourth new sauropod dinosaur from the Upper Jurassic of the Colorado Plateau and sauropod bipedalism. Great Basin Naturalist 48: 121–145.

Kvale, E.P., et al. 2001. Middle Jurassic (Bajocian and Bathonian) dinosaur megatracksites, Bighorn Basin, Wyoming, USA. Palaios 16: 233–254.

Lovelace, D.M., S.A. Hartman, and W.R. Wahl. 2007. Morphology of a specimen of *Supersaurus* (Dinosauria, Sauropoda) from the Morrison Formation of Wyoming, and a re-evaluation of diplodocid phylogeny. Arquivos Do Museu Nacional 65: 527–544.

Lull, R.S. 1919. The sauropodous dinosaur *Barosaurus* Marsh. Memoirs of the Connecticut Academy of Arts and Sciences 6: 1–42.

Madsen, J.H., J.S. McIntosh, and D.S. Berman. 1995. Skull and atlas-axis complex of the Upper Jurassic sauropod *Camarasaurus* Cope (Reptilia: Saurischia). Bulletin of Carnegie Museum of Natural History 31: 1–115.

Maidment, S.C.R., C. Brassey, and P.M. Barrett. 2015. The postcranial skeleton of an exceptionally complete individual of the plated dinosaur *Stegosaurus stenops* (Dinosauria: Thyreophora) from the Upper Jurassic Morrison Formation of Wyoming, U.S.A. PLoS One 10: e0138352.

Maidment, S.C.R., D. Balikova, and A.R. Muxworthy. 2017. Magnetostratigraphy of the Upper Jurassic Morrison Formation at Dinosaur National Monument, Utah, and prospects for using magnetostratigraphy as a correlative tool in the Morrison Formation. *In* K. Ziegler and W. Parker (editors), Deciphering complex depositional systems: 280–298. Amsterdam: Elsevier.

Maidment, S.C.R., D.C. Woodruff, and J.R. Horner. 2018. A new specimen of the ornithischian dinosaur *Hesperosaurus mjosi* from the Upper Jurassic Morrison Formation of Montana, U.S.A., and implications for growth and size in Morrison stegosaurs. Journal of Vertebrate Paleontology 38: e1406366.

Maltese, A., E. Tschopp, F. Holwerda, and D. Burnham. 2018. The real Bigfoot: a pes from Wyoming, USA is the largest sauropod pes ever reported and the northern-most occurrence of brachiosaurids in the Upper Jurassic Morrison Formation. PeerJ 6: e5250.

Mannion, P.D., P. Upchurch, O. Mateus, R.N. Barnes, and M.E.H. Jones. 2012. New information on the anatomy and systematic position of *Dinheirosaurus lourinhanensis* (Sauropoda: Diplodocoidea) from the Late Jurassic of Portugal, with a review of European diplodocoids. Journal of Systematic Palaeontology 10: 521–551.

Mannion, P.D., P. Upchurch, R.N. Barnes, and O. Mateus. 2013. Osteology of the Late Jurassic Portuguese sauropod dinosaur *Lusotitan atalaiensis* (Mac-

ronaria) and the evolutionary history of basal titanosauriforms. Zoological Journal of the Linnean Society 168: 98–206.

Mannion, P.D., R. Allain, and O. Moine. 2017. The earliest known titanosauriform sauropod dinosaur and the evolution of Brachiosauridae. PeerJ 5: e3217.

Mannion, P.D., P. Upchurch, D. Schwarz, and O. Wings. 2019. Taxonomic affinities of the putative titanosaurs from the Late Jurassic Tendaguru Formation of Tanzania: phylogenetic and biogeographic implications for eusauropod dinosaur evolution. Zoological Journal of the Linnean Society 185: 784–909.

Marsh, O.C. 1877a. A new order of extinct Reptilia (Stegosauria) from the Jurassic of the Rocky Mountains. American Journal of Science (Series 3) 14: 34–35.

Marsh, O.C. 1877b. Notice of new dinosaurian reptiles from the Jurassic formation. American Journal of Science (Series 3) 14: 514–516.

Marsh, O.C. 1878. Principal characters of American Jurassic dinosaurs, Part I. American Journal of Science (Series 3) 16: 411–416.

Marsh, O.C. 1879. Notice of new Jurassic reptiles. American Journal of Science (Series 3) 18: 501–505.

Marsh, O.C. 1881. Principal characters of American Jurassic dinosaurs. Part V. American Journal of Science (Series 3) 21: 417–437.

Marsh, O.C. 1884. Principal characters of American Jurassic dinosaurs. Part VII. On the Diplodocidae, a new family of the Sauropoda. American Journal of Science (Series 3) 27: 160–168.

Marsh, O.C. 1890. Description of new dinosaurian reptiles. American Journal of Science (Series 3) 39: 81–86.

Marsh, O.C. 1896. The dinosaurs of North America. U.S. Geological Survey Annual Report 16: 143–244.

Mateus, O., and E. Tschopp. 2013. *Cathetosaurus* as a valid sauropod genus and comparisons with *Camarasaurus*. Journal of Vertebrate Paleontology, Program and Abstracts 2013: 173.

Mateus, O., et al. 2011. *Angolatitan adamastor*, a new sauropod dinosaur and the first record from Angola. Anais da Academia Brasileira de Ciências 83: 221–233.

McHugh, J.B. 2018. Evidence for niche partitioning among ground-height browsing sauropods from the Upper Jurassic Morrison Formation of North America. Geology of the Intermountain West 5: 95–103.

McIntosh, J.S. 1981. Annotated catalogue of the dinosaurs (Reptilia, Archosauria) in the collections of Carnegie Museum of Natural History. Bulletin of Carnegie Museum of Natural History 18: 1–67.

McIntosh, J.S. 1990a. Species determination in sauropod dinosaurs with tentative suggestions for their classification. *In* K. Carpenter (editor), Dinosaur Systematics: Approaches and Perspectives: 53–69. Cambridge: Cambridge University Press.

McIntosh, J.S. 1990b. Sauropoda. *In* D.B. Weishampel, P. Dodson, and H. Osmólska (editors), The Dinosauria (1st ed.): 345–401. Berkeley: University of California Press.

McIntosh, J.S. 2005. The genus *Barosaurus* Marsh (Sauropoda, Diplodocidae). *In* V. Tidwell and K. Carpenter (editors), Thunder-lizards: the sauropodomorph dinosaurs: 38–77. Bloomington: Indiana University Press.

McIntosh, J.S., and M. Williams. 1988. A new species of sauropod dinosaur, *Haplocanthosaurus delfsi* sp. nov., from the Upper Jurassic Morrison Fm. of Colorado. Kirtlandia 43: 3–26.

McIntosh, J.S., C.A. Miles, K.A. Cloward, and J.R. Parker. 1996a. A new nearly complete skeleton of *Camarasaurus*. Bulletin of the Gunma Museum of Natural History 1: 1–87.

McIntosh, J.S., W.E. Miller, K.L. Stadtman, and D.D. Gillette. 1996b. The osteology of *Camarasaurus lewisi* (Jensen, 1988). Brigham Young University Geology Studies 41: 73–116.

McPhee, B.W., P.D. Mannion, W.J. de Klerk, and J.N. Choiniere. 2016. High diversity in the sauropod dinosaur fauna of the Lower Cretaceous Kirkwood Formation of South Africa: Implications for the Jurassic-Cretaceous transition. Cretaceous Research 59: 228–248.

Melstrom, K.M., M.D. D'Emic, D. Chure, and J.A. Wilson. 2016. A juvenile sauropod dinosaur from the Late Jurassic of Utah, U.S.A., presents further evidence of an avian style air-sac system. Journal of Vertebrate Paleontology 36: e1111898.

Mocho, P., R. Royo-Torres, and F. Ortega. 2014. Phylogenetic reassessment of *Lourinhasaurus alenquerensis*, a basal Macronaria (Sauropoda) from the Upper Jurassic of Portugal. Zoological Journal of the Linnean Society 170: 875–916.

Mocho, P., R. Royo-Torres, and F. Ortega. 2016. New data of the Portuguese brachiosaurid *Lusotitan atalaiensis* (Sobral Formation, Upper Jurassic). Historical Biology 29: 789–817.

Noto, C.R., and A. Grossman. 2010. Broad-scale patterns of Late Jurassic dinosaur paleoecology. PLoS One 5: e12553.

Osborn, H.F. 1904. Manus, sacrum, and caudals of Sauropoda. Bulletin of the American Museum of Natural History 20: 181–190.

Osborn, H.F., and C.C. Mook. 1921. *Camarasaurus*, *Amphicoelias*, and other sauropods of Cope. Memoirs of the American Museum of Natural History, new series 3 (3): 249–387, 85 pls.

Ostrom, J.H. 1970. Stratigraphy and paleontology of the Cloverly Formation (Lower Cretaceous) of the Bighorn Basin area, Wyoming and Montana. Bulletin of the Peabody Museum of Natural History 35: 1–234.

Ostrom, J.H., and J.S. McIntosh. 1966. Marsh's dinosaurs: the collections from Como Bluff. New Haven, CT: Yale University Press.

Owen, A., G.J. Nichols, A.J. Hartley, G.S. Weissmann, and L.A. Scuderi. 2015. Quantification of a distributive fluvial system: the salt wash DFS of the Morrison Formation, SW U.S.A. Journal of Sedimentary Research 85: 544–561.

Owen, A., G.J. Nichols, A.J. Hartley, and G.S. Weissmann. 2017. Vertical trends within the prograding Salt Wash distributive fluvial system, SW United States. Basin Research 29: 64–80.

Peterson, F. 1994. Sand dunes, sabkhas, streams, and shallow seas; Jurassic paleogeography in the southern part of the Western Interior basin. *In* M.V. Caputo, J.A. Peterson, and K.J. Franczyk (editors), Mesozoic systems of the Rocky Mountain region, USA: 233–272. Society of Economic Paleontologists and Mineralogists, Rocky Mountain Section.

Peterson, O.A., and C.W. Gilmore. 1902. *Elosaurus parvus*; a new genus and species of the Sauropoda. Annals of the Carnegie Museum 1: 490–499.

Poropat, S.F., et al. 2015. Revision of the sauropod dinosaur *Diamantinasaurus matildae* Hocknull et al. 2009 from the mid-Cretaceous of Australia: Implications for Gondwanan titanosauriform dispersal. Gondwana Research 27: 995–1033.

Rauhut, O.W.M., J.L. Carballido, and D. Pol. 2015. A diplodocid sauropod dinosaur from the Late Jurassic Cañadón Calcáreo Formation of Chubut, Argentina. Journal of Vertebrate Paleontology 35: e982798.

Remes, K. 2006. Revision of the Tendaguru sauropod dinosaur *Tornieria africana* (Fraas) and its relevance for sauropod paleobiogeography. Journal of Vertebrate Paleontology 26: 651–669.

Rothschild, B.M., and D.S. Berman. 1991. Fusion of caudal vertebrae in Late Jurassic sauropods. Journal of Vertebrate Paleontology 11: 29–36.

Royo-Torres, R., et al. 2017. Descendants of the Jurassic turiasaurs from Iberia found refuge in the Early Cretaceous of western USA. Scientific Reports 7: 14311.

Salgado, L., et al. 2015. Late Jurassic sauropods in Chilean Patagonia. Ameghiniana 52: 418–429.

Schwarz, D., T. Ikejiri, B.H. Breithaupt, P.M. Sander, and N. Klein. 2007. A nearly complete skeleton of an early juvenile diplodocid (Dinosauria: Sauropoda) from the lower Morrison Formation (Late Jurassic) of north central Wyoming and its implications for early ontogeny and pneumaticity in sauropods. Historical Biology 19: 225–253.

Schwarz-Wings, D., and N. Böhm. 2014. A morphometric approach to the specific separation of the humeri and femora of *Dicraeosaurus* from the Late Jurassic of Tendaguru, Tanzania. Acta Palaeontologica Polonica 59: 81–98.

Sekiya, T. 2011. Re-examination of *Chuanjiesaurus anaensis* (Dinosauria: Sauropoda) from the Middle Jurassic Chuanjie Formation, Lufeng County, Yunnan Province, southwest China. Memoir of the Fukui Prefectural Dinosaur Museum 10: 1–54.

Sellwood, B.W., and P.J. Valdes. 2008. Jurassic climates. Proceedings of the Geologists' Association 119: 5–17.

Sereno, P.C., et al. 1999. Cretaceous sauropods from the Sahara and the uneven rate of skeletal evolution among dinosaurs. Science 286: 1342–1347.

Stovall, J.W. 1938. The Morrison of Oklahoma and its dinosaurs. Journal of Geology 46: 583–600.

Tidwell, V., K. Carpenter, and W. Brooks. 1999. New sauropod from the Lower Cretaceous of Utah, USA. Oryctos 2: 21–37.

Tidwell, W.D., B.B. Britt, and S.R. Ash. 1998. Preliminary floral analysis of the Mygatt-Moore Quarry in the Jurassic Morrison Formation, West-Central Colorado. Modern Geology 22: 341.

Trujillo, K.C. 2006. Clay mineralogy of the Morrison Formation (Upper Jurassic–?Lower Cretaceous), and its use in long distance correlation and paleoenvironmental analysis. New Mexico Museum of Natural History and Science Bulletin 36: 17–23.

Trujillo, K.C., and B.J. Kowallis. 2015. Recalibrated legacy $^{40}Ar/^{39}Ar$ ages for the Upper Jurassic Morrison Formation, Western Interior, USA. Geology of the Intermountain West 2: 1–8.

Tschopp, E., and O. Mateus. 2012. A sternal plate of a large-sized sauropod dinosaur from the Late Jurassic of Portugal. ¡Fundamental! 20: 263–266.

Tschopp, E., and O. Mateus. 2013a. Clavicles, interclavicles, gastralia, and sternal ribs in sauropod dinosaurs: new reports from Diplodocidae and their morphological, functional and evolutionary implications. Journal of Anatomy 222: 321–340.

Tschopp, E., and O. Mateus. 2013b. The skull and neck of a new flagellicaudatan sauropod from the Morrison Formation and its implication for the evolution and ontogeny of diplodocid dinosaurs. Journal of Systematic Palaeontology 11: 853–888.

Tschopp, E., and O. Mateus. 2016. Case 3700 *Diplodocus* Marsh, 1878 (Dinosauria, Sauropoda): proposed designation of *D. carnegii* Hatcher, 1901 as the type species. Bulletin of Zoological Nomenclature 73: 17–24.

Tschopp, E., and O. Mateus. 2017. Osteology of *Galeamopus pabsti* sp. nov. (Sauropoda: Diplodocidae), with implications for neurocentral closure timing, and the cervico-dorsal transition in diplodocids. PeerJ 5: e3179.

Tschopp, E., et al. 2014. A specimen-level cladistic analysis of *Camarasaurus* and a revision of camarasaurid taxonomy. Journal of Vertebrate Paleontology, Program and Abstracts 2014: 241.

Tschopp, E., O. Mateus, and R.B.J. Benson. 2015a. A specimen-level phylogenetic analysis and taxonomic revision of Diplodocidae (Dinosauria, Sauropoda). PeerJ 3: e857.

Tschopp, E., O. Wings, T. Frauenfelder, and W. Brinkmann. 2015b. Articulated bone sets of manus and pedes of *Camarasaurus* (Sauropoda, Dinosauria). Palaeontologia Electronica 18: 1–65.

Tschopp, E., O. Mateus, and M. Norell. 2018a. Complex overlapping joints between facial bones allowing limited anterior sliding movements of the snout in diplodocid sauropods. American Museum Novitates 3911: 1–16.

Tschopp, E., D. Brinkman, J. Henderson, M.A. Turner, and O. Mateus. 2018b. Considerations on the replacement of a type species in the case of the sauropod dinosaur *Diplodocus* Marsh, 1878. Geology of the Intermountain West 5: 245–262.

Tucker, R.T. 2011. Taphonomy of Sheridan College Quarry 1, Buffalo, Wyoming: implications for reconstructing historic dinosaur localities including Utterback's 1902–1910 Morrison dinosaur expeditions. Geobios 44: 527–541.

Turner, C.E., and N.S. Fishman. 1991. Jurassic Lake T'oo'dichi': a large alkaline, saline lake, Morrison Formation, eastern Colorado Plateau. GSA Bulletin 103: 538–558.

Turner, C.E., and F. Peterson. 1999. Biostratigraphy of dinosaurs in the Upper Jurassic Morrison Formation of the Western Interior, USA. *In* D.D. Gillette (editor), Vertebrate Paleontology in Utah: 77–114. Salt Lake City, Utah, USA: Utah Geological Survey Miscellaneous Publication.

Turner, C.E., and F. Peterson. 2004. Reconstruction of the Upper Jurassic Morrison Formation extinct ecosystem—a synthesis. Sedimentary Geology 167: 309–355.

Upchurch, P., and P.M. Barrett. 2000. The evolution of sauropod feeding mechanisms. *In* H.-D. Sues (editor), Evolution of herbivory in terrestrial vertebrates: perspectives from the fossil record: 79–122. Cambridge: Cambridge University Press.

Upchurch, P., Y. Tomida, and P.M. Barrett. 2004. A new specimen of *Apatosaurus ajax* (Sauropoda: Diplodocidae) from the Morrison Formation (Upper Jurassic) of Wyoming, USA. National Science Museum Monographs 26: 1–118.

Wedel, M.J. 2001. The evolution of vertebral pneumaticity in the Sauropoda. Master's thesis, University of Oklahoma, Norman.

Wedel, M.J. 2003. The evolution of vertebral pneumaticity in sauropod dinosaurs. Journal of Vertebrate Paleontology 23: 344–357.

Wedel, M.J., and M.P. Taylor. 2013. Neural spine bifurcation in sauropod dinosaurs of the Morrison Formation: ontogenetic and phylogenetic implications. PalArch's Journal of Vertebrate Palaeontology 10: 1–34.

Wedel, M.J., R.L. Cifelli, and R.K. Sanders. 2000. Osteology, paleobiology, and relationships of the sauropod dinosaur *Sauroposeidon*. Acta Palaeontologica Polonica 45: 343–388.

Wedel, M.J., et al. 2018. Reconstructing an unusual specimen of *Haplocanthosaurus* using a blend of physical and digital techniques. PeerJ PrePrints 6: e27431v1.

Whitlock, J.A. 2011a. A phylogenetic analysis of Diplodocoidea (Saurischia: Sauropoda). Zoological Journal of the Linnean Society 161: 872–915.

Whitlock, J.A. 2011b. Inferences of diplodocoid (Sauropoda: Dinosauria) feeding behavior from snout shape and microwear analyses. PLoS One 6: e18304.

Whitlock, J.A. 2011c. Re-evaluation of *Australodocus bohetii*, a putative diplodocoid sauropod from the Tendaguru Formation of Tanzania, with comment on Late Jurassic sauropod faunal diversity and palaeoecology. Palaeogeography, Palaeoclimatology, Palaeoecology 309: 333–341.

Whitlock, J.A., K.C. Trujillo, and G.M. Hanik. 2018. Assemblage-level structure in Morrison Formation dinosaurs, Western Interior, USA. Geology of the Intermountain West 5: 9–22.

Wilhite, R. 2003. Biomechanical reconstruction of the appendicular skeleton in three North American Jurassic sauropods. Ph.D. dissertation, Louisiana State University, Baton Rouge.

Wilson, J.A. 1999. A nomenclature for vertebral laminae in sauropods and other saurischian dinosaurs. Journal of Vertebrate Paleontology 19: 639–653.

Wilson, J.A. 2002. Sauropod dinosaur phylogeny: critique and cladistic analysis. Zoological Journal of the Linnean Society 136: 215–275.

Wilson, J.A. 2006. Anatomical nomenclature of fossil vertebrates: standardized terms or "lingua franca"? Journal of Vertebrate Paleontology 26: 511–518.

Wilson, J.A. 2012. New vertebral laminae and patterns of serial variation in vertebral laminae of sauropod dinosaurs. Contributions from the Museum of Paleontology, University of Michigan 32: 91–110.

Wilson, J.A., and P.C. Sereno. 1998. Early evolution and higher-level phylogeny of sauropod dinosaurs. Society of Vertebrate Paleontology Memoir 5: 1–79.

Wilson, J.A., and P. Upchurch. 2003. A revision of *Titanosaurus* Lydekker (Dinosauria-Sauropoda), the first dinosaur genus with a "Gondwanan" distribution. Journal of Systematic Palaeontology 1: 125–160.

Wilson, J.A., R.N. Martinez, and O. Alcober. 1999. Distal tail segment of a titanosaur (Dinosauria: Sauropoda) from the Upper Cretaceous of Mendoza, Argentina. Journal of Vertebrate Paleontology 19: 591–594.

Wilson, J.A., M.D. D'Emic, T. Ikejiri, E.M. Moacdieh, and J.A. Whitlock. 2011. A nomenclature for vertebral fossae in sauropods and other saurischian dinosaurs. PLoS One 6: e17114.

Woodruff, D.C., and J.R. Foster. 2017. The first specimen of *Camarasaurus* (Dinosauria: Sauropoda) from Montana: The northernmost occurrence of the genus. PLoS One 12: e0177423.

Woodruff, D.C., et al. 2018. The smallest diplodocid skull reveals cranial ontogeny and growth-related dietary changes in the largest dinosaurs. Scientific Reports 8: 14341.

Xu, X., et al. 2018. A new Middle Jurassic diplodocoid suggests an earlier dispersal and diversification of sauropod dinosaurs. Nature Communications 9: 2700.